2013

Age-associated changes in the neuroinflammatory response to toll-like receptor 4 and 9 stimulation

Leah Beth Christensen
University of Montana, Missoula

AGE-ASSOCIATED CHANGES IN THE NEUROINFLAMMATORY RESPONSE TO TOLL-LIKE RECEPTOR 4 AND 9 STIMULATION IN YOUNG MICE

By

LEAH BETH CHRISTENSEN

Bachelors of Science, Microbiology, University of Minnesota, Minneapolis, MN, 2007

Dissertation

presented in partial fulfillment of the requirements
for the degree of

Doctor of Philosophy
in Integrative Microbiology and Biochemistry, Cellular and Molecular Biology

The University of Montana
Missoula, MT

May 2013

Approved by:

Dr. Sandy Ross, Dean of the Graduate School
Graduate School

Dr. Scott Wetzel, Co-Chair
Division of Biological Sciences

Dr. Byron Caughey, Co-Chair
Laboratory of Persistent Viral Disease, RML, NIAID, NIH /
Division of Biological Sciences

Dr. D. Scott Samuels,
Division of Biological Sciences

Dr. Jesse Hay
Division of Biological Sciences

ProQuest LLC.
789 East Eisenhower Parkway
P.O. Box 1346
Ann Arbor, MI 48106 - 1346

Dr. Karin Peterson
Laboratory of Persistent Viral Disease, RML, NIAID, NIH /
Division of Biological Sciences

Dr. Sue Priola
Laboratory of Persistent Viral Disease, RML, NIAID, NIH /
Department of Biomedical and Pharmaceutical Sciences

Christensen, Leah, Ph.D., Spring 2013 Integrative Microbiology and Biochemistry

Age-associated changes in the neuroinflammatory response to Toll-like receptor 4 and 9 stimulation in young mice

Co-Chairperson: Scott Wetzel, Ph.D.

Co-Chairperson: Byron Caughey, Ph.D.

During the perinatal time period, the mammalian brain is developing rapidly and is particularly sensitive to inflammation. Inflammation during this time period may be linked to later neurological illness in humans. Disease-associated alterations in learning and behavior can be modeled in rodents using perinatal immune stimulation with either infectious agents or Toll-like receptor (TLR) agonists. Although the gestational period is a particularly sensitive time for neurodevelopment, it is not known for how long after birth this sensitivity persists. In mice, susceptibility to neurological infection declines dramatically during the first weeks of life. Therefore, we sought to compare the neuroinflammatory responses of neonatal and weanling mice. To do so, we injected neonatal and weanling mice intracerebrally (IC) with lipopolysaccharide (LPS) or CpG oligodinucleotides (CpG), ligands of TLRs 4 and 9, respectively. We compared the production of inflammatory mediators and immune cell activation in the brain at each age. Despite lower *Tlr* mRNA expression in neonatal brains, TLR4 and TLR9 stimulation induced substantially higher levels of some cytokines in neonatal brains. We also detected age-associated differences in expression of a subset of microglial activating and inhibitory receptors, as well as age-associated differences in the immune populations present in the brain. We specifically examined whether the prion protein, PrP^{c}, plays an immunomodulatory role in the brain. PrP^{c} expression influences immune cell activation in the periphery, increases in the brain with age, and influences several aspects of glial cell function. Since glia are the primary immune-responsive cells in the brain, we hypothesized that PrP^{c} would influence the neuroinflammatory response. However, we found no PrP^{c}–dependent differences in cytokine production or glial activation *in vivo* in neonatal or weanling mice. Collectively, our data demonstrate that the neuroinflammatory response to TLR stimulation is developmentally regulated in young mice, although independent of PrP^{c} expression.

ACKNOWLEDGMENTS

I would like to start by thanking my advisor, Dr. Byron Caughey, for welcoming me into his lab, and for his guidance, encouragement, and giving me the freedom to explore new projects. I would also like to thank Dr. Karin Peterson for her assistance and invaluable insight. Thank you to my other committee members for taking the time to meet over the years, and for providing valuable input and discussion. I would like to thank former and current members of the Caughey and Peterson labs for your assistance, patience, and for creating such an enjoyable work environment. I would also like to thank DBS faculty and staff, who have always been helpful and welcoming.

I would especially like to thank my husband, Kevin, for his unconditional support and love, for his patience, flexibility and willingness to move to rural Montana, where there are no fine dining restaurants. Thank you to my parents and my sister, who have always believed in me and supported my every endeavor, no matter how unexpected. I would like to thank my little boys, Jack and Caleb, who inspire me and fill me with endless joy. Lastly, I would like to thank the many wonderful friends I have made here in Montana.

TABLE OF CONTENTS

LIST OF TABLES

261

LIST OF FIGURES

CHAPTER ONE

INTRODUCTION

Cells of the central nervous system

Neurons, astrocytes and oligodendrocytes in the central nervous system (CNS) arise from a common neuroepithelial progenitor cell. In contrast, microglia, the other prominent CNS cell type, are of myeloid origin. In humans, neurons constitute about half of the brain's cells (Azevedo et al., 2009; Lent et al., 2012). Glial cells—oligodendrocytes, astrocytes, and microglia largely account for the rest of the brain's cells, with a small percentage being epithelial and endothelial cells. In the human cortex, which is responsible for higher brain function, approximately 75% of glial cells are oligodendrocytes, about 20% are astrocytes and 5% are microglia (Pelvig et al., 2008). Despite accounting for a relatively small percentage of the brain's cells, astrocytes and microglia perform critical roles during development, disease and maintenance of homeostatic conditions. The percentage of each cell type in the rodent brain is not as well studied.

Neurons are highly specialized cells that transmit and accept electrical impulses and neurotransmitters. Neurotransmission occurs at specialized cellular junctions called synapses. Most neurons are terminally differentiated and generation of new neurons from neuroprogenitor cells is limited in adults. In contrast with most tissues, which undergo regular cellular turnover, neurons exist for the lifetime of the animal. Thus, one of the main functions of microglia and astrocytes is to protect neurons and aid their recovery from damage and disease.

Oligodendrocytes produce myelin, which sheaths neuronal axons, allowing rapid transmittance of impulses from one neuron to another. In the peripheral nervous system, this role is filled by Schwann cells. Myelination is absolutely essential for proper nervous system function in vertebrates.

Astrocytic processes envelope neurological synapses and rapidly take up excess neurotransmitters after neurotransmission (Danbolt, 2001). Prolonged exposure of neurons to neurotransmitters quickly leads to neurotoxicity (Rosenberg and Aizenman, 1989). Astrocytes also promote neuronal health by producing neurotrophic factors (Airaksinen and Saarma, 2002; Petrova et al., 2003; Rudge et al., 1995). Astrocytes are a critical part of the blood-brain-barrier (BBB) (Pekny et al., 1998; Wolburg and Lippoldt, 2002). Astrocytic endfeet are the primary component of the glia limitans, which separates the perivascular space from the brain parenchyma, or tissue proper (Bechmann et al., 2007). Although not considered an immune cell, astrocytes can produce inflammatory mediators, including cytokines and chemokines, in response to infection and damage (Bolin et al., 2005; Butchi et al., 2008; Butchi et al., 2010).

Microglia are the primary immune sentinels of the CNS. In addition to responding to pathogens and promoting inflammation, microglia clear cellular debris, and release trophic and anti-inflammatory factors that resolve the inflammatory response (Bessis et al., 2007; Prinz et al., 2011; Saijo and Glass, 2011). Microglia are involved in CNS development. They promote neurogenesis and synaptogenesis (Roumier et al., 2004; Sierra et al., 2010). Microglia also regulate synaptic pruning and programmed cell death of excess neurons (Frade and Barde, 1998; Paolicelli et al., 2011; Stevens et al., 2007; Wakselman et al., 2008).

The neonatal immune system

In some respects, the neonatal immune response is immature when compared with its adult counterpart. For example, immunological memory is not yet developed. However, in many ways the neonatal immune system is not immature as much as it is responding to the unique demands of its environment. At birth neonates are moving from a sterile intrauterine environment to one in which microbes, both pathogenic and commensal, are ubiquitous (Levy, 2007). The skin and gut, being subject to immediate colonization after birth, display a distinct immune response that balances the risk of infection with the danger of responding too strongly to commensal microbes (Dorschner et al., 2003; Lotz et al., 2006; Tollin et al., 2005). In the blood of neonates, some acute phase proteins are heightened in response to the mild hypoxia that results from normal labor and delivery (Jokic et al., 2000; Levy et al., 2006a). As a final example of the unique demands placed on the neonatal immune system, many inflammatory proteins have additional functions in neurological development. Complement proteins mediate neurogenesis and migration of neuroprogenitors to their proper location (Rutkowski et al., 2010). The cytokine IL-6 promotes neurite growth *in vitro*. Many immune molecules and cells are developmentally regulated during the period surrounding birth. In many tissues, neonatal immune stimulation can have consequences that differ from other ages (Chelvarajan et al., 2007; Ferret-Bernard et al.; Lotz et al., 2006).

Origins of CNS myeloid cell populations

Macrophages are highly heterogeneous cells that reside in every tissue in the body, their precise functions and capabilities dictated by the tissue they inhabit (Murray and Wynn,

2011). Tissue-specific macrophages derive from multiple origins (Schulz et al., 2012). Early in fetal development, a portion of the tissue-specific macrophage populations arise from extra-embryonic yolk sac macrophages (Ginhoux et al., 2010; Schulz et al., 2012). Later in development, hematopoietic stem cells (HSCs) give rise to myeloid progenitors (MPs). MPs can differentiate into monocytes and tissue macrophages. Monocytes circulating in the blood may also enter tissues and differentiate into macrophages (Auffray et al., 2007). Thus, tissue-specific macrophages may originate from yolk sac macrophages, HSCs, and blood monocytes.

In the CNS, cells of myeloid origin include microglia and macrophages. CNS macrophages reside within the perivasculature, meninges and choroid plexus. Resident macrophages derive from, and are regularly replenished by, blood monocytes (Bechmann et al., 2001; Chinnery et al., 2010). Microglia are the only CNS myeloid cells that reside beyond the blood brain barrier (BBB) in the brain parenchyma. Microglia probably differentiate from yolk sac macrophages and HSCs, although the precise contribution of each precursor to the microglial population is currently a matter of debate (Ginhoux et al., 2010; Samokhvalov et al., 2007; Schulz et al., 2012). In mice, the microglial population increases sixteen-fold during the first two post-natal weeks (Alliot et al., 1999). These new microglia derive from dividing resident microglia (Ginhoux et al., 2010). Microglia are one of the few tissue macrophage populations replenished through self-renewal and not blood-derived monocytes.

CNS myeloid cell functionality

Research has demonstrated important functional differences between the populations of CNS myeloid cells (El Khoury et al., 2007; Mildner et al., 2011; Simard et al., 2006).

Parenchymal microglia differ from resident macrophages in several ways. In addition to deriving, at least partially, from a different progenitor cell and being replenished by self-renewal, microglia express different patterns of cell surface markers than other CNS myeloid cells (Ransohoff and Cardona, 2010). Immune cell markers are frequently expressed at lower levels on microglia. For example, microglia express little MHC class II, which is in line with their reduced ability to present antigen. In contrast, resident macrophages are able to present antigens to T cells that have been previously activated in peripheral tissues (Hickey and Kimura, 1988). Unlike other myeloid cells, microglia express ion channels, neurotransmitter receptors, and a greater range of purinoceptors (Färber and Kettenmann, 2005; Färber and Kettenmann, 2006; Hanisch and Kettenmann, 2007).

Blood monocytes may be stimulated to enter the brain parenchyma under experimental conditions (Mildner et al., 2007; Simard et al., 2006). When this occurs they can differentiate into microglia-like cells. However, they have different functional capabilities than microglia. For example, blood monocytes are better able to phagocytize Aβ fibrils (El Khoury et al., 2007). Whether blood monocytes are able to enter the brain parenchyma in human neurological conditions is unclear.

Neonatal microglia are thought to exist in an elevated activation state due to their developmental roles in this time period (Bilbo and Schwarz, 2009). Whether neonatal CNS macrophages also have specific developmental roles that would influence their activation state in neonates is unknown. Thus, microglia, as well as resident macrophages, may contribute to age-dependent differences in responses to immune stimulation. It is also unclear whether age-associated differences in recruitment of blood monocytes occur after TLR stimulation (Levy,

2007). While neonatal monocytes are known to respond differently than adult monocytes in peripheral responses to immune stimulation, they may also behave differently than resident microglia (Kollmann et al., 2009; Nguyen et al., 2010).

Surveillant and activated microglia

Under normal conditions, microglia are often described as "resting" or "quiescent". These descriptions, which imply a degree of dormancy, are based on physical appearance and do not give an accurate indication of the cells' activity level. It is more accurate to refer to resting microglia as surveillant because they are active, but not in the proinflammatory way that is traditionally meant when microglia are described as active (Prinz et al., 2011). Surveillant microglia have a ramified phenotype, with many fine processes that are highly motile, constantly surveying their local environment for signs of disease or damage (Nimmerjahn et al., 2005). Their physical appearance is very different from "activated" microglia, which have retracted their processes and taken on an amoeboid appearance that is more similar to a typical macrophage. Amoeboid microglia have generally been activated by inflammation, produce large amounts of inflammatory molecules, and are highly phagocytic (Saijo and Glass, 2011). The switch from surveillant to amoeboid is not an all or nothing phenomenon. Activated microglial phenotypes often exist as gradations between ramified and amoeboid (Graeber, 2010). Complete retraction of processes into a fully amoeboid morphology is rare. Healthy microglia return to a ramified phenotype once the situation requiring their activation is resolved. Neonatal microglia have an amoeboid morphology, which is correlated with increased phagocytic ability (Fig 1.1). In contrast, weanling microglia have a ramified

phenotype with many fine processes. When microglia become over-activated by excessive inflammatory stimulation, they may be unable to transition to a surveillant state and instead chronically produce pro-inflammatory mediators, leading to significant tissue damage over time. This may occur in immune-stimulated neonatal microglia (Bilbo and Schwarz, 2009). Chronically over-activated microglia are not amoeboid but instead have several extremely thick processes (Bilbo and Schwarz, 2009). Additionally, acute encephalitic conditions can lead to activated microglia possessing a long and slender rod cell phenotype (Ackman et al., 2006; Graeber, 2010).

Toll-like receptors

Toll-like receptors (TLRs) are pattern recognition receptors (PRRs), a large and diverse family of proteins united in their ability to recognize pathogen-associated molecular patterns (PAMPs). PRR binding is often the first step in immune recognition and response to an invading pathogen. TLR stimulation activates production of cytokines and anti-microbial effector molecules (West et al., 2006). TLRs are prominently expressed on immune cells such as monocytes, macrophages and DCs (West et al., 2006). In the central nervous system (CNS), they are expressed on astrocytes and microglia and, to a lesser extent, neurons (McKimmie and Fazakerley, 2005). TLRs localize to either the plasma membrane or endosomal membranes (Barton and Kagan, 2009; Kagan et al., 2008). Plasma membrane-associated TLRs, such as TLR4, recognize components of bacterial outer membranes and viral envelopes. Endosomal TLRs, such as TLR9, recognize microbial nucleic acids. We have focused on TLR4 and TLR9 stimulation with their ligands, lipopolysaccharide (LPS) and CpG-rich oligonucleotides (CpG), respectively.

We chose TLRs 4 and 9 due to their potential to interact with the prion protein. This will be discussed further in chapter three.

TLR signaling

TLR4 signaling is often used as a model for TLR signaling because it is well-studied and TLR4 signals from both the plasma membrane and endosome (Fig 1.2). TLR4 stimulation leads to the production of pro-inflammatory cytokines through activation of several intracellular signaling pathways (Barton and Kagan, 2009; Ostuni et al., 2010). Upon ligand binding at the plasma membrane, TLR4 signaling leads to an initial activation of the transcription factors NFκB and AP-1. The TLR4 complex is then endocytosed. From the endosome, TLR4 stimulates a second round of NFκB and AP-1 activation, as well as activation of the transcription factor IRF3. The first round of NFκB and AP-1 activation is mediated by the adaptor MyD88. The second round of TLR4-mediated transcription factor activation is mediated by TRIF rather than MyD88. NFκB and AP-1 activation leads to the production of pro-inflammatory cytokines, with the exception of the type I interferons, which are induced by IRF3.

TLR signaling is complex; the precise outcomes of ligand binding are influenced by numerous intracellular adaptor proteins, which are modulated by the host cell's differentiation and activation state. Two features that guide TLR signaling are membrane phospholipid composition and polyubiquitin scaffolds. Membrane phospholipids control the cellular location of the TLR4 complex and provide binding sites for necessary intracellular adaptors (Kagan and Medzhitov, 2006; Triantafilou et al., 2004). Polyubiquitin scaffolds provide docking sites for

intracellular proteins critical to the activation of downstream transcription factors (Deng et al., 2000; Fan et al., 2010).

Recognition of LPS by TLR4 is aided by several accessory proteins. The secreted LPS binding protein (LBP) sequesters LPS monomers and presents them to CD14, which has an extremely high affinity for LPS (Gioannini et al., 2004; Wright et al., 1990). At the plasma membrane, CD14 transfers LPS to the TLR4:MD-2 complex (Gioannini et al., 2004). Concurrent with TLR4:MD-2 stimulation, CD14 interacts with CD11b (CR3) (Zarewych et al., 1996). CD11b may promote synthesis of the membrane lipid phosphatidylinositol 4,5-bisphosphate (PIP_2) by the kinase PI(4)P5K (Hynes, 2002; Ostuni et al., 2010). In response to TLR4 ligand binding, both PIP_2 and TLR4 are concentrated in lipid rafts. TLR4 is not normally found in lipid rafts but must be recruited and retained there for effective TLR signaling (Triantafilou et al., 2004).

On the cytosolic side of the plasma membrane, the sorting adaptor TIRAP is recruited by the relatively high concentrations of PIP_2 (Kagan and Medzhitov, 2006). TIRAP engages the signaling adaptor MyD88, which interacts sequentially with the IRAK effector proteins, leading to recruitment of the E3 ubiquitin ligase TRAF6 (Cao et al., 1996; Kagan and Medzhitov, 2006; Kawagoe et al., 2008; Suzuki et al., 2002). TRAF6 self polyubiquitination serves as a docking point for the IKK regulatory complex and the kinase TAK1 (Deng et al., 2000; Fan et al., 2010). Activated IKK promotes NFκB activation by phosphorylating IκB, leading to its degradation. NFκB, which is normally sequestered in the cytosol by IκB, is now able to translocate into the nucleus and induce pro-inflammatory gene expression (Doyle and O'Neill, 2006; Li and Stark, 2002). During inflammatory signaling, AP-1 activation is primarily regulated by the nuclear MAP kinases (MAPKs) p38, JNK, and ERK (Ostuni et al., 2010). Nuclear MAPK activation is connected

462 to the TLR signaling pathway by TAK1. As an activator of both IKK and the MAPKs p38 and JNK,
463 TAK1 is the branching point at which AP-1 activation diverges from NFκB activation in the
464 MyD88-dependent pathway (Sato et al., 2005; Wang et al., 2001).

465 The above events described for MyD88-dependent signaling from the plasma
466 membrane occur within 15-30 minutes of stimulation (Husebye et al., 2006; Kagan et al., 2008).
467 After this, the concentration of PIP_2 in the plasma membrane declines significantly, leading to
468 endocytosis of the TLR4 signaling complex (Botelho et al., 2000; Ostuni et al., 2010). Decreased
469 PIP_2 also results in TIRAP dissociating from the complex. With TIRAP gone, another sorting
470 adaptor, TRAM, is able to bind the intracellular domain of TLR4 (Yamamoto et al., 2003). TRAM
471 recruits the signaling adaptor TRIF, which engages the kinase RIP-1 (Meylan et al., 2004). From
472 this point on, the events leading to late NFκB signaling are similar to those described for early
473 NFκB signaling.

474 To activate IRF3, the signaling adaptor TRIF interacts with TRAF3, whose self-
475 ubiquitination leads to IRF3 activation (Hacker et al., 2006). Under basal conditions, IRF3 is a
476 cytosolic monomer but activating phosphorylation triggers dimerization and nuclear
477 translocation, permitting induction of the type I interferons, IFN-α and IFN-β (Honda et al.,
478 2006).

479 TLR4 signaling ends when the endosome matures. At this time the TRAM splice variant,
480 TAG, displaces TRIF in binding to TRAM, leading to endolysosomal degradation of TLR4
481 (Husebye et al., 2006; Palsson-McDermott et al., 2009).

482 TLR9 recognizes bacterial and viral unmethylated CpG DNA. In unstimulated cells, TLR9
483 is found in the endoplasmic reticulum (ER) (Latz et al., 2004; Leifer et al., 2004). In response to

immune stimulation, the sorting protein UNC93B1 transports inactive TLR9 from the ER to the endolysosomal pathway (Kim et al., 2008; Tabeta et al., 2006). Upon entering the endolysosome, TLR9 is proteolytically cleaved (Ewald et al., 2008; Park et al., 2008). Notably, full-length TLR9 can bind CpG DNA but cannot bind the intracellular signaling adaptor protein MYD88 (Barton and Kagan, 2009; Ewald et al., 2008). Therefore, proteolytic cleavage regulates the ability of TLR9 to transmit immune stimulatory signaling. Upon ligand binding and proteolytic cleavage, TLR9 binds MYD88, which leads to downstream signaling similar to what was previously described for endosomal TLR4 signaling (Fig 1.3) (Barton and Kagan, 2009; West et al., 2006). TLR9 signaling culminates in induction of cytokine genes, including the interferons, and other inflammatory mediators.

TLR signaling in development

Tlr4 and *Tlr9* mRNA expression are developmentally regulated in the murine brain. In mice, brain *Tlr9* expression increased from embryonic time points through adulthood (Kaul et al., 2012). In rats, brain *Tlr4* mRNA expression increased from birth through adulthood (Ortega et al., 2011). However, TLR4 protein levels in the rat brain remained stable over the same time period (Ortega et al., 2011). Among peripheral immune populations, *Tlr9* mRNA expression levels in human adult and cord blood monocytes were similar (Dasari et al., 2011), as were TLR9 protein levels on human plasmacytoid dendritic cells from adult peripheral blood and cord blood (Danis et al., 2008). Two human studies found no difference in monocytic *Tlr4* expression between neonates and adults (Dasari et al., 2011; Levy et al., 2004). However, in young mice

505 (9-12 days old), macrophage TLR4 expression was decreased when compared with expression
506 in adult macrophages (Chelvarajan et al., 2004).

507 A comprehensive analysis of TLR signaling pathway function in neonatal cells is
508 complicated by the fact that studies are often done in different species, using different cell
509 types and methods of harvesting cells, and different TLR ligands. Despite this, some general
510 patterns are emerging: Cord blood monocytes have reduced MyD88 expression, p38
511 phosphorylation, and IRF3 activation when TLR stimulation leads to reduced cytokine output
512 (Aksoy, 2006; Levy et al., 2004; Sadeghi et al., 2007; Yan et al., 2004). Enhanced cytokine
513 production by cord blood monocytes is associated with increased p38 phosphorylation and IκB
514 degradation (Levy et al., 2006b).

515

516 **The neonatal TLR response is stimulus- and cell type-specific**

517 Several cytokines, including IL-6 and IL-10, are elevated in neonates in numerous
518 conditions and cell types outside the CNS (Angelone et al., 2006; Chelvarajan et al., 2004;
519 Nguyen et al., 2010). In contrast, other cytokines, such as IL-1b, IL-12, TNF and the interferons,
520 are often expressed at reduced levels in neonatal immune cells that are isolated from
521 peripheral blood and tissues and stimulated with TLR agonists (Belderbos et al., 2009;
522 Chelvarajan et al., 2004; Islam et al., 2012b; Marodi, 2006). However, research is increasingly
523 showing that the neonatal cytokine response to TLR stimulation differs depending on the tissue
524 and cell type stimulated, as well as the TLR ligand. For example, in whole human blood
525 stimulated with LPS, production of IL-6, IL-8 and IL-10 was heightened in neonates when
526 compared with adult blood (Nguyen et al., 2010). In comparison, when the TLR9 ligand CpG

was used, in addition to IL-6, IL-8 and IL-10, IL-1β was also elevated (Nguyen et al., 2010). In sheep mesenteric lymph nodes, stimulation of TLR8 was able to potently overcome inhibition of T_h1-promoting responses to produce higher amounts of IL-12 and IFNγ in neonates than adults (Ferret-Bernard et al.). Stimulation with bacterial pathogens also leads to age-dependent cytokine responses in peripheral neonatal immune populations (Chelvarajan et al., 2007; Levy et al., 2006a).

Prion protein and transmissible spongiform encephalopathies (TSEs)

TSEs are a group of fatal neurodegenerative diseases that includes diseases of infectious, genetic, sporadic and iatrogenic origin (Caughey et al., 2009). TSE pathology and transmissibility requires expression of the endogenous prion protein (Bueler et al., 1993). In TSEs, the prion protein misfolds from its endogenous and non-pathogenic form, PrP^{c}, into a pathogenic form, PrP^{Sc}, whose name derives from the prototypical TSE, ovine scrapie. Conformationally, PrP^{c} has higher α-helical content while PrP^{Sc} contains reduced α-helix and increased levels of β-sheets. Although TSE disease progression has been closely studied, the underlying pathological causes remain unclear. Since misfolding of PrP^{c} into PrP^{Sc} may lead to subversion of normal function, knowledge of the normal function(s) of PrP^{c} may enlighten our understanding of TSE pathology.

PrP^{c} is a 254 amino acid protein that is glycosylated and primarily bound to the plasma membrane through a glycophosphatidyl inositol (GPI) anchor. Despite PrP^{c}'s apparent involvement in an array of physiological processes, its precise function remains poorly defined (Linden et al., 2008). Some proposed functions, such as adhesion and differentiation, are

applicable to many cell types and may reflect the near ubiquitous distribution of PrP^c. Others, such as mitigating excitotoxicity and acting as a scavenger receptor (Khosravani et al., 2008; Marc et al., 2007; Sunyach et al., 2003), could reflect functions in specific cell types like neurons and microglia. PrP^c functions associated with immunity and development are discussed in chapter three.

TLR signaling influences the TSE incubation period

Mice deficient in TLR4 signaling have a shortened scrapie incubation period (Spinner et al., 2008). Notably, MyD88 deficiency does not impact the scrapie incubation period (Prinz et al., 2003). This implies the MyD88-independent, TRIF-dependent TLR signaling pathway may influence scrapie disease progression. In agreement with this, a recently published paper demonstrates a shortened scrapie incubation period in mice lacking IRF3, a critical transcription factor in MyD88-independent signaling (Ishibashi et al., 2012). IRF3 activates many immune-responsive genes, including type I interferons. However, stimulation with interferons does not influence the scrapie incubation period (Field et al., 1969; Gresser et al., 1983). In addition, inoculation with the TLR9 ligand unmethylated CpG ODNs prolongs the scrapie incubation period (Sethi et al., 2002).

Overview

In mice, the neonatal brain is much more sensitive to infection than the weanling brain. Therefore, I hypothesized that the neuroinflammatory response would be altered in an age dependent manner in mice. To model neuroinflammation, I injected neonatal and weanling

mice intracerebrally (IC) with either the TLR4 agonist LPS or the TLR9 agonist CpG ODN. I aimed to compare expression of some neuroinflammatory mediators, including a subset of cytokines, at each age in order to gain insight into how the immune response changes with age. I was particularly interested in examining the activation profiles of microglia, as they are important mediators of the inflammatory response in the brain and their activation may be influenced by age. Therefore, for my second aim, I compared expression of activating and inhibitory markers on neonatal and weanling mice. Lastly, I aimed to determine whether PrP^{c} mediates neuroinflammation in an age-dependent manner, since PrP^{c} expression increases with age and has previously been associated with various immunological functions.

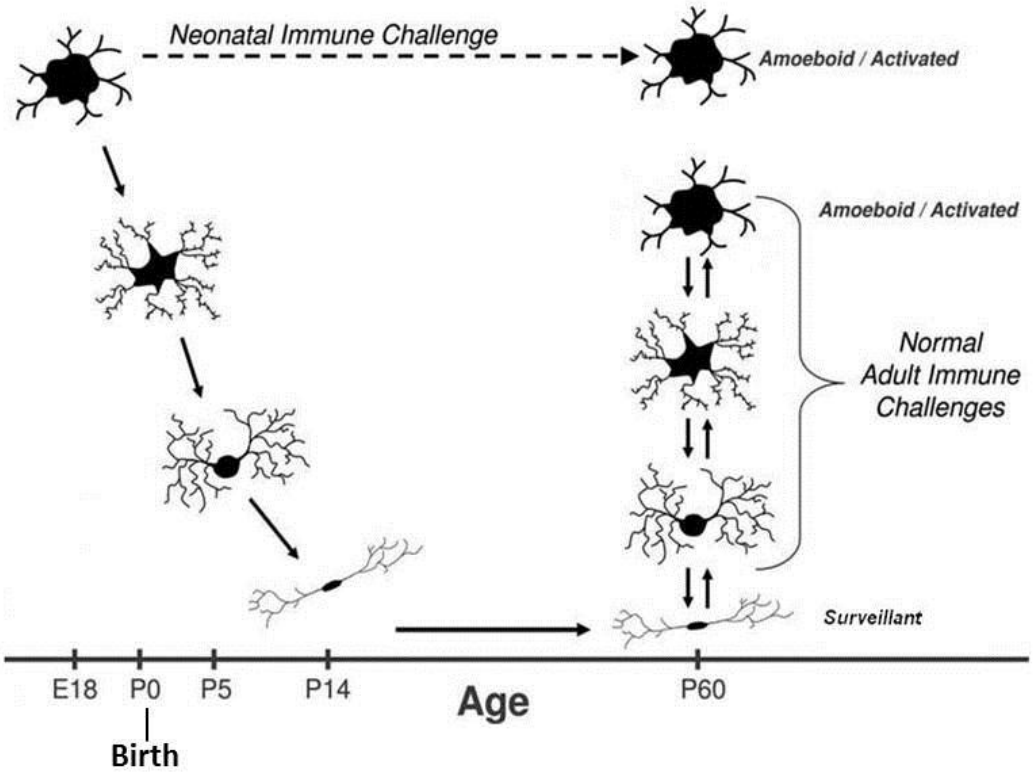

Figure 1.1 Microglial morphology is influenced by age and previous immune challenge.

Summary of how microglial phenotype changes with age and in response to immune challenge in murine models of development and disease. Time line shown is for mouse development. *Modified from Bilbo & Schwartz, Frontiers Behav. Neuro., 2009.*

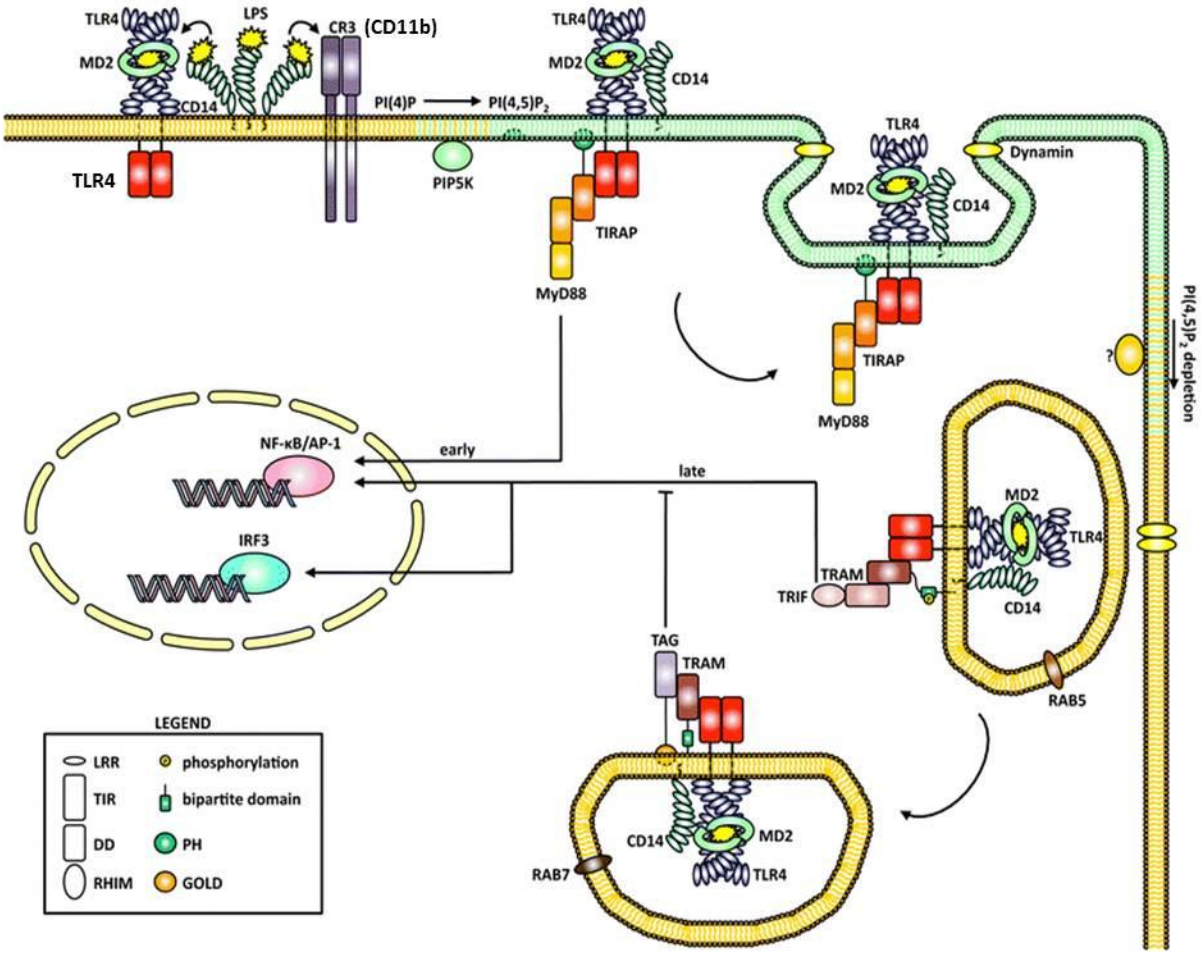

592

593 **Figure 1.2 Activated TLR4 signals from the plasma membrane and the endosome.** Ligand

594 binding stimulates recruitment of TLR4 into lipid rafts, where early TLR signaling is initiated.

595 Upon endocytosis, TLR4 activates late TLR signaling from the endosome. *From Ostuni et. al.,*

596 *Cell. Mol. Life Sci., 2010.*

597

598

599

600

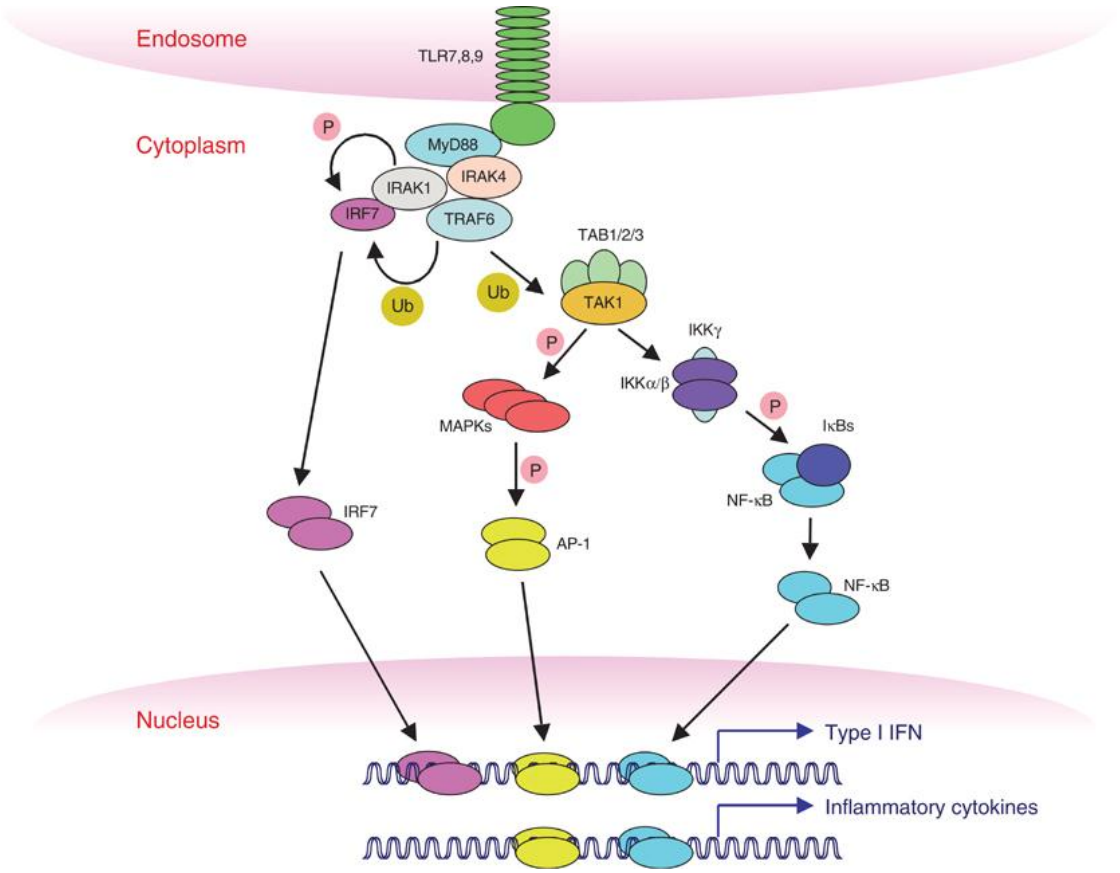

Figure 1.3 Activated TLR9 signaling from the endosome. Ligand binding and proteolytic cleavage lead to TLR9 signaling from the endolysosomal pathway. *From Kawai & Akira, Cell Death & Differentiation.*

CHAPTER TWO

SUPPORTING DATA FOR ANALYSIS OF AGE-ASSOCIATED CHANGES IN NEUROINFLAMMATORY RESPONSE

Background studies on influence of age and agonist concentration on *in vivo* cytokine production

In previous studies using the IRW mouse strain, a strong neuroinflammatory response was observed in neonatal mice after intracerebral (IC) inoculation with 1 μg LPS per gram of body weight (Butchi et al., 2008). To determine the best concentration of LPS to use in neonatal C57Bl/10 mice for IC inoculations, we tested 0.25, 0.5 and 1 μg LPS per gram of body weight. Cytokine protein levels in brain tissue were measured using a multiplex bead assay. Representative data are shown in Figure 2.1. One microgram LPS per gram of body weight was fatal to nearly fifty percent of C57Bl/10 mice (Fig 2.1A). We observed a similar mortality rate in C57Bl/10 $PrP^{-/-}$ mice (data not shown). With the exception of IL-6 ($p=0.0058$), the cytokine response to 0.5 μg LPS per gram body weight did not differ significantly from the cytokine response to 1 μg LPS per gram of body weight (Fig 2.1B). However, at 0.5 μg LPS per gram body weight, all mice survived. Therefore, we used 0.5 μg LPS per gram body weight in all future treatments. We also halved the CpG concentration that had been used in IRW mice to 0.125 μg CpG (40 picomole) per gram of body weight, in case the C57Bl/10 mice were also more reactive to this TLR ligand.

To better understand how the cytokine response to TLR 4 and 9 stimulation develops with age, we also examined IL-6 and CCL2 production in 10 and 42 day old (d.o.) mice. We chose the 10 d.o. age because susceptibility to Sindbis virus infection of the CNS decreases

dramatically by 11 days of age (Trgovcich et al., 1999). Since 21 d.o. mice are not yet adult, we also examined how the weanling response differs from that of a 42 d.o. adult.

Figure 2.2 shows the IL-6 and CCL2 protein production in response to TLR4 or TLR9 stimulation in 2, 10, 21 and 42 d.o. mice. Although the 2 and 21 d.o. samples were analyzed separately from the 10 and 42 d.o. samples, standards were comparable between experiments. The IL-6 response to TLR4 stimulation consistently declined with age over the time course analyzed. The CCL2 response to TLR4 stimulation showed an overall decline with age, although CCL2 levels were slightly higher in 21 d.o. mice than 10 d.o. mice. CCL2 production in response to TLR9 stimulation dramatically decreased in mice beyond the neonatal time period and remained low. In contrast, IL-6 production decreased from 2 to 21 days of age but sharply increased in 42 d.o. mice. Collectively, these data suggest that production of IL-6 and CCL2 depends not only on age, but also on the type of immune stimulant.

Developing a flow cytometry protocol for analysis of LPS-stimulated CNS immune populations

Many, if not all, cell types in the central nervous system can produce cytokines. However, we expected microglia and astrocytes to be important cytokine-producing cells in the brain during the response to TLR4 stimulation (discussed in Chapters 1 and 2). Initially, we planned to use flow cytometry to characterize and compare the activation states of neonatal and weanling microglia and astrocytes. A major hurdle to flow cytometric analysis of brain cell populations *ex vivo* is myelin. Contaminating myelin ovoids can be similar in size and shape to cells, making it impossible to gate them out based on size. Myelin can also mask epitopes and

lead to non-specific antibody binding. Myelination in the brain increases with age, so it is a bigger problem in weanlings than in neonates.

To remove the myelin from our samples, we initially tried using Miltenyi myelin depletion columns. With these columns, brain homogenates are pre-incubated with a myelin-specific antibody and then placed on the myelin depletion columns. Myelin should be retained on the column while cells are able to flow through. We encountered obstacles to the effective use of these columns for preparing samples for flow cytometry. First, the myelin removal columns did not satisfactorily remove non-myelin debris from the samples, which still allowed a high degree of non-specific antibody binding. However, the most challenging problem we faced when using the myelin depletion columns was the apparent loss of certain cell types, including microglia, in LPS-stimulated flow cytometry samples (Fig 2.3). This was observed in repeated experiments using mice of both ages. Representative samples pre-incubated with an antibody for CD11b are shown in Figure 2.3. Similar results were observed using antibodies targeting CD45 and CD80 (data not shown). The left graph shows the level of background fluorescence in an unstained control. In the center graph, $CD11b^+$ cells in PBS-treated samples are circled. The right graph shows the reduced number of $CD11b^+$ cells observed in LPS-treated samples.

We then tried isolating CNS immune cells using Percoll gradients, and with additional trituration, instead of myelin depletion columns. Percoll gradients are often used to isolate immune cells from other CNS components (Ford et al., 1995; Gelderblom et al., 2009; Mausberg et al., 2009; Peterson et al., 2006). We did not initially use Percoll gradients because we planned to examine both microglial and astrocytic populations. Using a 0/30/70% Percoll gradient, astrocytes primarily fractionate with myelin at the 0/30% interface [(Peterson et al.,

2006) and Fig 2.4]. Therefore, these Percoll gradients are not a suitable method for isolating astrocytes for flow cytometric analysis. As discussed in Chapter 2, the fraction at the 30/70% interface is enriched for microglia and other immune populations.

Figure 2.5 shows samples prepared either using myelin depletion columns (left) or Percoll gradients (right). Representative samples from neonatal (top) and weanling (bottom) uninoculated mice are shown. The region where cells are expected to be is circled on the graphs (solid line). Samples purified on myelin depletion columns contained more debris, as evidenced by the large number of events with high side scatter but little forward scatter. We also noted fewer cells in weanling samples (bottom) than neonatal samples (top).

Figure 2.6 compares CD45 and F4/80 staining on untreated cells isolated using either myelin depletion columns (A, C, E) or Percoll gradients (B, D, F). Cell gates for these samples are shown in Figure 2.5. Events within the cell gate of (A) myelin-depleted, or (B) Percoll gradient fractionated, neonatal samples are shown. (C) and (D) show the same samples, except Aqua Live/Dead stain was used to gate specifically on live cells. Comparing (A) with (C) demonstrates that gating specifically on live cells markedly reduced the noise in samples prepared using myelin depletion columns. In contrast, comparing (B) with (D) shows that live cell gating does not greatly change the plots of samples prepared using Percoll gradients. These results suggest that dead cells and debris are more effectively separated from CNS immune cells using Percoll gradients than myelin depletion columns. Similar results were observed in weanling samples (data not shown). A comparison of cells within the live cell gate of (E) myelin-depleted, or (F) Percoll gradient fractionated, weanling samples demonstrated that greater numbers of weanling microglia were isolated when samples were prepared using Percoll gradients.

Microglia are identified as $CD45^{lo}$ $F4/80^{+}$. Collectively, these results suggested that isolation and detection of microglia was improved by the use of Percoll gradients, rather than myelin depletion columns. In further experiments, Percoll gradients were used to isolate CNS immune cells.

While the use of Percoll gradients and trituration improved our isolation of microglia from untreated brain tissue, we still needed to improve recovery of LPS-stimulated CNS immune cells, particularly from weanling tissues. To address this, we tried enzymatically digesting the tissue. There are many published reports of successful preparation of CNS cells for flow cytometry using enzymatic digestion (Ford et al., 1995; Gelderblom et al., 2009; Gottfried-Blackmore et al., 2009; Mausberg et al., 2009). We adapted the protocol of Cardona *et al.* because it was developed specifically for isolation of microglia for both flow cytometry and RNA analysis (Cardona et al., 2006), which we also planned to do. In this protocol, homogenized brains are incubated with collagenase, dispase and DNase. Collagenase and dispase cleave collagen and fibronectin, respectively, while DNase removes extracellular DNA from lysed cells.

Figure 2.7 demonstrates that enzymatic digestion improved detection of LPS-stimulated CNS immune populations. In this experiment, digested and undigested samples from neonatal and weanling mice, with or without LPS stimulation, were examined. Enzymatic digestion did not markedly alter the detection of neonatal cell populations in untreated mice (A & E). However, in untreated weanling samples, digestion increased the number of microglia detected (C & G, solid line). Surprisingly, without enzymatic digestion, loss of $CD45^{hi}$ cells was not observed in LPS-treated samples (B & D, arrows), as we observed previously (Fig 2.3). The

results of the current experiment suggested that the modifications we previously made, namely the use of Percoll gradients and trituration, were sufficient to improve recovery of LPS-treated populations. However, enzymatic digestion led to additional recovery of $CD45^{hi}$ cells in LPS-treated samples (B & F, D & H, dashed line). Therefore, enzymatic digestion was added to the protocol for future flow cytometry studies.

Flow cytometry on *ex vivo* astrocytes

Although CNS immune cell detection was greatly improved by the use of Percoll gradients, our standard Percoll gradients are not appropriate for recovery of astrocytes for flow cytometry (discussed previously). Figure 2.8 demonstrates typical staining observed with an astrocyte-specific GFAP antibody. The sample in this figure is from a PBS-inoculated neonatal mouse and was prepared using a myelin depletion column. (A) shows staining of $CD11b^+$ cells in this sample. (B) demonstrates $GFAP^+$ staining. (C) contains antibodies for both GFAP and CD11b. Since GFAP and CD11b are found on separate populations, there should be no double-positive staining in (C). No distinct $GFAP^+$ populations are apparent, as there are for CD11b. Thus, GFAP staining may have been non-specific. Similar results were observed in weanling mice and in LPS-treated mice.

Since isolation of CNS immune cells improved when we used a Percoll gradient instead of a myelin depletion column, we attempted to modify our standard Percoll gradient in order to separate astrocytes from myelin. We tried a 0/15/70% gradient, hoping that myelin would stay at 0/15% interface and all cells would be at 15/70% interface. Unfortunately, this did not work (data not shown). We next tried a 0/20/30/70% Percoll gradient. In this gradient myelin was

found at both the 0/20% and 20/30% interfaces (data not shown). In summary, we were not able to find a satisfactory method to separate myelin and debris from $GFAP^+$ astrocyte populations *ex vivo*. Therefore, we limited our *ex vivo* flow cytometry analyses to CNS immune cell populations that could be effectively separated from debris through fractionation at the 30/70% interface of Percoll gradients.

Discussion

We were initially puzzled by the poor detection of CNS immune populations. However, through a number of modifications to our protocol, we were able to substantially recover these populations. The use of Percoll gradients and trituration led to recovery of microglia and a subset of $CD45^{hi}$ immune cells. One reason these cells may have been so challenging to recover is that they are extremely sticky, particularly when activated. They easily bind to one another or are lost during sample preparation through binding to the sides of tubes. The difficulties we initially had may have been due to these cells being non-specifically retained on the myelin depletion columns, a problem that was circumvented by the use of Percoll gradients. The additional trituration may have also assisted in the generation of detectable single cell suspensions.

Microglia are the largest immune population in the brain, so we were quite surprised when enzymatic digestion revealed large populations of $CD45^{hi}$ cells in LPS-treated tissues. Immune stimulation readily recruits peripheral immune populations into perivascular spaces within the blood brain barrier (BBB), although their ability to enter the brain parenchyma is much more limited (Bechmann et al., 2007; Ransohoff and Cardona, 2010). Therefore,

766 enzymatic digestion may be required to sufficiently dissociate the BBB and recover cells within
767 this space. In support of this, Dick *et al.* demonstrated that dissection of the meninges, choroid
768 plexus and ventricles away from the rest of the brain tissue reduced the number of $CD45^{hi}$ cells
769 detected in the brain by five-fold (Dick et al., 1995).
770 In summary, we have optimized a protocol for the efficient isolation of CNS immune
771 populations under both homeostatic and inflammatory conditions. Unfortunately, we were
772 unable to detect astrocytic populations without concomitant non-specific binding to myelin and
773 other debris.
774
775
776
777
778
779
780
781
782
783
784
785
786
787

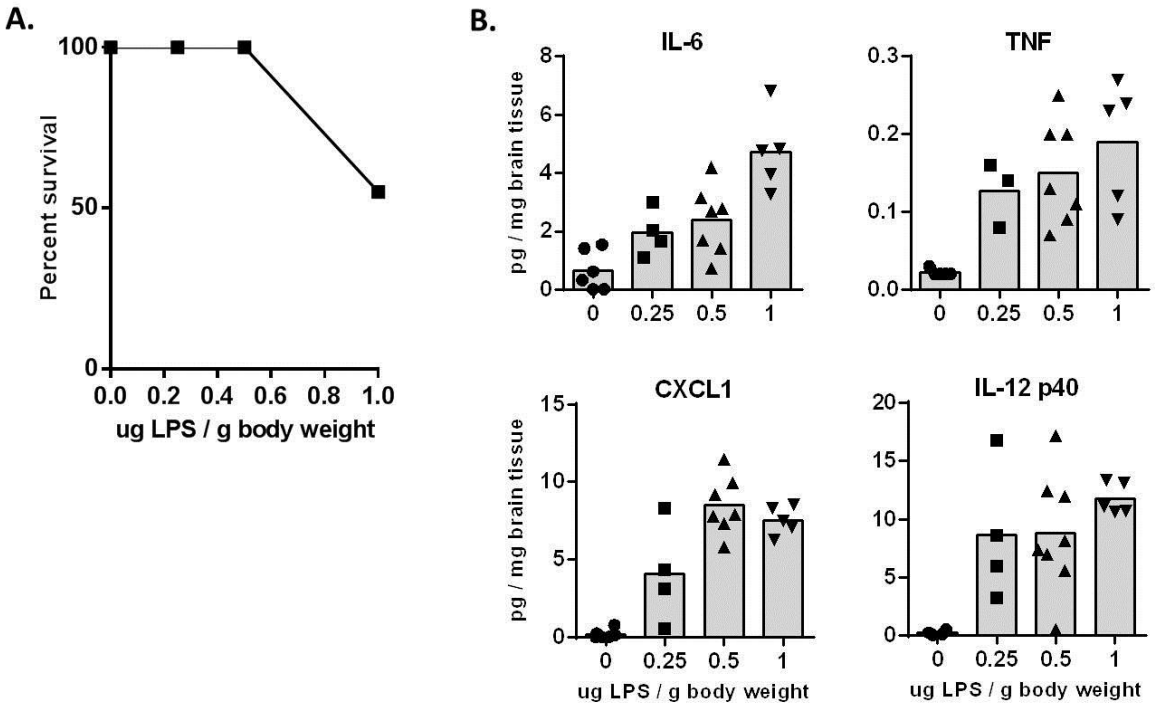

Figure 2.1 Determination of LPS dosage for intracerebral inoculation of neonatal mice. Newborn mice were inoculated IC with 0.25, 0.5 or 1 µg LPS per gram of body weight. **(A)** The highest dosage was fatal for nearly half the mice. n=8-9 per group. **(B)** Cytokine responses in whole brain tissue were measured in a multiplex bead assay at 12 hpi. Representative cytokines are shown here. n=3-8 per group.

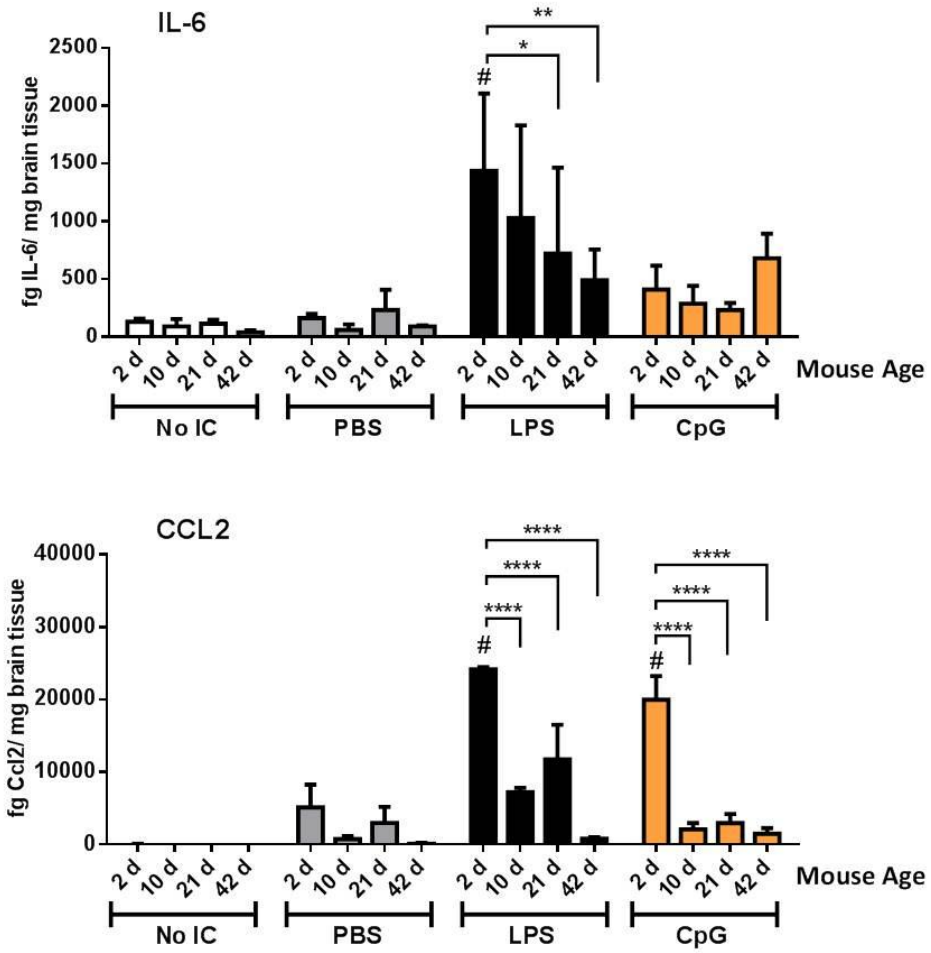

Figure 2.2 Cytokine responses differ with age and TLR agonist. IL-6 and CCL2 levels were measured in 2, 10, 21 and 42 day old brain tissue after IC inoculation with LPS or CpG. Protein concentrations were measured by ELISA and were calculated from in-plate standard curves generated with standards provided by manufacturer. n = 4 mice per group. Data are presented as mean +/- SD. # indicates treatment group contains samples above the dynamic range (based on standard curve). Statistical analysis was completed by two-way analysis of variance with Tukey's multiple comparisons test. Significant age-specific differences are as indicated: *p<0.05, **p<0.01, ***p<0.001, ****p<0.0001

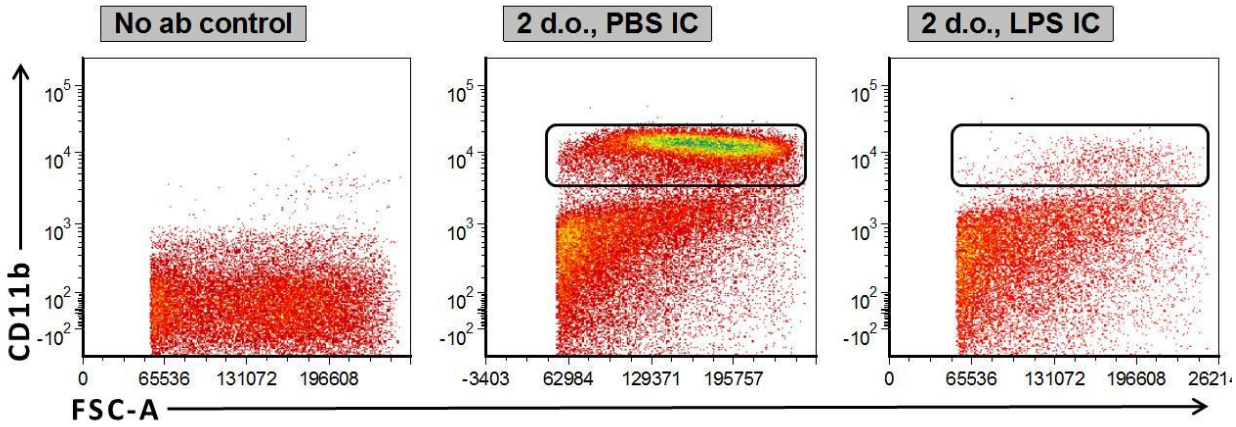

Figure 2.3 LPS-stimulated cells isolated using myelin depletion columns are poorly detected by flow cytometry. CD11b (AF700) staining is plotted against forward scatter for an unstained control, PBS- and LPS-treated neonatal samples. Positive CD11b staining is circled in PBS- and LPS-treated samples.

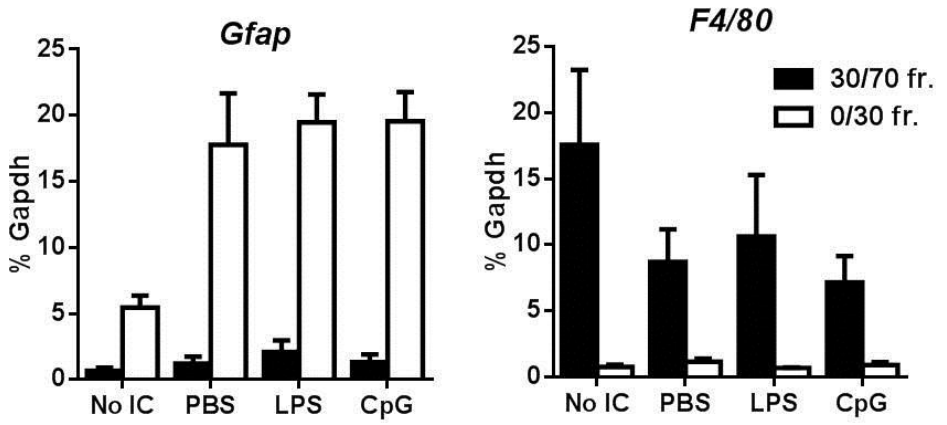

827

828 **Figure 2.4 Enrichment of astrocytic and microglial populations in separate Percoll gradient**

829 **fractions.** Whole brain homogenates were layered over 0/30/70% Percoll gradients. After

830 centrifugation, mRNA expression in the cellular fractions at the 0/30% and the 30/70%

831 interfaces was analyzed by qRT-PCR. **(A)** Expression of the astrocytic marker *Gfap* is detected

832 predominantly in the fraction at the 0/30% Percoll interface. **(B)** Expression of the microglial

833 marker *F4/80* is detected predominantly in the fraction at the 30/70% Percoll interface. Data

834 are presented as mean +/- SD. n = 4-5 per group.

835

836

837

838

839

840

841

842

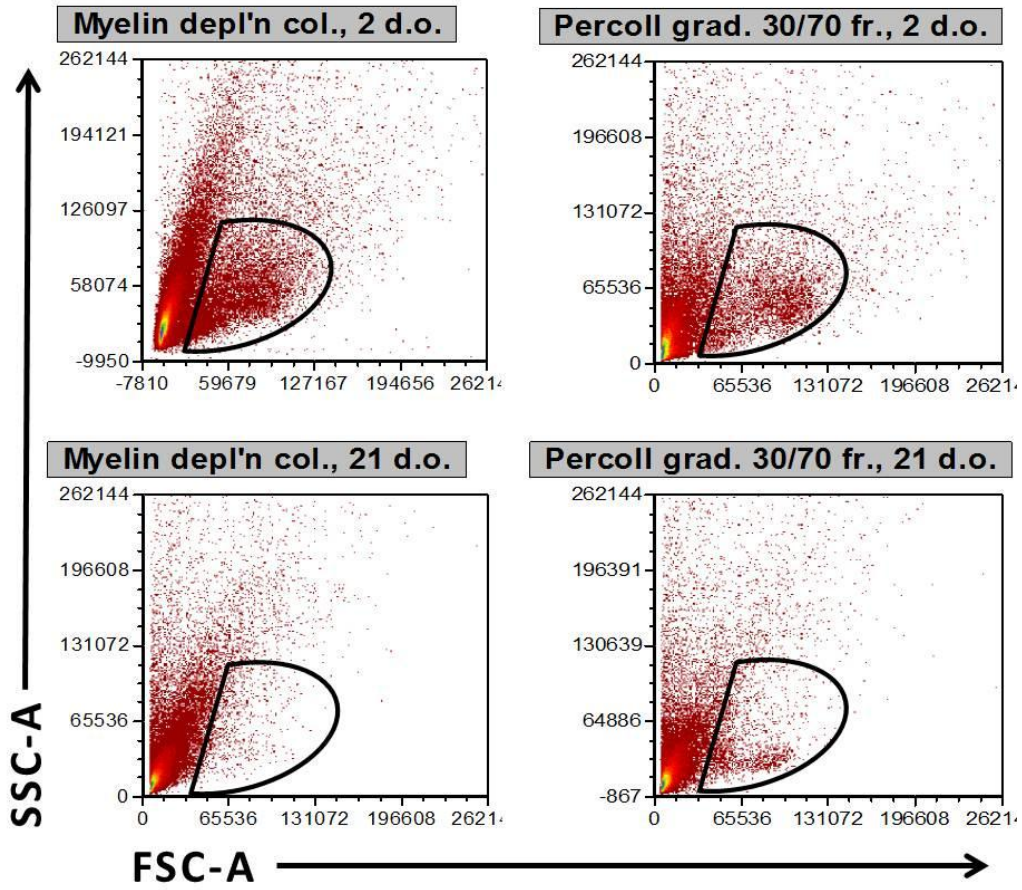

Figure 2.5 Comparison of cell populations isolated using myelin depletion columns or Percoll gradients. Cell density plots of forward scatter versus side scatter are shown for neonatal (top) and weanling (bottom) samples. Samples were prepared for flow cytometry either using myelin depletion columns (left) or Percoll gradients (right). Only the 30/70% fraction of the Percoll gradient, which is enriched for CNS immune cells, is shown. Cell population is outlined (not actual cell gate).

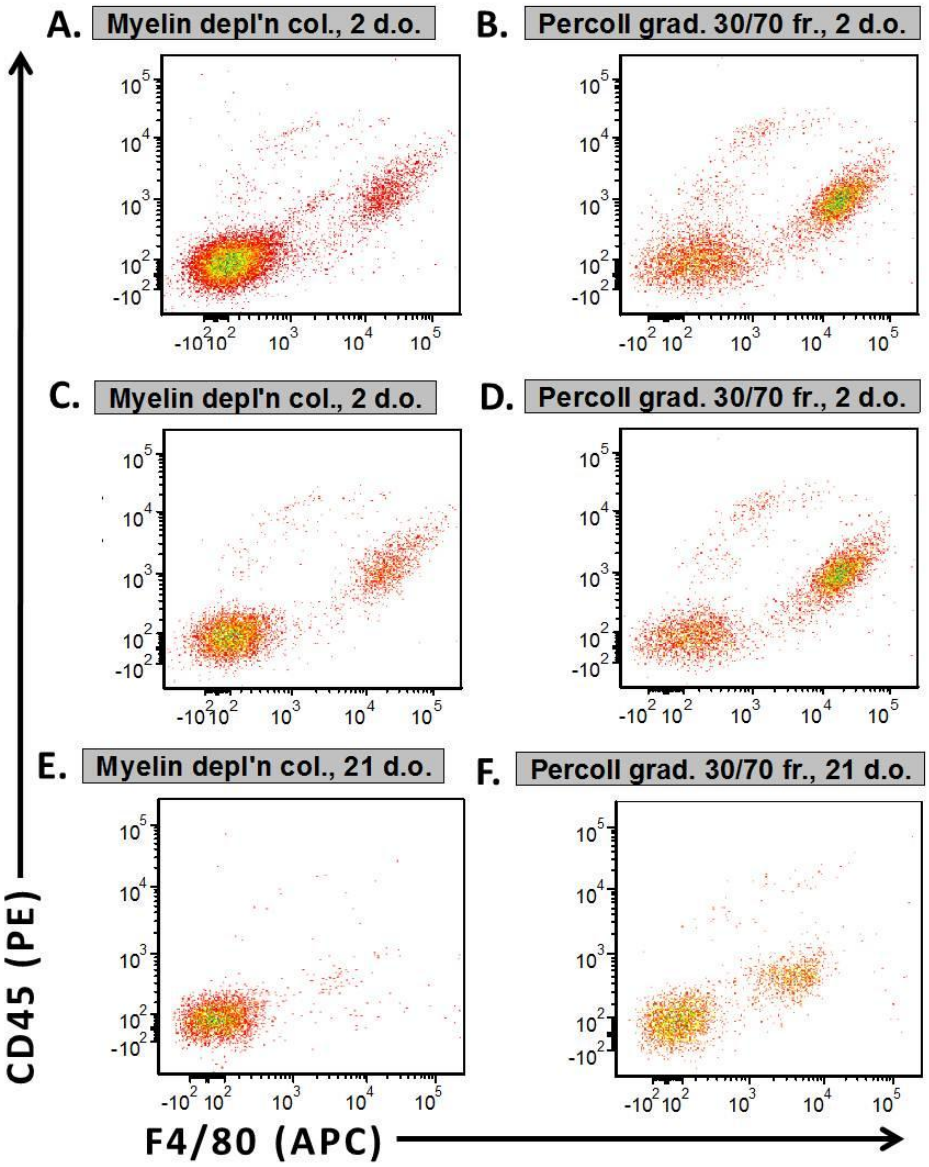

Figure 2.6 Comparison of CNS immune populations isolated using myelin depletion columns and Percoll gradients. Different sample preparation methods were compared using untreated neonatal **(A-D)** and weanling **(E-F)** brain tissue. Cell density plots of samples stained for the immune marker CD45 and the myeloid marker F4/80 are shown. **(A & B)** show events within the cell gate, while samples in **(C – F)** have been gated on both for events within the cell gate and for live cells. Cells were incubated with Aqua Live/Dead stain prior to fixation.

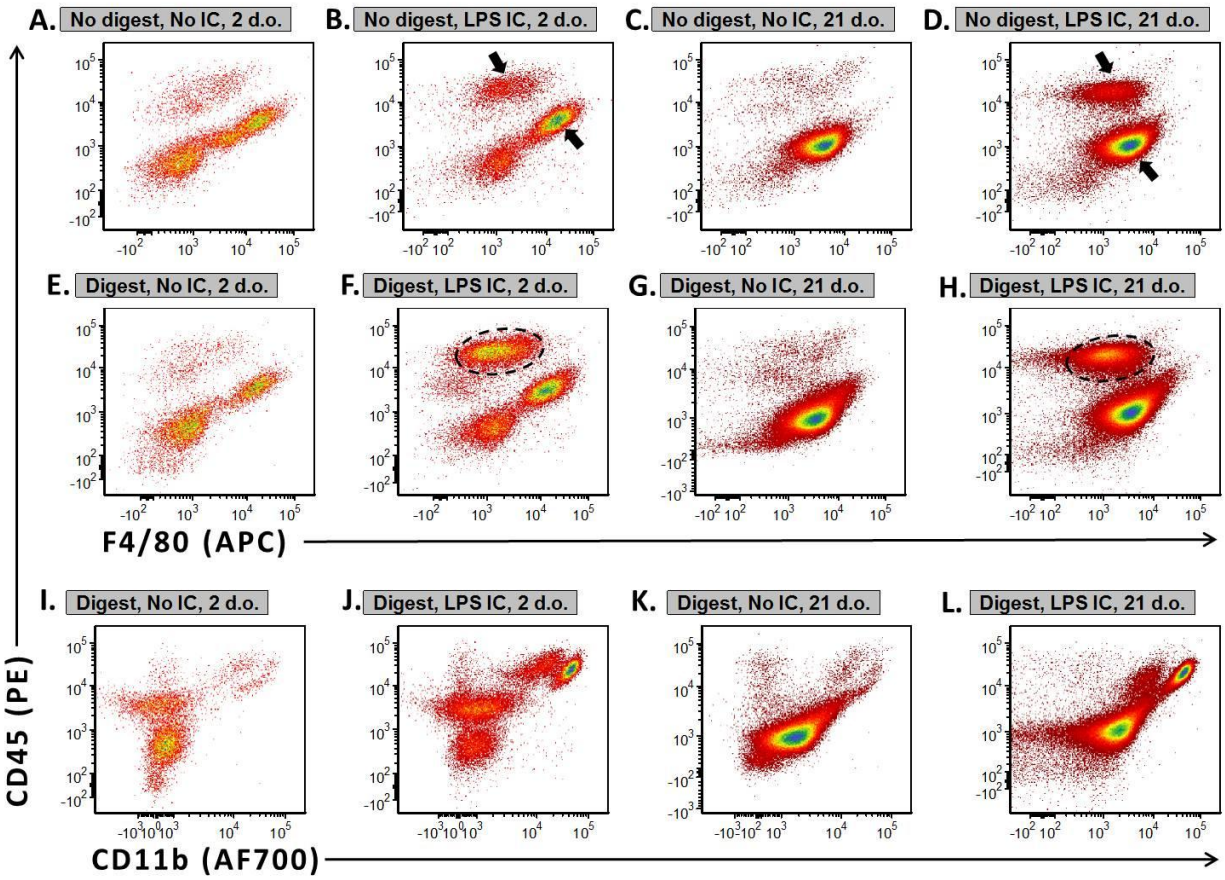

Figure 2.7 Enzymatic digest improves detection of LPS-stimulated CNS immune cells. Detection of CNS immune populations was compared after preparation of samples without **(A – D)** and with **(E – H)** enzymatic digestion (Collagenase D, Dispase I and DNase I) prior to Percoll gradient fractionation. Cell density plots of samples stained for the immune marker CD45 and the myeloid marker F4/80 are shown. Arrows indicate improved detection of LPS-stimulated immune populations, even in the absence of enzymatic digestion. Dashed line circles show even greater detection of LPS-stimulated $CD45^{hi}$ populations after enzymatic digestion.

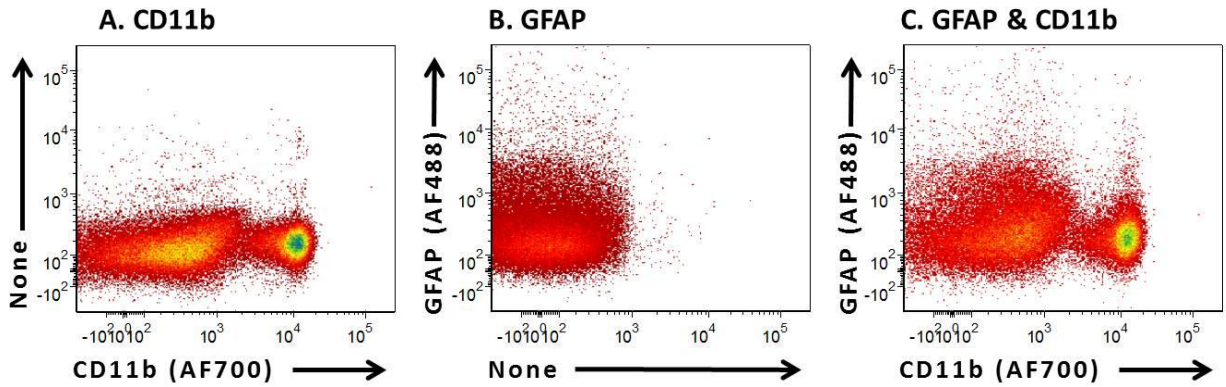

Figure 2.8 Flow cytometry of astrocytes *ex vivo*. Staining for the myeloid cell marker CD11b and the astrocyte cell marker GFAP in a neonatal PBS-treated sample is shown. These markers are not expected to exist on the same cell population in the brain, so double positive staining is not expected. **(A)** Sample is stained with antibody for CD11b only. **(B)** Sample is stained with antibody for GFAP only. **(C)** Sample includes antibodies for both GFAP and CD11b.

CHAPTER THREE

AGE-ASSOCIATED CHANGES IN THE ACUTE NEUROINFLAMMATORY RESPONSE TO TLR4 AND TLR9 STIMULATION IN YOUNG MICE

Introduction

During the perinatal period, the mammalian brain is developing rapidly and is particularly sensitive to inflammation. Gestational viral, bacterial and parasitic infections have been linked to neurological illnesses in offspring, including cerebral palsy, autism and schizophrenia (Brown et al., 2005; Mednick et al., 1988; Nelson and Willoughby, 2000; Shi et al., 2003; Sorensen et al., 2009). Additionally, perinatal infection may increase the risk of developing neurodegenerative diseases such as Alzheimer's and Parkinson's later in life (Chen et al., 2011; Ling et al., 2006). Current research suggests that it is not the infectious agent *per se* but the immune response that may cause neurological damage (Meyer and Feldon, 2010). Animal models of neurodevelopmental illnesses have demonstrated that perinatal immune stimulation with either infectious agents or Toll-like receptor (TLR) ligands can produce developmental and behavioral changes similar to those observed in human neurological illnesses, including alterations in learning and memory (Gilmore and Jarskog, 1997; Meyer et al., 2009). Moreover, the broad range of infectious organisms associated with neurodevelopmental dysfunction implies the etiology is not restricted to a specific organism. The fact that many immune molecules and cells have additional functions in neurological development also places unique demands on the neonatal immune system (Rolls et al., 2007; Rutkowski et al., 2010; Schafer et al., 2012; Ziv et al., 2006). Therefore, aberrant development

may be both an outcome of the immune system acting on the nervous system and a result of altered functionality within the nervous system.

A factor in how or whether perinatal infection leads to developmental abnormalities is the gestational age when insult occurs (Carvey, 2003; Meyer et al., 2006; Weinstock, 2008). For example, fetal rats exposed to LPS demonstrate progressive dopaminergic neuron loss throughout life only when exposure occurs between embryonic days 10.5 and 11.5 (Carvey, 2003; Ling et al., 2006). While the gestational period is a particularly sensitive time for neurodevelopment, it is not known for how long after birth this sensitivity persists. The exact relationship between age, immune response and specific developmental symptoms is not clear for many situations (Meyer and Feldon, 2010). However, the murine immune response to neurological infection develops dramatically during the first weeks of life, with two to three week old rodents being less susceptible to infection than neonates (Couderc et al., 2008; Ryman et al., 2007; Trgovcich et al., 1999).

In terms of cortical development, a newborn mouse or rat roughly corresponds to a human fetus midway through gestation (Clancy et al., 2001; Clancy et al., 2007a; Clancy et al., 2007b). Therefore, early postnatal immune activation in mice serves as a model to study the impact of infections corresponding with the mid to late gestational period in humans (Bonthius and Perlman, 2007; Hornig et al., 1999; Tohmi et al., 2007).

Many, if not all, cell populations in the brain can produce inflammatory mediators such as cytokines. As discussed in Chapter 1, both microglia and astrocytes regulate the neuroinflammatory response through production of pro- and anti-inflammatory mediators. Moreover, both microglia and astrocytes have developmental functions in the CNS [Chapter 1

and (Barres, 2008; Roumier et al., 2004; Ullian et al., 2001; Wakselman et al., 2008)]. Perinatal immune stimulation is thought to increase the risk of neurological illness by over-activating sensitive neonatal microglia [(Bilbo and Schwarz, 2009) and Chapter 1]. However, the developmental functions of astrocytes may also require neonatal astrocytes to exist in a heightened activation state under basal conditions. In addition, and as discussed in the introduction (Chapter 1), age-specific differences in inflammatory responses have been noted in peripheral immune populations stimulated with TLR ligands (Belderbos et al., 2009; Chelvarajan et al., 2007; Ferret-Bernard et al.; Nguyen et al., 2010). Therefore, microglia, as well as astrocytes and infiltrating peripheral immune populations, may contribute to age-associated differences in the inflammatory response in the CNS.

Here we have compared neuroinflammation in neonatal and weanling mice by inoculating them with lipopolysaccharide (LPS) or CpG oligodinucleotides (CpG), ligands of TLRs 4 and 9, respectively. We measured production of pro- and anti-inflammatory mediators in brain tissue. To better understand the processes leading to heightened neonatal inflammation, we also analyzed usage of common signaling pathways and activation of CNS immune-reactive cell populations.

Results

Neonatal cytokine responses to TLR4 stimulation are heightened and sustained

To characterize how the cytokine response changes during the first weeks of life, we examined cytokine production in neonatal (2 day old) and weanling (21 day old) C57Bl/10 mice after intracerebral (IC) inoculation with LPS or CpG. Control mice were either uninoculated or

inoculated IC with PBS. LPS was used at a concentration of 0.5 µg LPS per gram of body weight, based on the average mouse weight at each age. CpG was used at a concentration of 0.125 µg CpG (40 picomoles) per gram of body weight. These concentrations of LPS and CpG elicit strong neonatal cytokine responses (Fig 3.1 and Fig 3.2) but are not fatal (Fig 2.1 and data not shown).

We characterized the cytokine response using a multiplex bead assay, which is an antibody-based assay that simultaneously measures the protein levels of twenty common cytokines and growth factors. Cytokine levels were calculated using in-plate standards provided by the manufacturer. In response to intracerebral TLR9 stimulation, measured cytokine protein levels were high at 12 hpi but low or undetectable at 24, 48, 72 and 96 hpi [(Butchi et al., 2011) and data not shown]. Similarly, for detectable cytokines, IC TLR4 stimulation led to strong cytokine production at 12 hpi but cytokine levels were low to undetectable at 48 and 96 hpi (data not shown). Therefore, we compared cytokine protein levels at 12 hpi. We focused on the 13 cytokines in the multiplex bead assay that were detectable in brain tissue. In response to LPS, production of the inflammatory cytokines IL-1α, IL-1β, IL-2, IL-5, IL-6, TNF, CXCL9, CCL2 and CCL3 was significantly higher in neonatal brain tissue than in weanling brain tissue (Fig 3.1A). In response to CpG, IL-2, IL-5, TNF, CXCL9 and CCL2 production was elevated in neonatal brains, when compared with weanling brains. In order to confirm our results by an additional method, IL-6 and CCL2 protein levels in neonatal and weanling brains were examined by ELISA (Fig 3.1B). The ELISA findings agreed with trends observed in our multiplex data.

Not all cytokines were up-regulated to higher levels in neonates, when compared with weanling mice. Inflammatory cytokines whose protein levels did not show a statistically

significant age-dependent difference after TLR4 or TLR9 stimulation included IL-12, CXCL1 and CXCL10 (Fig 3.2). However, CXCL10 expression shows the same trend in age-dependent differences that was observed for the cytokines in Figure 3.1. Since several neonatal LPS- and CpG-treated samples were above the standard curve for CXCL10, whether or not age-dependent differences in CXCL10 expression occur cannot be conclusively determined from these data. In addition, significant age-dependent differences in the CpG response were not observed for IL-1α, IL-1β, IL-6 or CCL3. Production of the anti-inflammatory cytokine IL-10 also did not vary significantly with age (Fig 3.2). The multiplex bead assay also tested for IL-4, IL-13, IL-17, IFNγ and GM-CSF, but they were not present at detectable levels at either age. In conclusion, these results indicate that TLR stimulation can provoke elevated cytokine responses in the neonatal CNS. The cytokine response in neonates is further summarized in Table 3.1.

Since the prion protein, PrP^{c}, is developmentally expressed in the brain and may play a role in immune cell activation, we also examined cytokine production in neonatal and weanling C57Bl/10 $PrP^{-/-}$ mice. Although PrP^{c} knock out did not lead to detectable changes in the neuroimmune response (see Chapter 4), similar age-dependent differences in cytokine production were observed in both wild-type and $PrP^{-/-}$ mice, including age-dependent differences in IL-6, CCL2 and CXCL9 (compare Fig 4.3 with 4.4).

We considered the possibility that the age-associated differences in the cytokine response reflected differences in timing, rather than the magnitude of the cytokine response (Ortega et al., 2011). To examine this, we looked at mRNA expression levels from 2 to 48 hpi after treatment with either PBS or LPS. Significant differences in *Ccl2, Ccl3* and *Ifn b1* mRNA levels in PBS-treated neonatal and weanling brains were observed at 2 hpi but not at other time

points. Age significantly influenced LPS-induced mRNA expression of *Il6, Ccl2, Ccl3* and *Ifn b1* (Fig 3.3). At 2 hpi after stimulation with LPS, *Ccl2* and *Il6* levels were comparable between the two ages. By 6 hpi, the LPS response in weanling mice had dropped nearly to basal levels while neonatal *Il6* and *Ccl2* levels remained high. In contrast, *Ifn b1* levels were higher in neonates at 2 hpi but had returned to basal levels in mice of both ages by 6 hpi. *Ccl3* mRNA levels were significantly higher in neonates than weanling mice for the duration of the response (Fig 3.3). In summary, we observed that some cytokine mRNA levels were both prolonged and heightened in neonates in response to immune stimulation.

Age-dependent differences in expression of inflammatory signaling markers

We noted that basal *Tlr* mRNA levels in the brain and spleen increase with age (Fig 4.2), which contrasts with the age-associated difference in ability to respond to TLR stimulation (Fig 3.1 & Fig 3.3). To examine whether the heightened neonatal cytokine response was a global response, we looked at gene expression in 18 common signaling pathways, including pathways involved in inflammation, survival and development, using a Signal Transduction Pathway Finder SuperArray. Neonatal and weanling brain samples from PBS- and LPS-treated mice were assessed at 6 hpi. Among genes whose expression was altered at least two fold in response to LPS, differences were considered to be age-associated if the LPS-stimulated response between neonates and weanlings was statistically significant and at least two fold different. A minimum difference of two fold was required because each PCR cycle amplifies samples two fold, therefore this is the limit of resolution for PCR. Genes whose expression met these criteria are graphed in Fig 3.4. LPS-stimulated expression of the pro-inflammatory genes *Icam1, Nos2,*

Cxcl9 and *Ccl2* was significantly higher in neonates than weanling mice (Fig 3.4). We also noticed a trend in increased neonatal expression of *Birc3, Nfkbia*, *Il1a*, *TNF* and *Irf1* in response to LPS, although these age-associated differences were less than two-fold (data not shown). Collectively, our SuperArray gene expression analysis suggested differential age-associated regulation of the NFκB signaling pathway, which promotes inflammatory signaling downstream of TLR stimulation (Ostuni et al., 2010).

In contrast with the elevated expression of some inflammatory markers in neonates, *Bmp4* and *Csf2* levels were higher in weanling mice after stimulation with LPS (Fig 3.4). *Bmp4*, a signaling molecule critical for the development of many organs (Czyz and Wobus, 2001; Hamilton and Anderson, 2004; Ishibashi et al., 2005), was significantly down-regulated in neonatal, but not weanling, brains in response to LPS ($p=0.0495$). *Csf2,* a cytokine that promotes the differentiation of granulocytes, monocytes and dendritic cells (Hamilton and Anderson, 2004; Hesske et al., 2010), was induced in weanling, but not neonatal, brains in response to LPS.

Glia contribute to the heightened neonatal response to TLR4 and TLR9 stimulation

To investigate which cell types contribute to the heightened neonatal inflammatory response, we compared mRNA expression levels of glial markers in brain tissue from 2 to 48 hpi (Fig 3.5A-D). mRNA levels of the astrocytic activation marker *Gfap* were greater in weanling brain tissue at 48 hpi (Figure 3.5A). The activation marker *Cd80* is expressed by myeloid cells, including microglia, in the CNS (Hesske et al., 2010; Mausberg et al., 2009; Zhang et al., 2002). *Cd80* was significantly heightened in LPS-treated neonatal brains, when compared with

weanling brains, at 12 hpi (Figure 3.5B). In addition, mRNA levels of *Slamf7*, whose expression we have found primarily in microglia in the CNS (Fig 3.10), were significantly higher in neonates at 6 and 12 hours after LPS inoculation (Fig 3.5C). In contrast, expression of the myeloid marker *F4/80* expression increased in parallel in mice of both ages at 48 hours after LPS inoculation (Fig 3.5D) (Lin et al., 2005; Lin et al., 2010).

We also considered whether a peripheral immune cell type, recruited into the brain early in the inflammatory response, could contribute to the acute neonatal response. We examined mRNA levels of the T cell markers *Cd3* and *Cd8*, the dendritic cell (DC) marker *Itgax,* and the neutrophil marker *Ela2*. We did not observe a significant increase in expression of any of these markers until 48 hpi (Fig 3.5E-H). Neonatal *Ela2* expression was slightly elevated at 12 hpi but strongly induced at 48 hpi (Fig 3.5H). In contrast, *Itgax* levels were higher, and relatively stable, in neonates from 2 to 12 hpi. However, by 48 hpi, *Itgax* levels were much higher in weanling mice in response to LPS (Figure 3.5G). Both PBS- and LPS-stimulated levels of the pan T cell marker *Cd3* were significantly higher at 48 hpi in neonatal mice (Figure 3.5E). However, *Cd8*, which is expressed by $CD8^+$ T cells and NKT cells, was similarly induced in mice of both ages (Fig 3.5F). Collectively, the only cell markers that differed at early time points after LPS stimulation were *Cd80* and *Slamf7*. Since both markers are expressed by microglia, these cells may contribute to the heightened inflammatory response in neonates.

To better assess which cell types are contributing to heightened neonatal inflammation, we separated brain tissue into two populations using a 0/30/70% Percoll gradient. After centrifugation, astrocytes, a cell type known to respond to TLR stimulation (Butchi et al., 2010), are predominantly found in the 0/30% fraction [(Butchi et al., 2011) & (Fig 2.4)]. The 30/70%

fraction contains myeloid cells, including microglia and macrophages, and infiltrating immune cells (Peterson et al., 2006). The immune response cannot be quantitatively compared between the two fractions because the individual cell types that make up each fraction are quite different.

Although basal *Tlr4* expression in whole brain tissue increases with age (Fig 3.2), we did not observe any significant age-dependent changes in *Tlr4* mRNA levels in gradient fractions enriched for either microglia or astrocytes (Fig 3.6A). Higher overall *Tlr4* mRNA levels were found in the 30/70% fraction, when compared with the 0/30% fraction, and were strongly down-regulated in the 30/70% fraction in response to LPS. *Tlr9* mRNA, which was also found primarily in the 30/70% fraction, increased significantly in this fraction with age (Fig 3.6B). We examined *Il6* and *Ccl2* mRNA levels in these fractions because we previously observed age-dependent expression of these genes and their encoded proteins (Fig 3.1 & Fig 3.3). We also examined mRNA expression of *Nos2* and *Icam1* in these fractions because we found them to be expressed at higher levels in neonates in whole brain homogenates (Fig 3.4). Although populations in both fractions contributed to heightened neonatal expression of these genes (Fig 3.6C-F), we observed trends towards higher IL-6 and CCL2 expression in the 30/70% fraction but higher *Nos2* and *Icam1* expression in the 0/30% fraction.

Age-associated expression of microglial activating and inhibitory proteins

To better understand the microglial contribution to neuroinflammation, we assessed expression of microglial activating and inhibitory proteins in neonatal and weanling brains at 6 hpi. We chose the 6 hour time point because this is when production of many cytokine mRNAs

peak in neonates. We sought to correlate the microglial activation profile with cytokine production. After IC inoculation with PBS or LPS, brain tissue was harvested, and then cells within the 30/70% fraction of Percoll gradients were analyzed by flow cytometry. Representative samples are shown in Figure 3.7. Plots of forward scatter (FSC-A) versus side scatter (SSC-A) were initially used to set cell gates that excluded dead cells and debris (Fig 3.7A-D). Weanling cells consistently had lower side scatter than neonatal cells. Since side scatter is a measure of granularity, and active cells are more granular, this may be due to an increased activity level in neonatal CNS myeloid cells. Distinct cell populations were initially visualized and gated on based on their expression of the leukocyte common antigen CD45 and the myeloid-specific marker F4/80 (Fig 3.7E-H) (Irie-Sasaki et al., 2001; Lin et al., 2010). Microglia are known to express lower levels of CD45 than macrophages, as well as some other immune cell populations, and so were identified as $CD45^{lo}$ $F4/80^{+}$ (solid line in Fig 3.7E-H) (Ford et al., 1995; Sedgwick et al., 1991). Different cell gates were required for neonatal and weanling microglia because neonatal microglia expressed higher levels of CD45 and F4/80. Macrophages were identified as $CD45^{hi}$ $F4/80^{+}$ (dotted line in Fig 3.7E-H). Additional cells with $CD45^{hi}$ staining and little to no F4/80 expression ($F4/80^{lo}$) were also observed (dashed line in Fig 3.7E-H). Neonatal samples tended to contain larger amounts of $CD45^{-}$ $F4/80^{-}$ cells and had more intense staining in the F4/80 (APC) channel (double solid line in Fig 3.7E-H).

We examined expression of the cell surface proteins CD11b, CD11a, CD86, CD172a, CD200R, LY6C and SLAMF7 on CD45 high and low populations (Figures 3.8 & 3.9). CD11a, CD11b and CD86 are activation markers (Kettenmann et al., 2011; Kurpius et al., 2006; Liu et al., 2008). In contrast, CD172a and CD200R inhibit activation (Gitik et al., 2011; Hernangómez et

al., 2012; Liu et al., 2008; Masocha, 2009). SLAMF7 can act either as an activating or inhibitory receptor, depending on the adaptor molecules present (Cruz-Munoz et al., 2009). LY6C expression can help distinguish between different myeloid cell populations (Auffray et al., 2007; Geissmann et al., 2003; Jutila et al., 1994).

In Figure 3.8, populations were color-coded to illustrate age-associated differences CD11b and LY6C expression, as well as in side scatter and forward scatter, which is a measure of size. In Figure 3.8, cells within the microglial gate (solid line in Fig 3.7E-H) are blue, macrophages (dotted line in Fig 3.7E-H) are green, and $CD45^{hi}$ $F4/80^{lo}$ cells (dashed line in Fig 3.7E-H) are pink and aqua. $CD45^{-}$ $F4/80^{-}$ cells are yellow (double solid line in Fig 3.7E-H). The phenotypes of these cell populations are summarized in Table 3.2. When cells were plotted based on CD45 and CD11b expression, the $CD45^{hi}$ $F4/80^{lo}$ cells could be separated into two distinct populations with CD11b high and low expression, which segregated to either side of the macrophage population (Fig 3.8 B & F). The $CD45^{hi}$ $F4/80^{lo}$ $CD11b^{hi}$ cells are pink while the $CD45^{hi}$ $F4/80^{lo}$ $CD11b^{lo}$ cells are aqua. In the $CD45^{hi}$ $F4/80^{lo}$ population, CD11b expression also correlated with LY6C expression (Fig 3.8 D & H). Examination of F4/80 expression on $CD45^{hi}$ $F4/80^{lo}$ cells in which the $CD11b^{hi}$ and $CD11b^{lo}$ populations were separately colored demonstrated that both of these populations had variable F4/80 expression (Fig 3.8 C & G). Macrophages expressed an intermediate amount of CD11b, high levels of LY6C, and were larger and of intermediate granularity (Fig 3.8 A & E). Microglia were similar to the $CD45^{hi}$ $F4/80^{lo}$ $CD11b^{lo}$ cells in their size, granularity, and expression of CD11b and LY6C (Fig 3.8). $CD45^{hi}$ $F4/80^{lo}$ $CD11b^{hi}$ cells were the least uniform in size and granularity. Neonatal samples

contained fewer macrophages and $CD45^{hi}$ $F4/80^{lo}$ $CD11b^{lo}$ cells, but more $CD45^{-}$ $F4/80^{-}$ cells, than weanling samples.

In neonatal PBS-treated samples, we also observed a population of cells with very high forward and side scatter (Fig 3.8 A, dashed red line). Gating on this population shows an additional population of cells in graphs of antibody staining (CD45, F4/80, CD11b, LY6C) that are always to the upper right of the $CD45^{hi}$ $F4/80^{lo}$ $CD11b^{lo}$ population (pink) for all antibodies (data not shown), indicating proportionally higher staining for these antibodies. These cells could be doublets or an additional, uncharacterized population.

Based on the greater overall responsiveness of neonates to neuroinflammatory stimuli, we expected to observe increased expression of activation markers and decreased expression of inhibitory receptors on neonatal microglia in response to LPS, when compared with weanling microglia. Indeed, expression of the activation markers CD11a and CD11b was consistently higher on neonatal microglia when compared with weanling microglia (Fig 3.9 A-C). Unexpectedly, expression of the inhibitory receptor CD172a was also higher on neonatal microglia than weanling microglia. In addition, these microglial protein levels did not significantly change in response to LPS in mice of either age (Fig 3.9 D-F), possibly due to the early time point post-treatment (6 hpi). Significant age-dependent differences in levels of the activation marker CD86 and in inhibitory CD200R were not observed in microglia (data not shown).

SLAMF7 has been shown to be expressed by a variety of peripheral immune populations (Beyer et al., 2012; Cruz-Munoz et al., 2009; Llinas et al., 2011). However, SLAMF7 expression on microglia has not previously been described. After observing elevated *Slamf7* expression in

neonatal whole brain homogenates in response to LPS (Fig 3.5C), we examined *Slamf7* expression in the 0/30% and 30/70% fractions of centrifuged neonatal and weanling Percoll gradients (Fig 3.10A). In response to LPS stimulation, *Slamf7* was primarily up-regulated in the neonatal 30/70% fraction. *Slamf7* expression was also up-regulated in the weanling 30/70% fraction in response to stimulation with CpG. We looked at SLAMF7 expression on $CD45^{+}$ populations (Fig 3.10B) and found that SLAMF7 protein levels were higher on neonatal microglia than on all other populations examined ($p < 0.0001$), although it was not elevated following LPS stimulation.

Collectively, our flow cytometry data suggest there may be differences in the ratios of $CD45^{hi}$ populations in neonatal and weanling brains, based on expression of CD11b and LY6C. This difference could contribute to the differing cytokine responses observed at each age. Our data also suggest that there are age-associated differences in expression of CD11a, CD11b, CD172a and SLAMF7 on microglia.

We also examined expression of CD11b and CD45 in the spleen. The spleen serves as the primary reservoir for monocytes (Swirski et al., 2009). In response to immune stimulation, splenic monocytes migrate into tissues and differentiate into macrophages and dendritic cells (Geissmann et al., 2010; Swirski et al., 2009). Although we did not observe LPS-specific differences in the CNS at 6 hpi by flow cytometry, CD11b was up-regulated in the spleen in an LPS-dependent manner at this time point (Fig 3.11). In addition, CD45 expression was up-regulated on LPS-stimulated $CD11b^{+}$ spleen cells. This suggests that the peripheral immune response to TLR4 agonist inoculation in the brain is detectable at least as early as 6 hpi. There were no age-dependent differences in splenic CD11b or CD45 expression.

Discussion

The immune response at birth is immature and infants are often unable to mount an effective response to infection (Levy, 2007). Therefore, we were initially surprised to find that some cytokine levels were higher in neonatal brains than weanling brains in response to TLR4 and TLR9 stimulation. However, as detailed in Chapter 1, recent studies in peripheral tissues and immune cells have demonstrated that age-associated differences in cytokine production can also differ based upon the cell or tissue type being examined (Aksoy, 2006; Chelvarajan et al., 2007; Chelvarajan et al., 2004; Ferret-Bernard et al.; Islam et al., 2012b). In addition, the immune response is uniquely regulated in the brain (Carson et al., 2006; Ransohoff and Cardona, 2010). Therefore, conclusions about the neonatal TLR response in the brain cannot be inferred from studies of other tissues.

Our results extend current knowledge of the neonatal neuroinflammatory response by directly comparing the responses of neonatal and weanling mice to TLR4 or TLR9 stimulation. We demonstrate that production of many cytokines is higher in neonatal brains than in weanling brains. TLR4 stimulation in neonates leads to elevated production of cytokines that are an important part of the inflammatory response in many neurological conditions, including the cytokines IL-1β, TNF and IL-6. TLR9 stimulation also led to increased neonatal cytokine expression, albeit for a smaller subset of cytokines. Our research suggests some cytokine responses to TLR stimulation in the brain are elevated in neonates. This includes higher neonatal levels of IL-1b, TNF and Cxcl9, cytokines whose expression is often inhibited during the neonatal TLR response in the periphery (Angelone et al., 2006; Chelvarajan et al., 2004; Islam et

al., 2012a; Levy et al., 2006a; Nguyen et al., 2010). In contrast, we were unable to detect significantly higher neonatal levels of IL-10, an anti-inflammatory cytokine whose production is often elevated in neonatal peripheral immune cells (Chelvarajan et al., 2007; Ferret-Bernard et al.; Martino et al., 2012). IL-12, which is often expressed at reduced levels in neonatal responses to TLR stimulation in the periphery (Belderbos et al., 2009; Chelvarajan et al., 2004; Islam et al., 2012a), did not differ significantly with age in the brain. Thus, the neonatal response in brain tissue appears to differ from that reported for peripheral tissues.

Although elevated levels of IL-6, IL-1β and TNF in the neonatal brain have been correlated with later cognitive disability and behavioral changes (Bilbo and Schwarz, 2009), few published studies directly compare the neuroinflammatory response of neonates with that of older animals. Ortega *et al.* recently examined cytokine responses in the brains of neonatal and weanling rats to intraperitoneal LPS administration (Ortega et al., 2011). They found that mRNA levels of *Il-6, Il-1β* and *Tnf* peak at 2-6 hpi in weanling brains, but peak at 6-24 hpi in neonatal brains. In contrast, we did not find that cytokine mRNA expression in response to IC LPS occurred sooner in weanling mice. However, we did observe that for the cytokine mRNAs examined, expression was prolonged in neonatal mice. Therefore, whether age-dependent differences in the timing of the CNS cytokine response occur may be influenced by either the location or the trafficking of the immune stimulus in the body.

As described in Chapter 1, altered activation and expression of molecules involved in TLR signaling has been implicated in distinct neonatal immune responses in the periphery (Levy, 2007). In parallel with this, we noted heightened CD11b levels on neonatal microglia when compared with weanling microglia. CD11b is thought to be involved in TLR4 signaling by aiding

the recruitment of intracellular TLR signaling adaptor proteins to lipid rafts, where LPS-bound TLR4 is localized (Chapter 1). Therefore, elevated microglial CD11b levels could promote neonatal TLR4 signaling.

In addition to increased microglial CD11b protein levels, CD11a protein levels on microglia and CD11c (*Itgax*) mRNA levels in whole brain tissue were also increased in neonates. CD11a, CD11b and CD11c belong to the β_2-integrin family of adhesion molecules. Increased neonatal expression of β_2-integrins supports the theory that neonatal microglia exist in a heightened activation state because β_2-integrins are involved in migration and phagocytosis (Hu et al., 2010; Liu et al., 2008). Our observations on the age-associated changes in β_2-integrin expression on microglia agree with the morphological studies of others (see Chapter 1) and suggest that neonatal microglia are in a more active state under basal conditions than microglia from older animals.

We were initially surprised that CD11a and CD11b levels did not change in response to TLR4 stimulation. However, we examined the protein levels of microglial activation markers at the early time point of 6 hpi. In a study of the neonatal microglial response to neuronal damage, new protein synthesis was not required for early microglial responses, including migration (Kurpius et al., 2006). This implies that proteins involved in microglial migration, such as CD11a and CD11b, exist at high enough levels under homeostatic conditions to allow neonatal microglia to begin to respond to trauma without waiting for new proteins to be synthesized. While microglial activation in response to other stimuli was not examined, it may be that new protein synthesis is not required for the early response of neonatal microglial to LPS. If protein synthesis is not required for the initial changes in microglia associated with

activation, this may explain why we observe age-dependent, but LPS-independent, changes in microglial activation markers involved in adhesion and migration.

In addition to increased expression of some pro-inflammatory mediators in neonates, we observed increased expression of the anti-inflammatory mediator CD172a in neonates. CD172a negatively regulates CD11b-mediated adhesion, migration and phagocytosis (Liu et al., 2008). Heightened CD172a expression could provide a counterbalance to the elevated levels of β_2-integrins on neonatal microglia.

We found SLAMF7 expression in the brain to be of particular interest because SLAMF7 levels were highest on neonatal microglia. Microglia express lower levels of many immune receptors than other macrophage populations (Ransohoff and Cardona, 2010). Therefore, it is somewhat surprising that we detected the highest SLAMF7 expression on neonatal microglia. SLAMF7 was the only immune cell marker examined in this study whose expression was higher on microglia than on all other cell populations examined. As mentioned above, SLAMF7 can be either an activating or inhibitory receptor. The activity of SLAMF7 on microglia is not yet clear.

We observed age-dependent differences in the CNS immune populations found in the brain. Neonatal samples contained fewer macrophages and $CD45^{hi}$ $F4/80^{lo}$ $CD11b^{lo}$ cells than weanling samples. The identities of the $CD45^{hi}$ $F4/80^{lo}$ $CD11b^{hi}$ and $CD11b^{lo}$ populations are unclear. They may include monocytes, as circulating monocytes have been shown to express lower levels of F4/80 than tissue resident macrophages (Lin et al., 2010). However, the $CD45^{hi}$ populations could also include T cells, neutrophils and DCs. Other studies have noted small endogenous populations of dendritic cells, T cells and neutrophils in murine and primate brains under homeostatic conditions (Bischoff et al., 2011; Dick et al., 1995; Ford et al., 1995;

Gottfried-Blackmore et al., 2009). In addition, intracerebral immune stimulation can lead to a large influx of peripheral immune cells, including DCs (Gelderblom et al., 2009; Hesske et al., 2010; Mausberg et al., 2009).

The number of $CD45^{hi}$ cells detected in LPS-treated samples was reduced when compared with PBS-treated samples. These results were observed in both neonatal and weanling tissues. It is unclear why fewer $CD45^{hi}$ cells were detected in LPS-stimulated samples because immune stimulation is expected to increase recruitment of peripheral immune cells. Montero-Menei *et al.* reported a similar phenomenon in rats that were either inoculated IC with LPS or received an IC stab lesion (Montero-Menei et al., 1996). At 5 hpi, greater infiltration of $CD11b^{+}$ cells was observed in the stab lesioned brains than in the LPS inoculated brains. However, at 15 hours and later there was greater $CD11b^{+}$ infiltration into LPS-treated brains than into stab lesioned brains (Montero-Menei et al., 1996). If IC LPS initially suppresses immune cell recruitment but later promotes it, as suggested by Montero-Menei *et al.*, then LPS-specific recruitment of peripheral immune cells could also be delayed in our model.

In neonatal PBS-treated samples we also observed a population of cells with very high forward and side scatter (dashed red line in Fig 3.8 A). This population may include doublets, perhaps due to the rapid cell division occurring at this age. Alternatively, this could be a distinct population of cells.

We found that mRNA levels of the astrocyte activation marker *Gfap* were higher in weanling mice. However, we suspect that, in this situation, *Gfap* expression does not accurately reflect the activation state of neonatal astrocytes. *Gfap* is an intermediate filament protein involved in cytoskeletal structure. *Gfap* levels may more accurately reflect that

weanling astrocytes have more, and larger, processes than neonatal astrocytes. We expect that astrocytes contribute to the elevated inflammatory response observed in neonatal brains because astrocytes are a component of the 0/30% Percoll gradient fraction, which contributes to the elevated neonatal response. Other cells, such as oligodendrocytes or ependymal cells, may also contribute to the inflammatory response observed in the 0/30% fraction.

In addition to shedding light on the etiology of neurodevelopmental disorders, a better understanding of the unique pro- and anti-inflammatory aspects of the neonatal immune response may lead to the development of more effective treatments for the initial infection as well as its long term consequences.

Table 3.1 Age-associated changes in cytokine responses.

	Overall significant interaction between age and treatment?	Change in response to LPS	Neonatal response to CpG
IL-2	Y	↑*	↑*
IL-5	Y	↑*	↑*
TNF	Y	↑*	↑*
CCL2	Y	↑*	↑*
CXCL9	Y	↑*	↑*
IL-1a	Y	↑*	↔
IL-1b	Y	↑*	↔
IL-6	N	↑*	↔
CCL3	N	↑*	↔
IL-10	N	↔	↔
IL-12	N	↔	↔
CXCL1	N	↔*	↔
CXCL10	N	↔*	↔*

Overall significant interactions between age and treatment are listed in the first column. Arrows indicate direction of response in neonates when compared with weanling mice. Asterisk indicates whether cytokine was significantly induced in neonates in response to the given agonist. Statistical analysis was completed by two-way analysis of variance with Sidak's multiple comparisons test.

Table 3.2 Phenotypes of examined cell populations.

Population	Color in Figure 3.8					
Microglia	Blue	$CD45^{lo}$	$F4/80^{+}$	$CD11b^{lo}$	$Ly6C^{-}$	SSC^{lo}
Macrophages	Green	$CD45^{hi}$	$F4/80^{+}$	$CD11b^{int}$	$Ly6C^{hi}$	SSC^{int}
Other cell populations:						
Unknown	Pink	$CD45^{hi}$	$F4/80^{lo}$	$CD11b^{hi}$	$Ly6C^{hi}$	SSC^{hi}
Unknown	Aqua	$CD45^{hi}$	$F4/80^{lo}$	$CD11b^{lo}$	$Ly6C^{-}$	SSC^{lo}
Unknown	Yellow	$CD45^{-}$	$F4/80^{-}$	$CD11b^{lo}$	$Ly6C^{-}$	n.d.

n.d. = not determined

Table 3.3 Percentage of cells in examined populations.

	Color in Figure 3.8	2 d, PBS	2 d, LPS	21 d, PBS	21 d, LPS
Microglia	**Blue**	**20.1 ± 7.4**	**43.2 ± 3.7**	**56.3 ± 7.2**	**79.1 ± 6.0**
Macrophages	**Green**	**2.0 ± 0.2**	**1.8 ± 0.4**	**13.1 ± 1.5**	**3.2 ± 0.9**
Unknown $CD11b^{hi}$	**Pink**	**58.2 ± 8.9**	**15.9 ± 0.3**	**19.6 ± 7.4**	**4.8 ± 0.9**
Unknown $CD11b^{lo}$	**Aqua**	**0.5 ± 0**	**0.5 ± 0.2**	**3.6 ± 0.8**	**0.7 ± 0.1**
$CD45^{-}$	**Yellow**	**15.6 ± 0.8**	**35.6 ± 4.4**	**3.8 ± 0.7**	**6.9 ± 3.8**

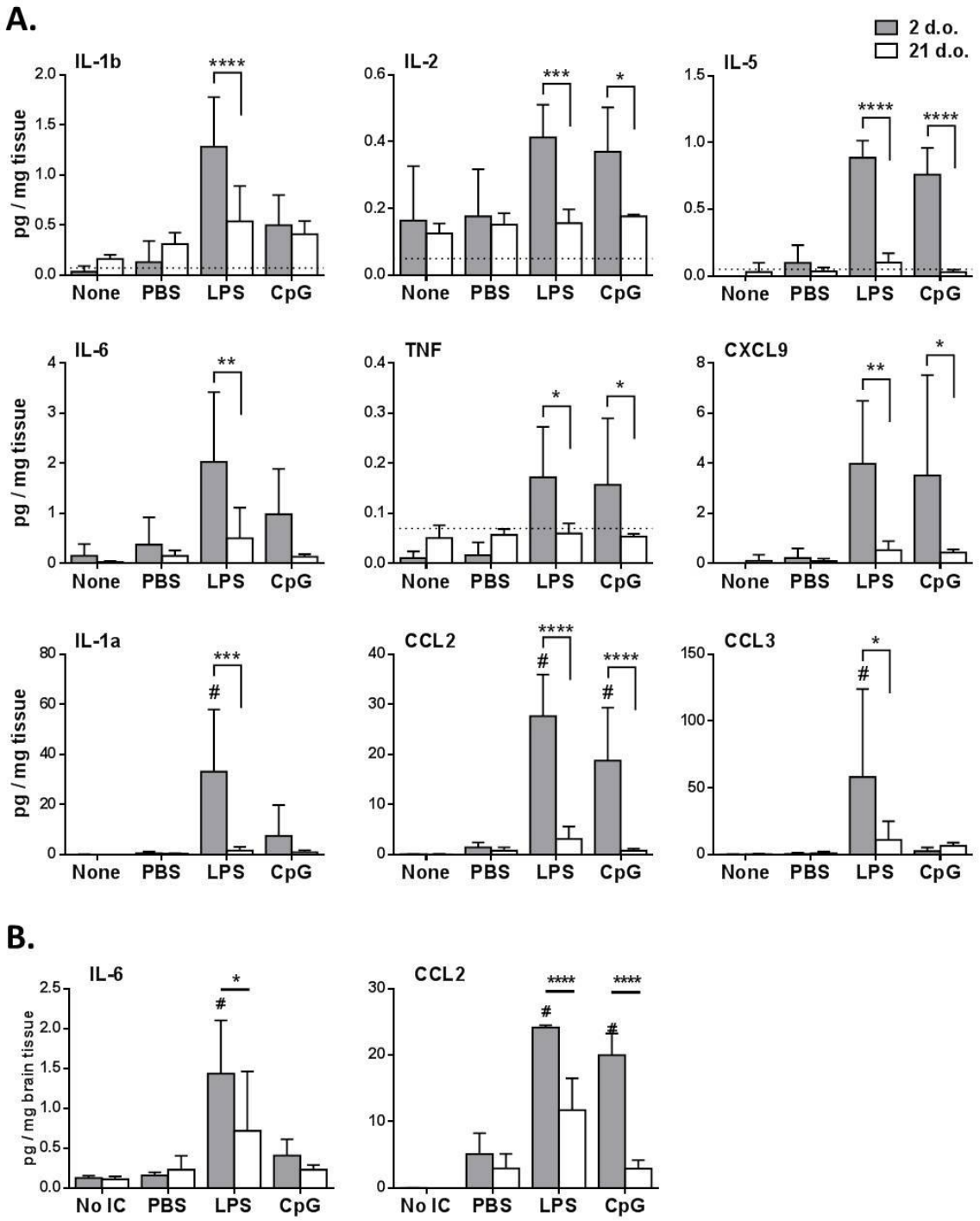

Figure 3.1 Heightened neonatal cytokine responses to IC TLR4 and TLR9 stimulation. Neonatal (2 d.o.) and weanling (21 d.o.) mice were inoculated intracerebrally (IC) with LPS or CpG. Control groups were either not inoculated or inoculated IC with PBS. **(A)** Cytokine protein levels

in brain homogenates from neonatal and weanling mice were measured at 12 hpi using a multiplex bead assay. n = 10-12 for 2 d.o. mice and includes the combined results from two independent experiments, n = 5-6 for 21 d.o. mice from one independent experiment. **(B)** Age-dependent differences in cytokine production were confirmed by ELISA for IL-6 and Ccl2. n = 5 mice per group. Data are presented as mean +/- SD. For both assays, protein concentrations were calculated using in-plate standard curves derived from manufacturer-provided protein standards. Dotted line indicates lower limit of detection (based on standard curve). # indicates treatment group contains samples above the dynamic range (based on standard curve). Outliers detected by Grubbs' test were excluded. Statistical analysis was completed by two-way analysis of variance with Sidak's multiple comparisons test. Significant age-specific differences are as indicated: *p<0.05, **p<0.01, ***p<0.001, ****p<0.0001.

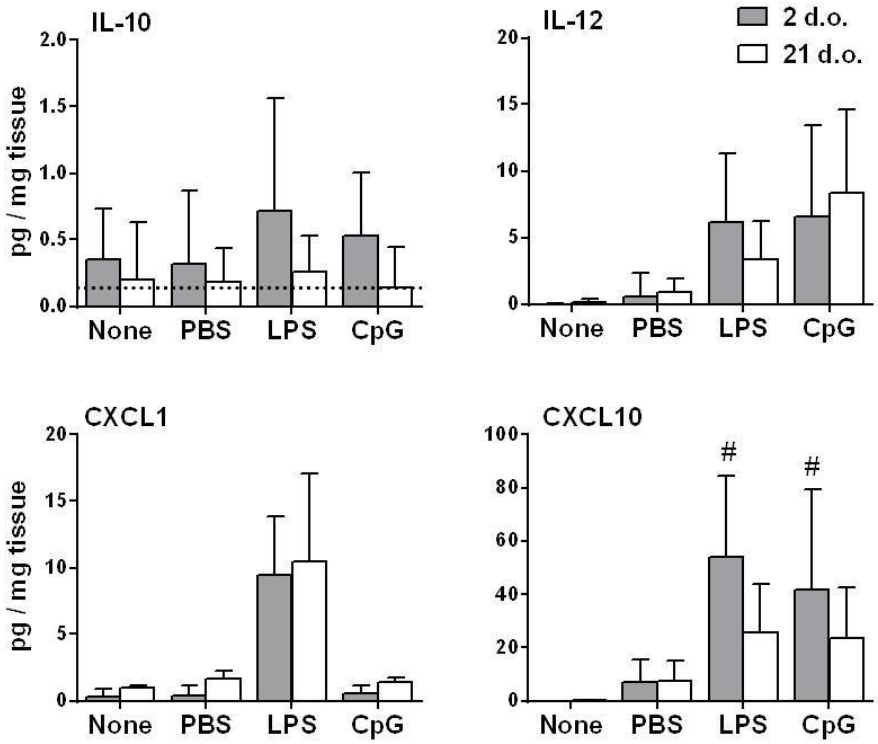

Figure 3.2 Production of some cytokines does not differ with age in response to IC LPS or CpG. Neonatal and weanling mice were inoculated IC with PBS, LPS or CpG, or remained uninoculated. Cytokine protein levels in whole brain homogenates were measured at 12 hpi using a multiplex bead assay. n = 10-12 for 2 d.o. mice and includes the combined results from two independent experiments, n = 5-6 for 3 w.o. mice from one independent experiment. Dotted line indicates lower limit of detection (based on standard curve). # indicates treatment group contains samples above the dynamic range (based on standard curve). Outliers detected by Grubbs' test were excluded. Statistical analysis was completed by two-way analysis of variance and Sidak's multiple comparisons test. Data are presented as mean +/- SD.

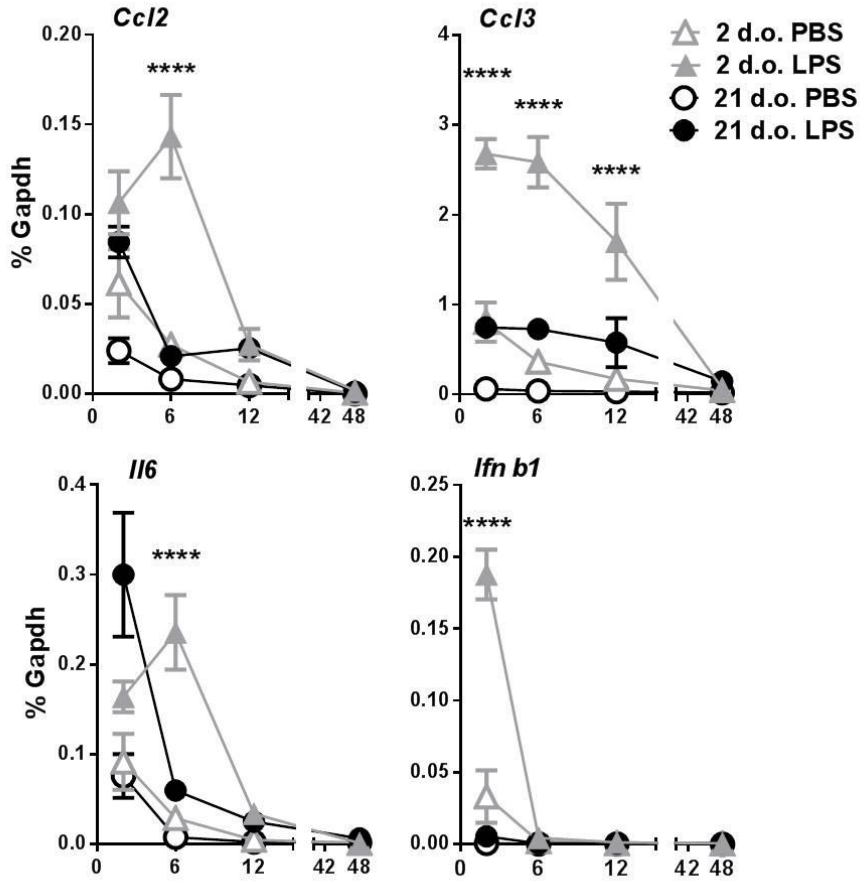

Figure 3.3 Heightened and prolonged inflammatory cytokine responses in neonates. Cytokine mRNA levels in whole brain homogenates from neonatal and weanling mice were assayed at 2, 6, 12 and 48 hpi after IC inoculation with PBS or LPS. n = 4-6 mice per group. No statistically significant differences in *Il6* levels were observed between PBS treated neonatal and weanling mice. Neonatal PBS treated mice expressed significantly higher levels of *Ccl2*, *Ccl3* and *Ifn β1* than weanling PBS treated mice at 2 hpi only (p=0.0339 for *Ccl2*, p=0.0143 for *Ccl3*, p=0.0075 for *Ifn β1*). Data are presented as mean +/- SE. Statistical analysis was completed by two-way analysis of variance with Tukey's multiple comparisons test. Significant age-specific differences in the LPS response are indicated in the figure as: **p<0.01, ***p<0.001, ****p<0.0001.

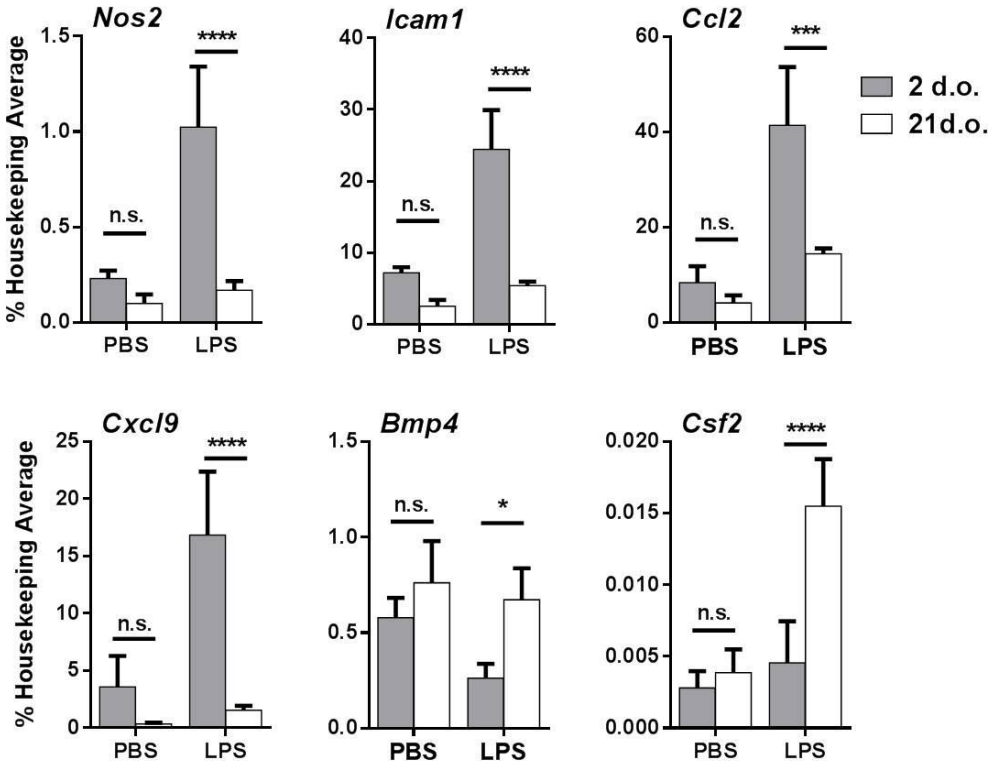

Figure 3.4 Age-associated differences in expression of signaling markers. Age-dependent differences in the LPS response were analyzed using a PCR SuperArray designed to detect differential usage of 18 common signaling pathways, including pathway involved in inflammation, survival and development. mRNA expression levels in whole brain homogenates of neonatal and weanling mice were tested at 6 hpi with PBS or LPS. Data presented here include genes whose expression showed a statistically significant change in response to both LPS and age. n = 4 mice per group. Data are presented as mean +/- SD. Statistical analysis was completed by two-way analysis of variance with Tukey's multiple comparisons test. Significant age-specific differences are as indicated: *p<0.05, **p<0.01, ***p<0.001, ****p<0.0001

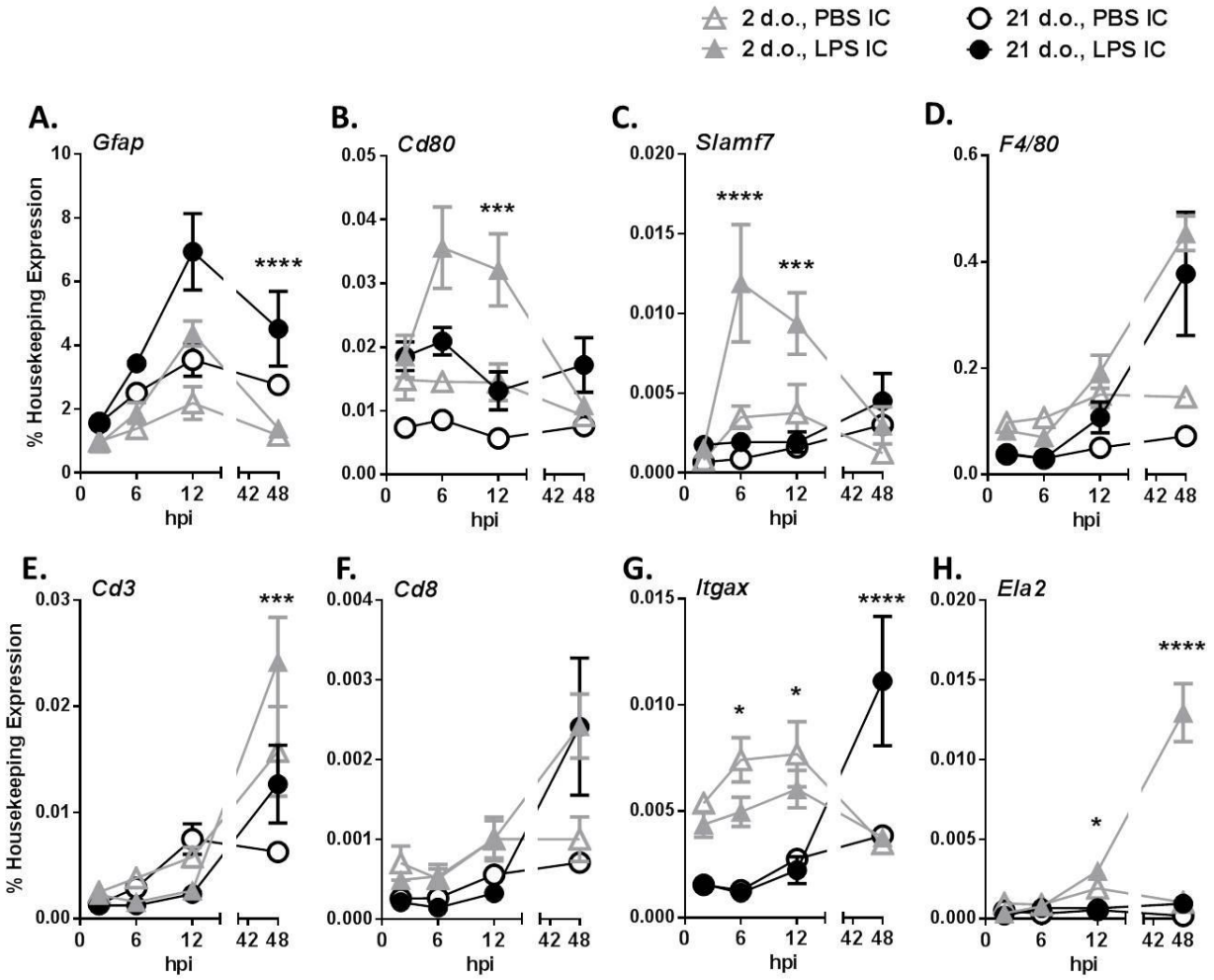

Figure 3.5 Temporal expression of glial and immune cell markers after TLR4 stimulation. mRNA levels of glial and immune cell markers in whole brain homogenates from neonatal and weanling mice were tested at 2, 6, 12 and 48 hpi with PBS or LPS. **(A)** mRNA levels of the astrocytic marker *Gfap* are higher in weanling mice. **(B)** *Cd80*, which is expressed by microglia and macrophages in the CNS, is induced early in the inflammatory response, and to a greater degree, in neonates. **(C)** *Slamf7*, which is expressed by microglia, is also induced early, and to a greater degree, in neonates. **(D)** The myeloid marker *F4/80* is not strongly induced until 48 hpi and is not induced in an age-specific manner. **(E)** Neonatal expression of the pan T cell marker

Cd3 is higher under mock- and LPS-inoculated conditions at 48 hpi. **(F)** No age-associated differences were observed for *Cd8*, which is expressed by a T cell subset and NKT cells. **(G)** The dendritic cell marker *Itgax* is expressed at higher levels in neonates at early time points, but not significantly more in response to LPS. At 48 hpi, *Itgax* levels are significantly higher in LPS-stimulated weanling mice. **(H)** The neutrophil marker *Ela2* is expressed at higher levels in neonates in response to LPS at 12 and 48 hpi. No statistically significant differences in *Cd80*, *F4/80*, *Slamf7*, *Gfap, Cd8* or *Ela2* levels were observed between PBS-treated neonatal and weanling mice. *Cd3* levels were significantly higher in PBS-treated neonates than in weanling mice at 48 hpi. *Itgax* levels were significantly higher in neonates in response to PBS at 2, 6 and 12 hpi. n = 4-6 mice per group. Data are presented as mean +/- SE. Statistical analysis was completed by two-way analysis of variance with Tukey's multiple comparisons test. Significant age-specific differences in the LPS response are as indicated: *p<0.05, **p<0.01, ***p<0.001, ****p<0.0001

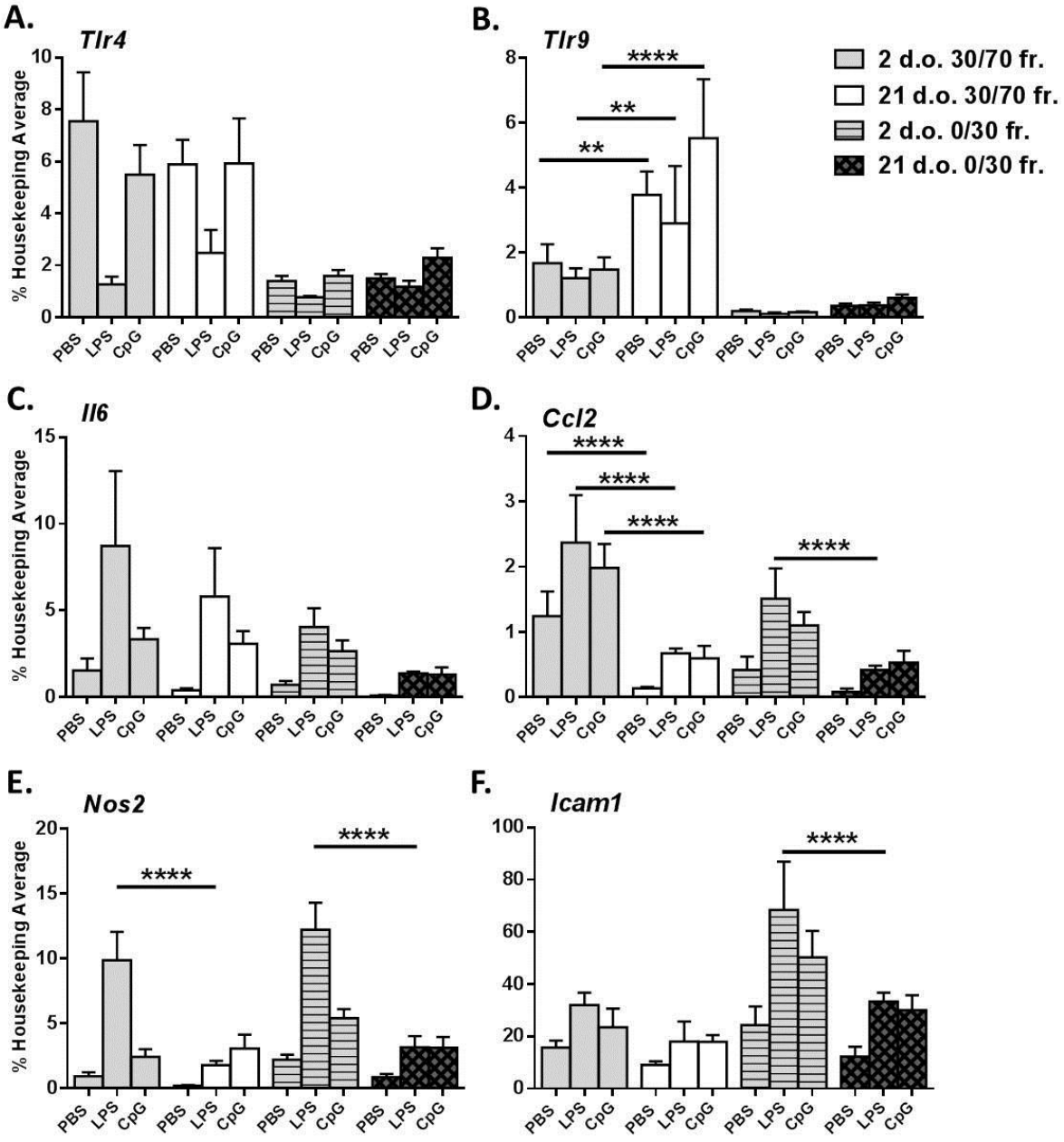

Figure 3.6 Both astrocyte- and microglia-enriched fractions contribute to heightened neonatal expression of inflammatory genes. At 6 hours after IC inoculation with PBS, LPS, or CpG, brain homogenates from neonatal and weanling mice were fractionated on Percoll gradients, and mRNA expression levels were analyzed by qRT-PCR. **(A & B)** *Tlr4* and *Tlr9* are predominantly

expressed in the 30/70 % fraction, which is enriched for microglia. **(A)** *Tlr4* levels did not vary with age. LPS stimulation leads to significant down-regulation of *Tlr4* in neonatal and weanling 30/70 % fractions ($p<0.0001$). A similar trend in *Tlr4* down-regulation is observed in the 0/30% fraction, which is enriched for astrocytes. **(B)** Under all conditions tested, *Tlr9* expression significantly increases with age in the 30/70 % fraction. **(C)** *Il6* production is significantly higher in the neonatal 30/70% fraction, when compared with weanling mice. **(D)** *Ccl2* expression is significantly elevated under all conditions in neonatal 30/70% fractions, as well as the neonatal 0/30% fraction in response to LPS. **(E)** In response to LPS, *iNOS* levels are significantly higher in both neonatal fractions than in weanling fractions. In response to CpG, the 0/30% fraction expresses significantly higher *iNOS* mRNA levels in neonates. **(F)** *Icam1* expression is significantly higher in LPS-stimulated 0/30% fractions. n = 4-5 per group. Data are presented as mean +/- SD. Statistical analysis was completed by two-way analysis of variance with Tukey's multiple comparisons test. Significant age-specific differences in the response to LPS or CpG are as indicated: *$p<0.05$, **$p<0.01$, ***$p<0.001$, ****$p<0.0001$

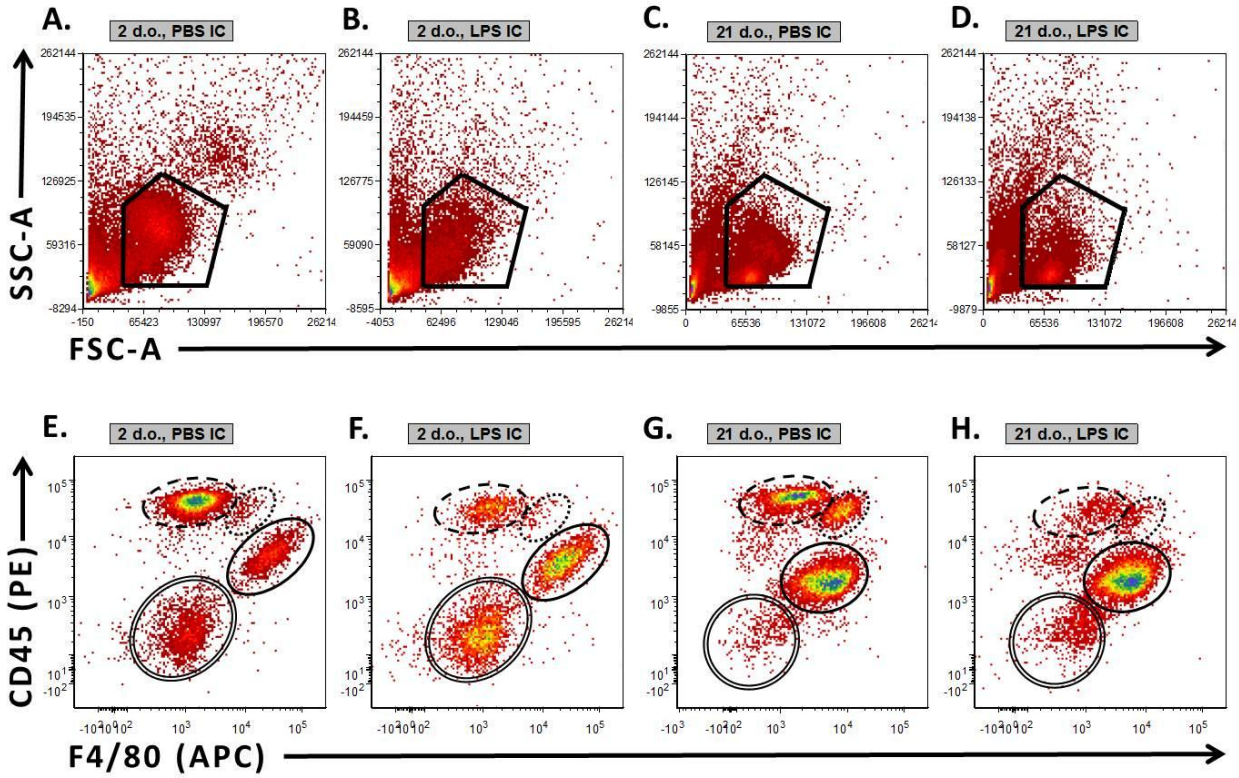

Figure 3.7 Cell population gates used for analysis by flow cytometry. At 6 hours after inoculation, samples were isolated on Percoll gradients, then analysis of CNS immune cell populations was performed using flow cytometry. **(A-D)** Side scatter (SSC) and forward scatter (FSC) were used to create cell gates and exclude debris and apoptotic cells (gate shown). Cell populations were separated by their expression of CD45 and F4/80. **(E-H)** Microglia were identified as $CD45^{lo}$ $F4/80^{+}$ (solid line). Macrophages were identified as $CD45^{hi}$ $F4/80^{+}$ (dotted line). Other immune cells were $CD45^{hi}$ $F4/80^{lo}$ (dashed line). Unstained cells were $CD45^{-}$ $F4/80^{-}$ (double line). Representative samples are shown. **(A & E)** 2 d.o., PBS IC; **(B & F)** 2 d.o., LPS IC; **(C & G)** 21 d.o., PBS IC; **(D & H)** 21 d.o., LPS IC. Circles are for illustrative purposes only and are not the actual cell gates.

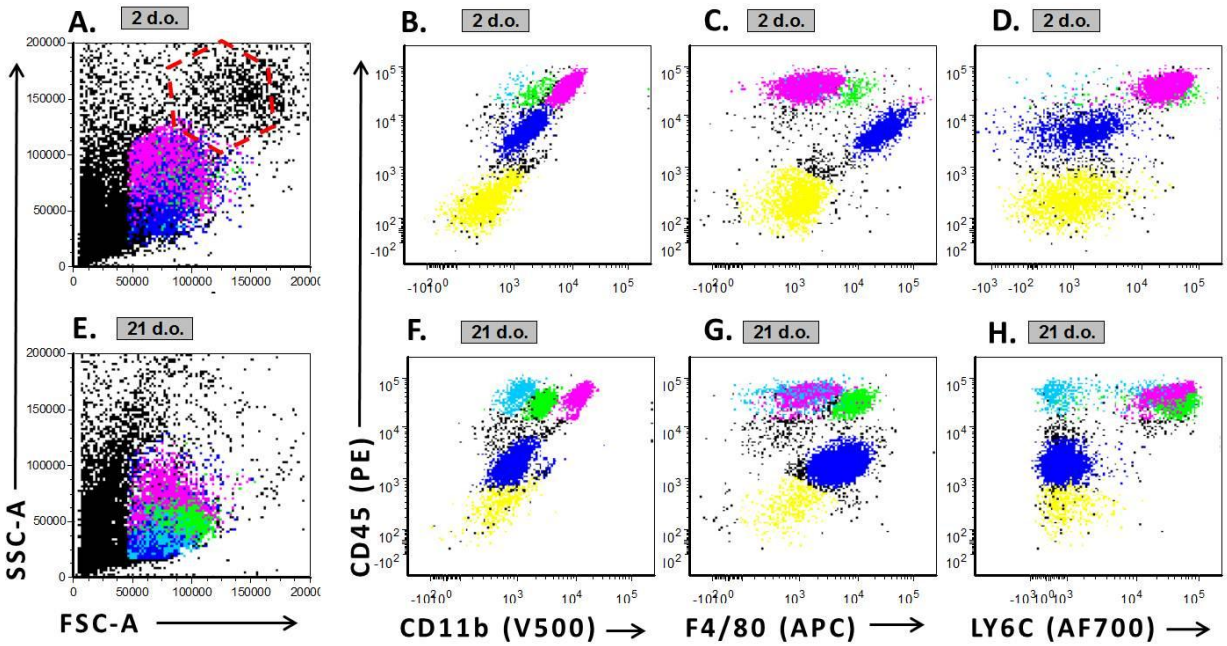

Figure 3.8 CNS immune cell populations. Cell populations could be further distinguished by their **(A & E)** side and forward scatter, **(B & F)** CD11b and **(D & H)** Ly6C expression. **(C & G)** F4/80 expression is also shown. **(B-D, F-H)** For reference, all samples were plotted against CD45 expression on the y-axis. Representative samples from PBS-treated mice are shown. **(A-D)** Neonatal; **(E-H)** Weanling. Cell populations are color-coded: $CD45^{lo}$ $F4/80^{+}$ microglia (blue), $CD45^{hi}$ $F4/80^{+}$ macrophages (green), $CD45^{hi}$ $F4/80^{lo}$ immune cells (aqua and pink), $CD45^{-}$ $F4/80^{-}$ cells (yellow).

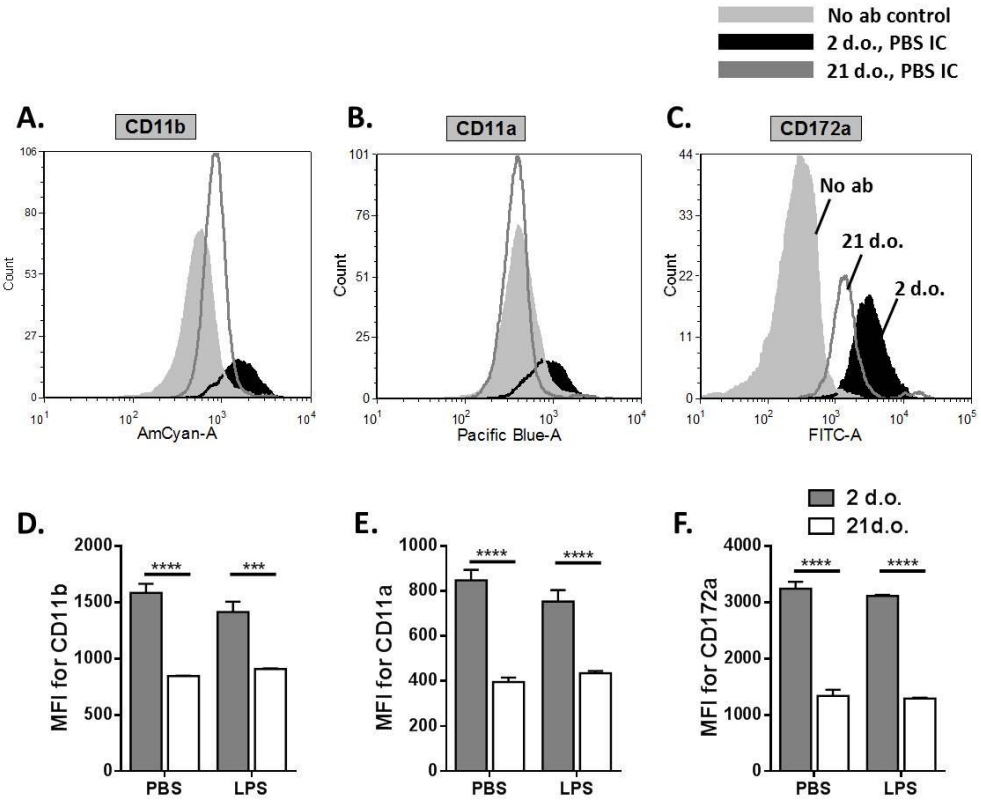

Figure 3.9 Increased expression of activating and inhibitory markers on neonatal microglia. Microglial populations were analyzed *ex vivo* at 6 hpi after IC PBS or LPS inoculation. Neonatal microglia exhibit increased expression of **(A & D)** CD11b, **(B & E)** CD11a and **(C & F)** CD172a. Histograms in **(A-C)** show representative PBS-treated neonatal and weanling samples, as well as unstained control. Mean fluorescence intensity (MFI) after PBS or LPS treatment is plotted for each antigen in **(D-F).** Protein levels differed significantly in an age-dependent, but LPS-independent, manner at this time point. Data was reproduced in an additional experiment that used lower antibody concentrations. n = 2-3 mice per group. Data are presented as mean +/- SD. Statistical analysis was completed by two-way analysis of variance with Tukey's multiple comparisons test. Significant age-specific differences are as indicated: **p<0.01, ***p<0.001, ****p<0.0001

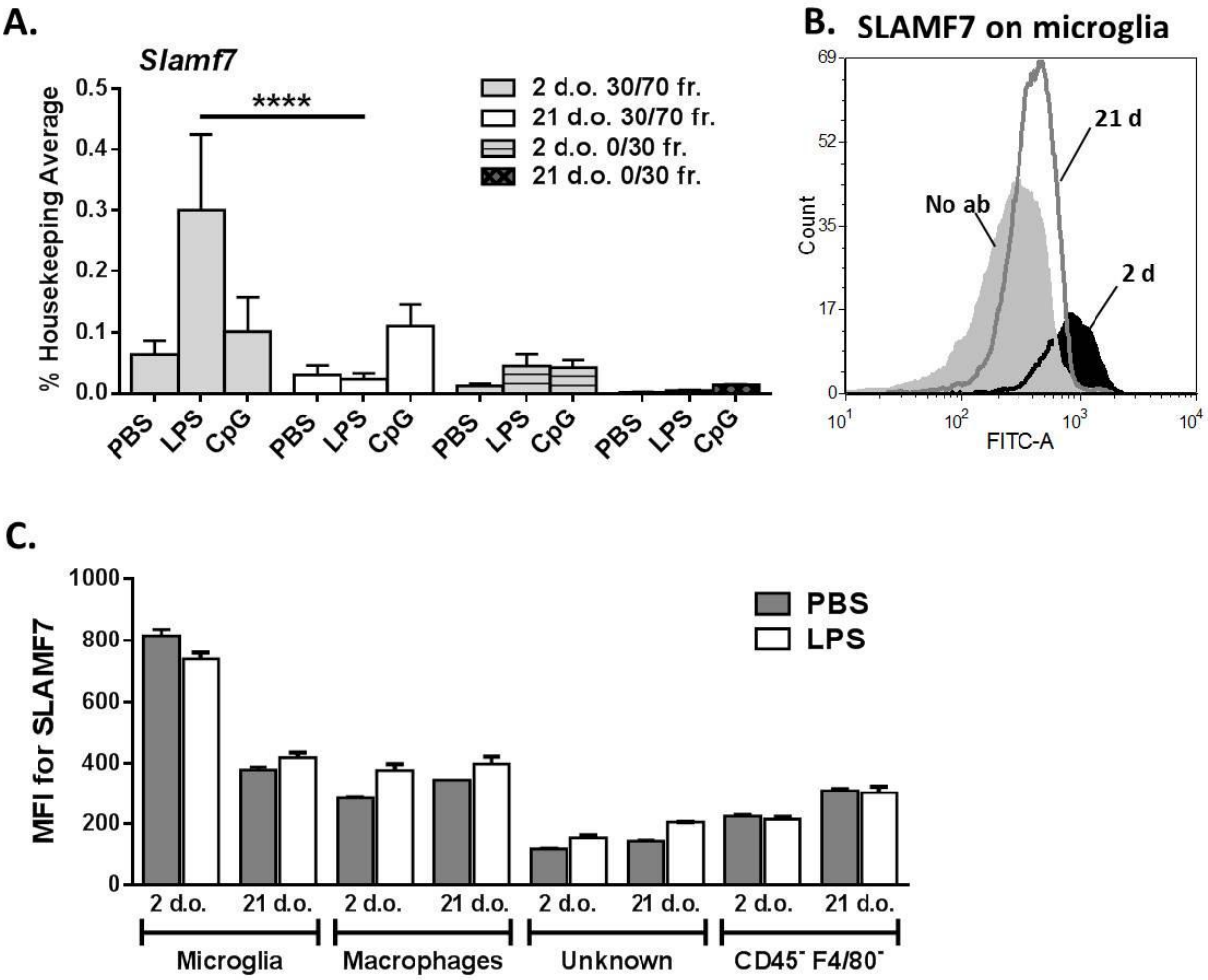

Figure 3.10 SLAMF7 is strongly expressed by neonatal microglia. (A) *Slamf7* expression in neonatal and weanling Percoll gradient fractions in shown at 6 hours after IC stimulation with PBS, LPS or CpG. *Slamf7* was significantly induced in the neonatal 30/70% LPS-stimulated fraction. A similar trend was observed, but to a lesser extent, in the weanling 30/70% CpG-stimulated fraction. Statistical analysis was completed by two-way analysis of variance with Tukey's multiple comparisons test. n=4-5 per group. **(B)** SLAMF7 mean fluorescence intensity (MFI) for neonatal and weanling populations separated by CD45 and F4/80 staining (see Figure 3.7). 'Unknown' refers to CD45hi population. Expression of SLAMF7 was significantly elevated

in neonatal microglia when compared with other populations shown ($p<0.0001$). Statistical analysis was completed by two-way analysis of variance with Dunnett's multiple comparisons test and Tukey's multiple comparisons test. n=2-3 per group.

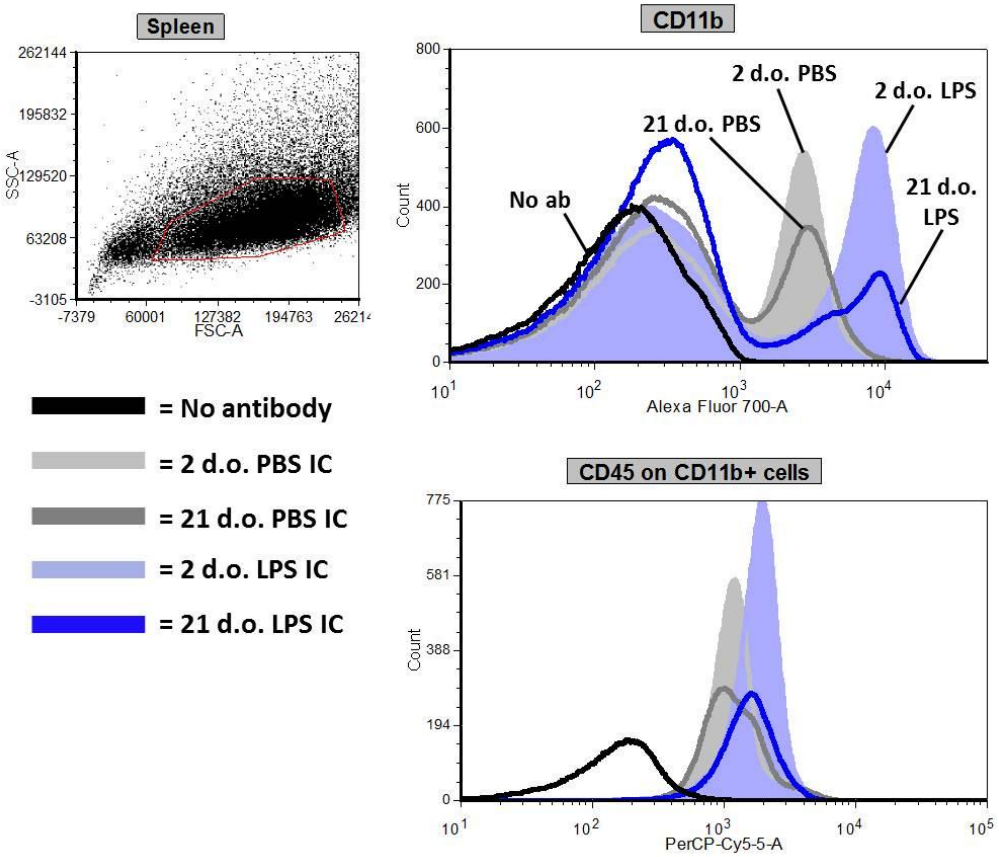

Figure 3.11 Increased expression of CD11b in the spleen after IC LPS. Forward scatter and side scatter were used to gate on cells (red line) in the spleen. CD11b expression is shown for representative neonatal and weanling spleen samples after IC treatment with PBS or LPS. CD45 expression is shown for $CD11b^{+}$ populations only. Splenic CD11b and CD45 expression was analyzed in two independent experiments in weanling mice and one experiment in neonatal mice.

CHAPTER FOUR

PRION PROTEIN AND THE NEUROINFLAMMATORY RESPONSE TO TOLL-LIKE RECEPTOR 4 AND 9 STIMULATION IN YOUNG MICE

Introduction

PrP^c is expressed in most tissues but expression is highest in neurons (Bendheim et al., 1992). There are also significant PrP^c levels in microglia, astrocytes and many peripheral immune cell types (Arantes et al., 2009; Brown et al., 1998; Dodelet and Cashman, 1998; J. D. Isaacs, 2006). PrP^c is developmentally regulated (Lazarini et al., 1991; Lieberburg, 1987; Manson et al., 1992; Moser et al., 1995) and influences neuronal survival, astrocyte development, and the acute stress response (Arantes et al., 2009; Lima et al., 2007; Nico et al., 2005). However, PrP knock out ($PrP^{-/-}$) mice do not exhibit any gross phenotypic abnormalities (Bueler et al., 1992; Manson et al., 1994) and the precise role of PrP^c remains poorly defined.

PrP^c expression is differentially regulated in activated immune cells and influences several aspects of immune cell function. PrP^c expression regulates macrophage phagocytosis and stimulates signaling pathways involved in phagocytosis, cellular migration and cytokine production *in vitro* (de Almeida et al., 2005; Krebs et al., 2006). Dendritic cell expression of PrP^c is required for dendritic cell activation of T cells (Ballerini et al., 2006). *In vivo*, PrP^c expression alters macrophage phagocytosis and recruitment of immune cells to the site of inflammation in the periphery (de Almeida et al., 2005). Several papers report altered cytokine production in $PrP^{-/-}$ tissues and cells, including reduced production of TNF in injured $PrP^{-/-}$ muscles, less IL-2 and IL-4 production by stimulated $PrP^{-/-}$ splenocytes, and increased IL-6 expression in inflamed $PrP^{-/-}$ colons (Bainbridge and Walker, 2005; Martin et al., 2011; Stella et al.).

Despite the high expression of PrP^{c} in the central nervous system (CNS) and the influence of PrP^{c} over the immune response, research examining the role of PrP^{c} in the neuroimmune response is limited. In cultured microglia, PrP^{c} expression is proportional to the degree of microglial proliferation and activation, with $PrP^{-/-}$ microglia being the least responsive to activation (Brown et al., 1996; Brown et al., 1998; Herms et al., 1997). Nasu-Nishimura *et al.* reported that $PrP^{-/-}$ mice infected with encephalomyocarditis viral (ECMV) display reduced microglial activation and recruitment of peripheral immune cells into the brain when compared with wild-type (WT) mice (Nasu-Nishimura et al., 2008). PrP^{c} exerts a neuroprotective effect in the CNS in response to sterile inflammation caused by ischemia (McLennan et al., 2004; Sakurai-Yamashita et al., 2005).

In the present study, we examined how PrP^{c} influences the neuroinflammatory response *in vivo* using a model system that activates Toll-like receptor (TLR) signaling pathways. TLRs activate the innate immune system through binding to conserved molecular patterns associated with both infection and sterile inflammation. We chose to use the TLR9 ligand, CpG-rich DNA (CpG), and the TLR4 ligand, lipopolysaccharide (LPS), both of which also bind PrP^{c}. PrP^{c} binds nucleic acids with high affinity but low specificity (Cordeiro et al., 2001; Gabus et al., 2001; Weiss et al., 1997). DNA binding leads to conformational changes and aggregation of the prion protein (Cordeiro et al., 2001; Nandi et al., 2002; Yin et al., 2008). Additionally, nucleic acid and phosphorothioated nucleic acid binding to prion protein causes internalization of the PrP:DNA complex while PrP^{c} expression promotes uptake of DNA (Kocisko et al., 2006; Yin et al., 2008). Such molecules can also strongly influence conversion of PrP^{c} to PrP^{Sc} both *in vivo* and *in vitro* (Cordeiro et al., 2001; Deleault et al., 2003; Kocisko et al., 2006). LPS binds PrP^{c} under

conditions of normal and low pH (Pasupuleti et al., 2009) and is reported to up-regulate PrP^c expression in spleens, as well as in macrophage and microglial cell lines (Gilch et al., 2007; Lotscher et al., 2007).

Here, we have tested whether PrP^c influences cytokine production and glial activation in response to TLR stimulation with LPS or CpG by comparing responses in WT, $PrP^{-/-}$, and Tg7 mice. In Tg7 mice, mouse prion protein has been knocked out and hamster prion protein, which is similar in sequence, in expressed at three to four fold higher levels than normal. We examined these responses shortly following birth, when mice are undergoing rapid neurological development, and at 21 days, when physiological levels of PrP^c are higher in the brain.

Results

PrP^c expression in the brain changes with age but not in response to LPS or CpG stimulation

As the $PrP^{-/-}$ mice that we used had been bred extensively onto the C57Bl/10 background, we used WT C57Bl/10 mice as our PrP^C positive controls. Tg7 PrP^c overexpressing mice were also on a C57Bl/10 background and overexpress hamster PrP^c, which is similar in sequence to mouse PrP^c. We examined the neuroinflammatory response in neonatal (2 d.o.) and weanling (21 d.o.) mice because the developmental increase in brain *Prnp* expression leveled off at 21 days of age in C57Bl/6 mice (Lazarini et al., 1991). However, when we later looked at *Prnp* mRNA levels in WT C57Bl/10 mice from 2 to 42 days of age using quantitative real-time PCR (qRT-PCR), we observed that basal brain *Prnp* levels continued to rise over the entire time period examined (Fig 4.1A). Although C57Bl/10 *Prnp* levels increased approximately five-fold in the brain in the first six weeks of life, *Prnp* levels in the peripheral immune organs of

the spleen and thymus remained constant over this period (Fig 4.1A). We also examined whether TLR4 stimulation influenced PrP^{c} expression. *Prnp* mRNA levels in WT mice were monitored by qRT-PCR from 2-48 hpi after TLR4 stimulation in 2 and 21 day old mice (Fig 4.1B). No significant differences in brain PrP^{c} mRNA levels were observed in response to TLR 4 stimulation in mice of either age over the time course examined.

Tlr4 and Tlr9 gene expression is not affected by a lack of PrP^{c} under homeostatic or inflammatory conditions

We next tested whether PrP^{c} influences *Tlr* mRNA expression. Basal mRNA levels of *Tlrs 3, 4, 7, 8* and *9* were examined in the brain, spleen and thymus of WT and $PrP^{-/-}$ mice at 2, 14 and 42 d.o. (Fig 4.2 A-C). Over the time period examined, mRNA levels of *Tlrs 3, 4, 7* and *9* rose four- to six-fold in the brains of both WT and $PrP^{-/-}$ mice, while *Tlr8* levels remained unchanged. Splenic *Tlr* levels increased two- to five-fold in WT and $PrP^{-/-}$ mice while thymic *Tlr* levels were unchanged with age. Lack of PrP^{c} did not significantly influence basal *Tlr* expression in any tissue or time point examined. The effect of $PrP^{-/-}$ on *Tlr4* and *9* mRNA levels after TLR stimulation was also examined (Fig 4.2 D & E). We saw no significant differences in brain *Tlr4* or *Tlr9* mRNA levels between WT and $PrP^{-/-}$ mice of either age in response to LPS or CpG, nor were agonist-specific alterations in *Tlr4* or *Tlr9* levels were detected.

Lack of effect of PrP^{c} expression on cytokine responses to intracerebral TLR4 or TLR9 stimulation

To determine whether PrP^c influences cytokine responses, we treated mice with LPS or CpG by IC inoculation. As controls, mice were either left uninoculated or inoculated with PBS. Cytokine and growth factor protein levels in whole brain homogenates were examined by multiplex bead assay at 12 hpi in WT and $PrP^{-/-}$ neonatal (Fig 4.3) and weanling (Fig 4.4) brain tissue. Although strong inflammatory cytokine induction was observed, no differences in production of the inflammatory cytokines IL-1b, IL-6, IL-12, Cxcl1, Cxcl9, Ccl2 or Ccl3 were detected between WT and $PrP^{-/-}$ brain tissue in 2 or 21 d.o. mice. Additionally, no PrP^c-dependent differences were noted for the anti-inflammatory cytokine IL-10. Similar results were observed for the cytokines IL-1a, IL-2, IL-5 and TNF and the growth factors FGF and VEGF (data not shown). IL-4, IL-13, IL-17, IFNγ and GM-CSF were also assayed but were not present at detectable levels under the conditions tested.

Due to limited quantities of mice available in the Tg7 strain, we only examined the cytokine responses to IC PBS or CpG in weanling mice of this strain. Figure 4.5 shows production of IL-1b, IL-12, CCL3, CXCL9 and CXCL10 in Tg7, WT and $PrP^{-/-}$ brains and is representative of the cytokine responses observed in weanling Tg7 mice. PrP^c overexpression in Tg7 mice did not influence cytokine production in the brain.

In previous studies using the IRW mouse strain, some cytokine levels in the brain remained heightened at 48 and 96 hpi after TLR stimulation (Butchi et al., 2008). Therefore, we also examined neonatal brain homogenates at 48 and 96 hpi to determine whether PrP^c influenced late cytokine responses. However, all cytokines had returned to basal levels in C57Bl/10 WT and $PrP^{-/-}$ mice by 48 hpi (data not shown).

PrP^C expression did not influence glial activation

To test for effects of PrP^C on other aspects of glial activation, we assessed induction of glial activation markers by qRT-PCR in neonatal WT and $PrP^{-/-}$ brains (Fig 4.6). We examined mRNA expression of glial activation markers at 6 and 12 hpi after TLR4 or TLR9 stimulation. However, most mRNAs had returned to basal levels by 12 hpi, so only the 6 hour data are shown here. *Cd80* is expressed by activated microglia while *Nos2*, *Gpr84* and *Icam1* are induced in both microglia and astrocytes in response to neuroinflammation. No significant differences were detected between WT and $PrP^{-/-}$ brains in the mRNA levels of any of the glial activation markers tested.

We also performed histologic analyses of WT and $PrP^{-/-}$ brain sections that were taken at 12, 48 and 96 after inoculation with PBS, LPS, CpG, as well as uninoculated controls. Tissues were stained with hematoxylin and eosin, glial fibrillary acidic protein (GFAP), or ionized calcium binding adaptor molecule 1 (IBA1). No significant differences in inflammation, peripheral immune cell infiltration, astrocytic activation or microglial activation were observed (data not shown).

Discussion

Microglia and astrocytes are the primary immune-responsive cells of the brain and have many overlapping functions, including release of inflammatory and neurotrophic factors and phagocytosis of debris. Prion protein has been demonstrated to influence microglial activation *in vitro* (Brown et al., 1996; Brown et al., 1998; Herms et al., 1997). Astrocytic PrP^C plays a role in both astrocytic and neuronal development (Arantes et al., 2009; Lima et al., 2007). PrP^C has

not yet been shown to influence the immune-specific functions of astrocytes. We hypothesized that PrP^{c} expression would influence the neuroimmune response *in vivo*. However, after measuring several parameters of the neuroinflammatory response, we have not observed any differences between WT, $PrP^{-/-}$ and PrP^{c} overexpressing mice.

The apparent discord between our results and published studies may be because our experiments utilized *in vivo* models while most published studies were restricted to *in vitro* models. Discrepancies between *in vitro* and *in vivo* responses were recently noted by Mariante *et al.*, who observed that TNF up-regulates neutrophil expression of PrP^{c} *in vitro* but not *in vivo* (Mariante et al., 2012). This group also noted that neutrophil, but not brain, PrP^{c} was up-regulated in response to LPS. Another possibility is that PrP^{c} influences the inflammatory response of a specific cell type in wild-type mice but in a manner that is undetectable in $PrP^{-/-}$ mice due to compensation by another molecule or cell type.

It is possible that purified TLR agonist is not sufficient to stimulate PrP^{c}-dependent differences in the neuroinflammatory response. TLR 4 and 9 agonists were chosen because interactions between PrP^{c} and nucleic acids are well-documented and PrP^{c} has recently also been shown to bind LPS. However, upon intracranial inoculation of mice with ECM virus, Nasu-Nishimura *et al.* reported that $PrP^{-/-}$ mice displayed reduced recruitment of peripheral immune cells into the brain and reduced microglial activation when compared with WT cells (Nasu-Nishimura et al., 2008). Since ECM virus infection activates a broader range of immune pattern recognition receptors, it is conceivable that PrP^{c}-dependent modulation of the immune system occurs through a mechanism independent of TLR signaling.

The above PrP^{C}-associated differences were only apparent when using 15 week old mice but not in experiments with 6 week old mice (Nasu-Nishimura et al., 2008). Similarly, Keshet *et al.* found that age influences the activity and subcellular localization of neuronal nitric oxide synthase (nNOS) (Keshet et al., 1999). In 30 day old mice, PrP knock out did not impair nNOS function or localization to lipid rafts. Both localization and enzymatic activity were impaired in 100 day old $PrP^{-/-}$ brains. These results imply that either PrP^{C} influences the neuroinflammatory response only in mature mice, or compensatory mechanisms for mitigating the loss of PrP^{C} decline with age. We did not examine the PrP^{C}-dependent response in mature mice. It is possible that PrP^{C} could influence the TLR response in older mice.

The cellular differentiation state of astrocytes and microglia may influence the function of PrP^{C} within these cell types. Although PrP^{C} is expressed in astrocytes and microglia in young mice, it does not appear to influence the inflammatory response in these cells. PrP^{C} is involved in development of the central nervous system. Conceivably, PrP^{C} in young glial cells could be restricted to developmental functions but in older glial cells takes on immunoregulatory functions.

PrP^{C} and TLR4 share several physiological characteristics. Both PrP^{C} and TLR4 are plasma membrane proteins that migrate into lipid rafts upon ligand binding, which stimulates endocytosis (Husebye et al., 2006; Lee et al., 2007; Marella et al., 2002; Triantafilou et al., 2004). In addition to binding PAMPs, TLRs bind damage-associated molecular patterns (DAMPs), which can elicit an inflammatory response in the absence of infection. Both TLR4 and PrP^{C} interact with the DAMPs heparan sulfate and hyaluronan (Johnson et al., 2002; Pan et al., 2002; Termeer et al., 2002). It is unclear which accessory proteins mediate the transfer of

DAMPs to TLR4. Although we have not found PrP^C to influence the inflammatory response to TLR signaling in response to PAMPs, it is intriguing to consider whether PrP^C could be an accessory protein in TLR4 DAMP signaling.

PrP^C appears to be developmentally regulated in the brain and plays a role in many developmental functions. Additionally, PrP^C has been shown to influence immune cell function, primarily in the periphery. We hypothesized that PrP^C would influence the neuroinflammatory response in young mice, perhaps by acting as a scavenger receptor for TLR ligands. However, in our investigation of the inflammatory response to IC TLR 4 or 9 stimulation, we did not observe PrP^C–dependent differences in the acute neuroinflammatory response, as measured by cytokine production and glial activation.

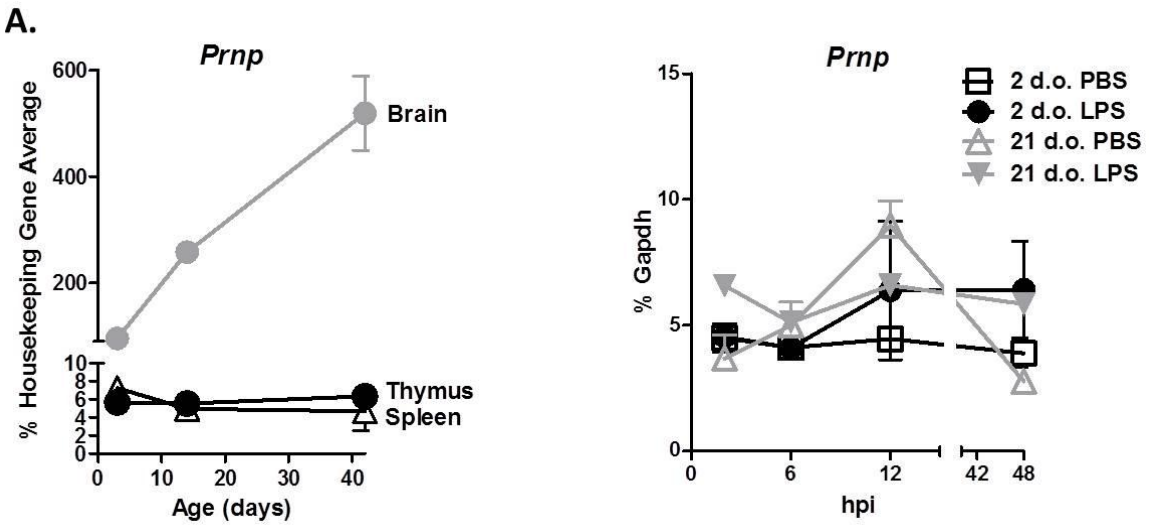

Figure 4.1 Brain PrP^{c} expression is influenced by age but not TLR4 or TLR9 stimulation. (A) Prion protein (*Prnp*) transcript levels were measured in the brain, spleen and thymus of C57Bl/10 WT untreated mice at 2, 14 and 42 days old. Only brain tissue showed an age-dependent increase in *Prnp* expression. Housekeeping gene expression was averaged using *Gusb*, *Actb* and *Rpl32*. n=4-5 per group. **(B)** *Prnp* mRNA levels in WT neonatal and weanling brains were analyzed from 2 to 48 hpi after inoculation with either PBS or LPS. No differences in *Prnp* levels were observed. Data are presented as mean +/- SE. n=5-6 per group.

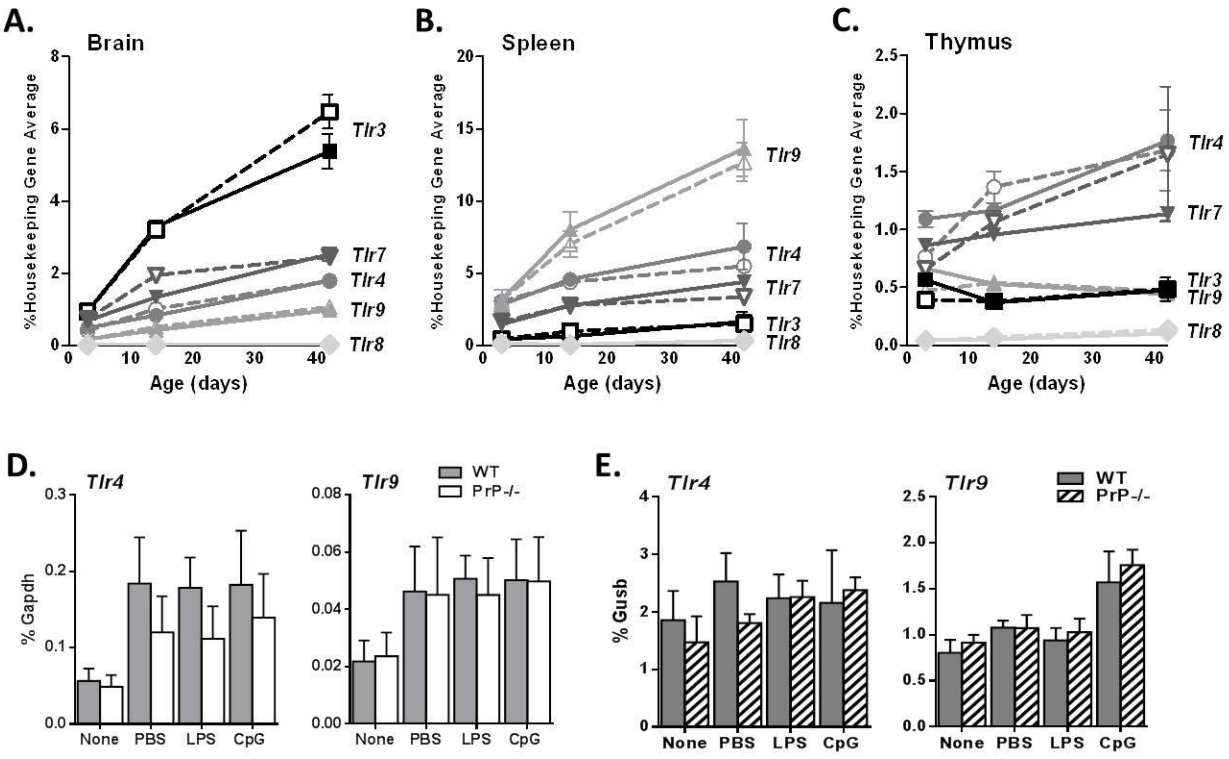

1726

1727 **Figure 4.2 *Tlr* mRNA expression is influenced by age but not PrP^{c} expression.** *Tlr* transcript

1728 levels were measured in the brain **(A)**, spleen **(B)** and thymus **(C)** of WT and PrP$^{-/-}$ untreated

1729 mice at 2, 14 and 42 days old. mRNA expression levels of *Tlrs 3, 4, 7* and *9* increased steadily

1730 with age in the brain and spleen. A similar trend was observed in the thymus for *Tlr4* and *Tlr7*

1731 expression. No differences in basal *Tlr* mRNA levels were observed between WT and PrP$^{-/-}$

1732 tissues. Housekeeping gene expression was averaged using *Gusb*, *Actb* and *Rpl32*. Data are

1733 presented as mean +/- SE. **(D & E)** At 12 hpi after TLR4 or 9 stimulation, *Tlr4* and *Tlr9* mRNA

1734 levels in WT and PrP$^{-/-}$ brains were examined. No significant PrP^{c}-dependent differences were

1735 noted in neonatal **(D)** or weanling **(E)** mice. Data are presented as mean +/- SD. n=3-5 per

1736 group.

1737

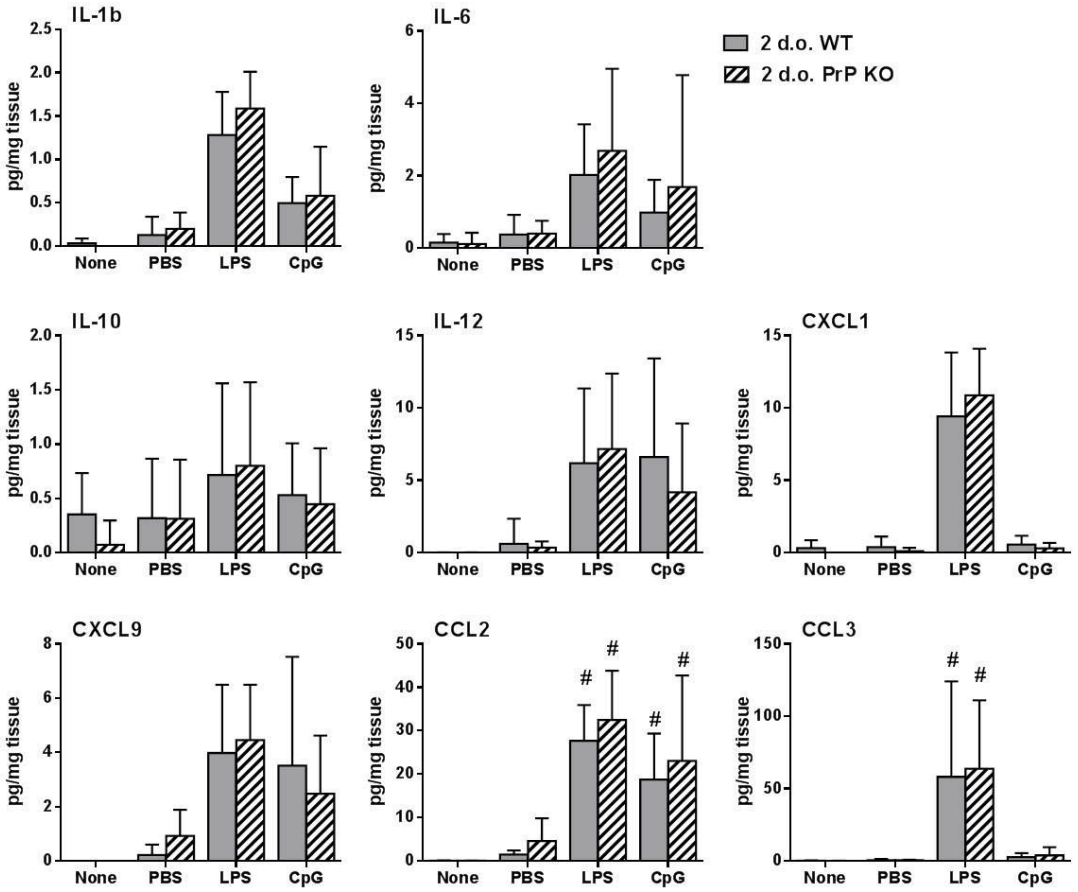

Figure 4.3 PrP^{c} expression does not alter cytokine responses to TLR 4 or 9 stimulation in neonatal brains. WT and PrP$^{-/-}$ mice were inoculated with PBS, LPS or CpG intracerebrally (IC). Uninoculated controls were used as an additional control group. Cytokine protein levels at 12 hpi were measured in neonatal brain tissue by multiplex. Representative cytokines are shown here. WT data was previously shown in Figures 3.1 and 3.2. No significant differences in cytokine production were observed between WT and PrP$^{-/-}$ brains. Data are presented as mean +/- SD. # indicates treatment group contains samples above the dynamic range (based on standard curve). Outliers detected by Grubbs' test were excluded. Statistical analysis was completed by two-way analysis of variance with Sidak's multiple comparisons test. For both

WT and $PrP^{-/-}$ mice, data contain the combined results of two independent experiments. n=10-13 per group.

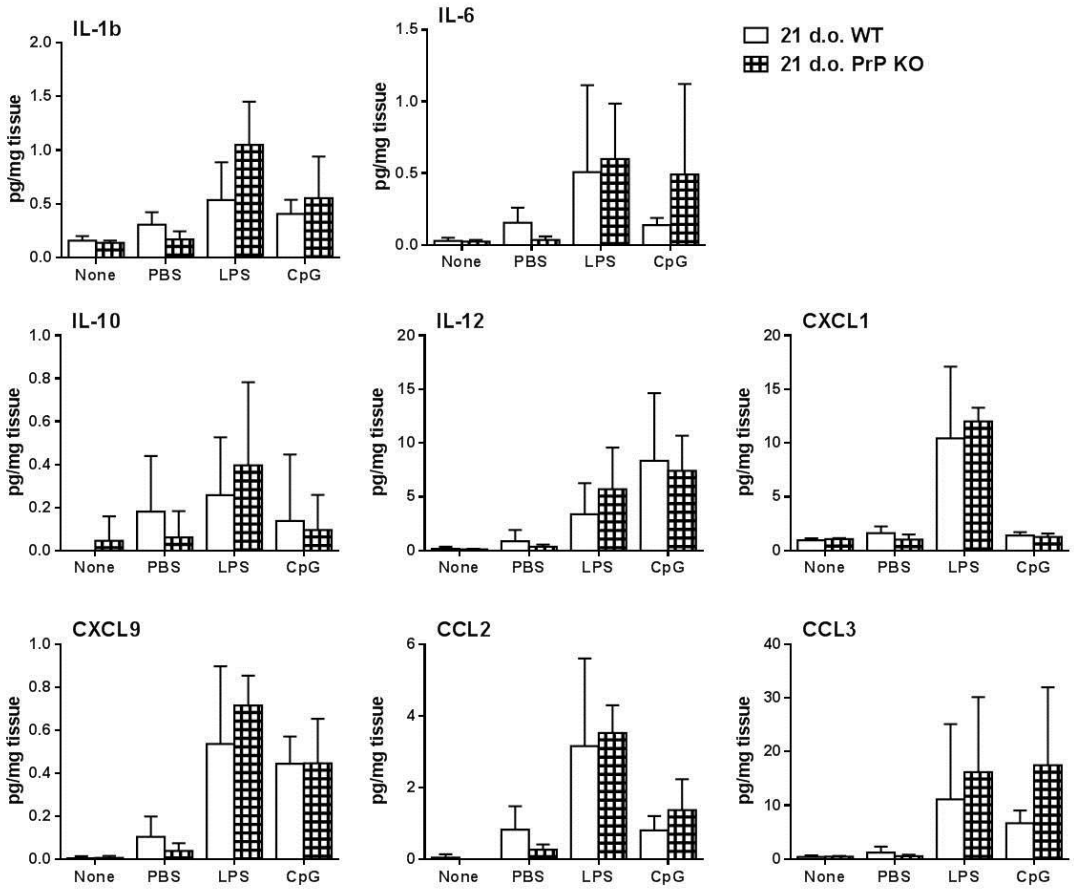

Figure 4.4 PrP^{c} expression does not alter cytokine responses to TLR 4 or 9 stimulation in weanling brains. WT and PrP$^{-/-}$ mice were inoculated with PBS, LPS or CpG intracerebrally (IC). Uninoculated controls were used as an additional control group. Cytokine protein levels at 12 hpi were measured in weanling brain tissue by multiplex. Representative cytokines are shown here. WT data was previously shown in Figures 3.1 and 3.2. No significant differences in cytokine production were observed between WT and PrP$^{-/-}$ tissue. Data are presented as mean +/- SD. Outliers detected by Grubbs' test were excluded. Statistical analysis was completed by two-way analysis of variance with Sidak's multiple comparisons test. n=5-6 per group.

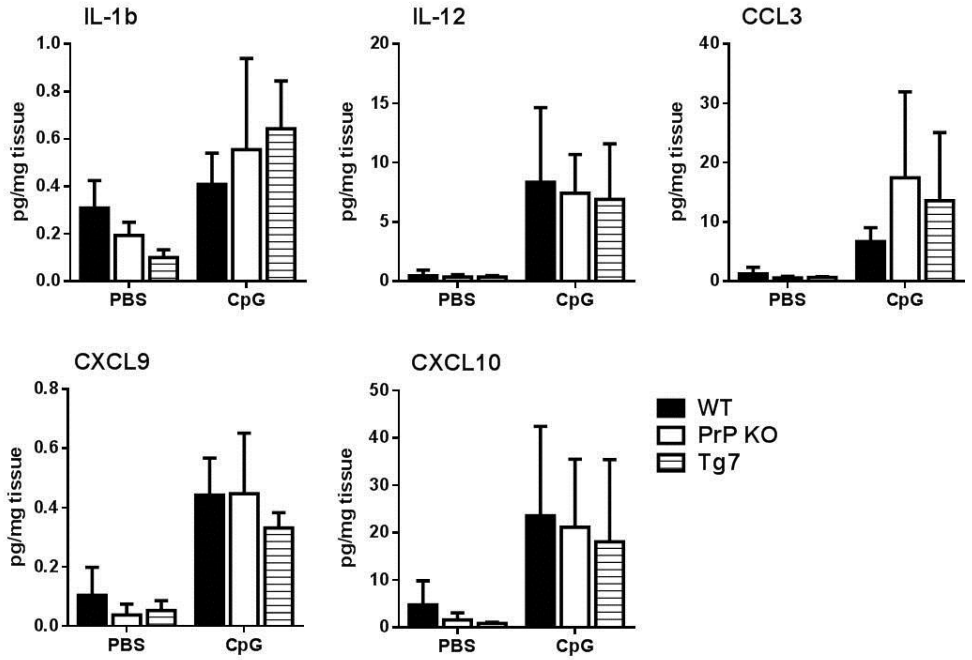

Figure 4.5 PrP^{c} overexpression does not influence cytokine responses to TLR9 stimulation in weanling brains. Cytokine responses in Tg7 PrP^{c} overexpressing mice were compared to responses in WT and PrP$^{-/-}$ weanling mice. WT and PrP$^{-/-}$ data are also shown in Figure 4.5. Brain cytokine levels were measured at 12 hpi by multiplex. Representative data are shown here. No significant differences in cytokine levels were detected between WT, PrP$^{-/-}$ and Tg7 mice. Data are presented as mean +/- SD. Outliers detected by Grubbs' test were excluded. Statistical analysis was completed by two-way analysis of variance with Sidak's multiple comparisons test. n=5-6 per group.

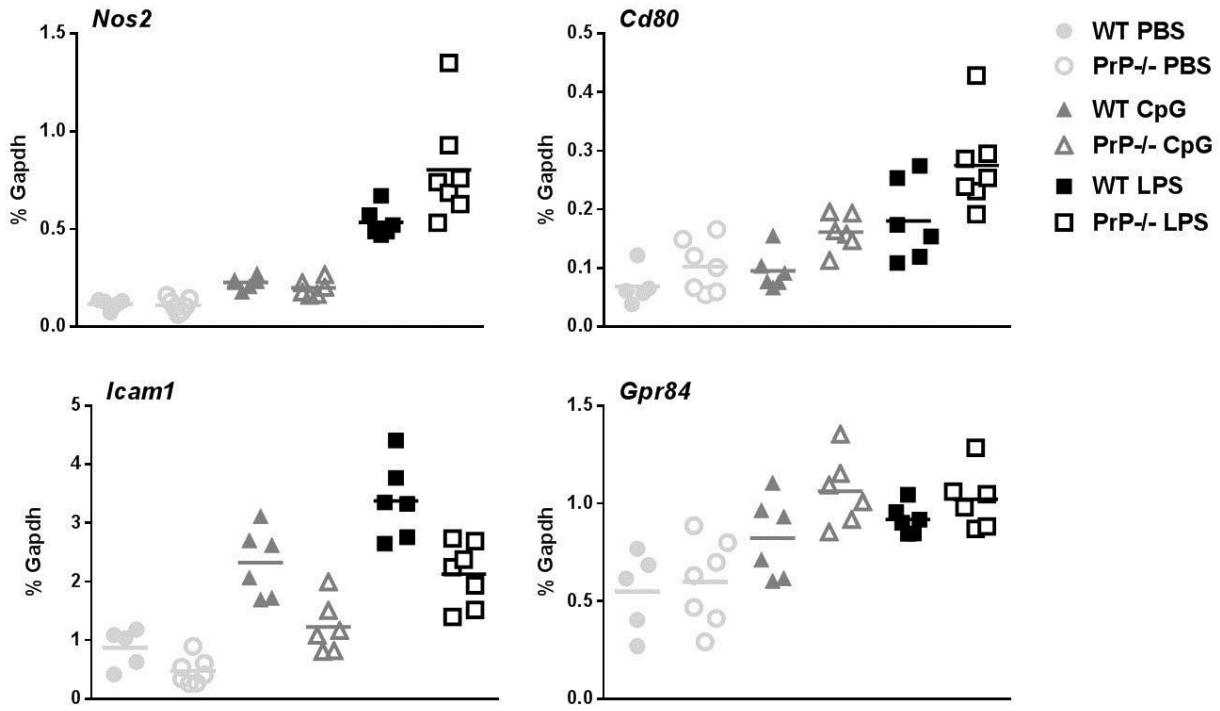

Figure 4.6 PrP expression does not alter expression of glial activation markers in response to LPS or CpG. Expression of astrocytic and microglial activation markers was examined in WT and $PrP^{-/-}$ brains at 6 hours after TLR stimulation. Since a two-fold change is the smallest change that can be observed by qRT-PCR, differences in mRNA expression that were less than two-fold were not considered significant. No significant differences in expression of the glial activation markers *Nos2, Cd80, Icam1* and *Gpr84* were observed between WT and $PrP^{-/-}$ brains. n=5-7 per group.

CHAPTER FIVE

EXPERIMENTAL METHODS

Ethics statement

All animal research was carried out in adherence with protocols approved by the National Institutes of Health Rocky Mountain Laboratories Animal Care and Use Committee.

Animal models and inoculation of TLR agonists

All mice were housed and maintained by the Rocky Mountain Laboratories Veterinary Branch (Hamilton, MT). Mice were maintained under pathogen-free conditions with regular light/dark cycles and given food and water *ad libitum*. WT C57Bl/10 and $PrP^{-/-}$ C57Bl/10 mice were inoculated at 36-48 hours of age. Newborn mice were anaesthetized by hypothermia prior to intracerebral (IC) inoculations using a Hamilton syringe with a 33-gauge needle. Three week old mice were anaesthetized by isofluorane inhalation prior to inoculation. Mice were inoculated once in each hemisphere with a solution volume of 3 µl per hemisphere. Mice were inoculated with one of two TLR agonists, lipopolysaccharide (LPS) or unmethylated CpG-rich oligonucleotides (CpG), or with a phosphate-buffered saline (PBS) control. Mice were weighed and amount of TLR agonist used was based on average weight at each age. For TLR stimulation, mice were inoculated with either 0.5 µg LPS per gram of body weight or 0.125 µg CpG per gram of body weight. For neonatal mice, this meant a total inoculum of 1 µg LPS or 0.25 µg (40 picomoles) CpG. For three week old mice, this translated to 3.8 µg LPS or 0.95 µg CpG. As an

additional control, another group of mice remained completely uninoculated. All experimental and control groups contained mice from multiple litters that were inoculated on different days.

Harvesting of tissues for mRNA and protein analysis

Prior to harvesting of tissues, all animals were anaesthetized by inhalation of isofluorane, followed by axillary incision and cervical dislocation at the specified time point. Brains were snap frozen in liquid nitrogen and stored at -80˚C.

TLR agonists

TLR4 agonist ultra pure LPS (Cat. No. tlrl-3pelps) and TLR9 agonist phosphorothioated CpG type B [5'-tcc atg acg ttc ctg acg tt-3'] (Cat. No. tlrl-1826) were purchased from InvivoGen. Agonist stocks were suspended in endotoxin-free water, aliquoted and stored at -20˚C. Immediately prior to use, agonists were diluted in endotoxin-free, PBS-buffered solution.

Protein quantification

For protein quantification, brains were weighed and homogenized in Bio-Plex cell lysis buffer (Bio-Rad Cat. No. 171-304012) containing PMSF (Sigma Cat. No. P-7626) and Complete Mini Protease Inhibitor Cocktail (Roche Cat. No. 11836153001). Brains in cell lysis buffer were homogenized using Kontes pellet pestles (Fisher Scientific) and diluted to a final concentration of 300 mg/ml wet weight. Samples were centrifuged at 4,500 × *g* for 15 minutes at 4˚C and supernatants collected for further analysis. Cytokine and chemokine protein levels in brain homogenate supernatants were analyzed using the Invitrogen Mouse Cytokine Twenty-Plex

Antibody Bead kit (Cat. No. LMC006) on a Bio-Rad Bio-Plex 200 system. Individual protein concentrations were calculated using standard curves generated from standards provided with the Twenty-Plex kit. IL-6 (Cat. No. M6000B) and CCL2 (Cat. No. MJE00) protein levels were also analyzed using R & D Systems ELISA kits. Individual protein concentrations were calculated using standard curves generated from standards provided with the ELISA kits.

Quantification of mRNA Expression by Real-Time PCR

Total RNA was extracted using the Qiagen RNeasy Mini Kit (Cat. No. 74106) per manufacturer's instructions. RNA was then treated with DNase (Ambion Cat. No. AM2224) for 30 min at 37˚C, followed by a final purification and concentration using the Zymo Research RNA Clean-up kit (Cat. No. R1018). Complimentary DNA (cDNA) was generated from the isolated RNA using the iScript cDNA Synthesis kit (Bio-Rad Cat. No. 170-8891). All primers were designed using Primer3 and were gene-specific in blast searches performed using the National Center for Biotechnology Information database. Real-time PCR was performed using iTAQ SYBR Green Supermix with ROX (Bio-Rad Cat. No. 1725852) on an Applied Biosystems PRISM 7900HT instrument. All samples were run in triplicate. The baseline was automatically set and the C_T was manually set to intersect the mid-log phase of PCR curves at 0.19. Dissociation curves were used to verify that only a single gene product was amplified in each sample. RNA that was not reverse transcribed and water were used as negative controls. Primers used are listed in Table 6.1.

Preparation of brain tissue for flow cytometry

Animals were anaesthetized by inhalation of isofluorane, followed by perfusion through the left ventricle of the heart with ice cold 1x Hank's balanced salt solution (HBSS) without calcium and magnesium (Gibco Cat. No. 14185). Whole brains were removed and sliced into several pieces using a razor. Weanling brain homogenates were then Dounce homogenized while neonatal brain homogenates were triturated using a 5 ml pipet. Neonatal and weanling brain homogenates were further triturated using a 20G needle. For samples that were enzymatically digested, brain homogenates were incubated in 0.05% Collagenase D (Roche Cat. No. 11 088 882 001), 0.09 U/ml Dispase I (Sigma Cat. No. D4818) and 0.025 U/ml DNase I (Sigma Cat. No. D4527) in 1x HBSS at room temperature for 30 minutes with continuous rocking. Neonatal tissue was digested in 5 mls per brain, 10 mls per brain was used for weanling tissue. Vigorous pipetting was used to dislodge any cells that may have adhered to the sides of tubes during enzymatic digestion. Cell suspensions were then placed on 0/30/70% Percoll gradients. Percoll (Sigma Cat. No. P4937) was diluted to the appropriate concentration using HBSS. One Percoll gradient was used per neonatal brain and two Percoll gradients per weanling brain. After centrifugation for 20 minutes at 4° C, the fraction at the 30/70% interface was removed for further analysis of CNS immune cells. For samples that were prepared using myelin depletion columns, brain homogenates were pre-incubated with myelin removal beads (Miltenyi Biotec Cat. No. 130-094-544) following manufacturer's instructions. One neonatal brain homogenate was placed on an LS column (Miltenyi Biotec Cat. No. 130-042-401) while two LD columns (Miltenyi Biotec Cat. No. 130-042-901) were used per weanling brain homogenate.

Flow cytometric analysis of CNS populations *ex vivo*

After generation of single cell suspensions using either enzymatic digestion and Percoll gradients, or myelin depletion columns, cells were then counted by hemocytometer. Aqua Live/Dead staining (Life Technologies Cat. No. L34657) was performed at this time on some samples. During development of the flow cytometry protocol, as described in Chapter 4, samples of the same age and treatment group were pooled. For flow cytometry experiments described in Chapter 2, samples were not pooled, permitting the analysis of biological replicates. Neonatal and weanling samples that were compared to one another were examined in the same experiment, as were PBS- and LPS-treated samples. Samples were plated onto 96-well plates. Similar numbers of cells were added to each well. Cells were fixed in 2% paraformaldehyde, then permeabilized in 0.1% saponin/2% bovine serum albumin (BSA)/1x PBS. Samples were incubated in an F_C blocking solution containing rat anti-mouse CD16/CD32 Fcγ III/II antibody (BD Pharmingen Cat. No. 553142) in 2% donkey serum/0.1% saponin/2% BSA/1x PBS. Cells were incubated with fluorescently-conjugated antibodies at room temperature. After washing twice, cells were resuspended in PBS and analyzed on a FACSAria flow cytometer (BD Biosciences) using FACSDiva software (BD Biosciences). Data were analyzed using FCS Express. A list of antibodies used is given in Table 6.2.

Harvesting and preparation of spleen tissue for flow cytometry

Spleens were Dounce homogenized, then incubated in Ammonium-Chloride-Potassium (ACK) buffer to lyse red blood cells. Samples were then centrifuged, resuspended in PBS, and single cell suspensions were prepared for flow cytometry as described for brain cells (above).

1924 **Table 6.1 Primers used for qRT-PCR**

Gene name	Forward primer	Reverse primer
Actb	CAGCTTCTTTGCAGCTCCTT	CACGATGGAGGGGAATACAG
Rpl32	ACATCGGTTATGGGAGCAAC	CACCTCCAGCTCCTTGACAT
Gapdh	AACGACCCCTTCATTGAC	TCCACGACATACTCAGCA
Gusb	CAATGAGCCTTCCTCTGCTC	CTGCATCATATTTGGCGTTG
Cd3e	GAGCACCCTGCTACTCCTTG	TGAGCAGCCTGATTCTTTCA
Cd80	CCTTGCCGTTACAACTCTCC	CAGGCCCAGGATGATAAGAG
Cd8a	TCAGTTCTGTCGTGCCAGTC	GCCGACAATCTTCTGGTCTC
Ela2	CTTCGAGAATGGCTTTGACC	ACGTTGGCGTTAATGGTAGC
F4/80	ACAAGTGTCTCCCTCGTGCT	AACAT GTGCTTTCCACAGTC
Gfap	CGTTTCTCCTTGTCTCGAATGAC	TCGCCCGTGTCTCCTTGA
Gpr84	CTGACTGCCCCTCAAAAGAC	GGAGAAGTTGGCATCTGAGC
Icam1	AGGGCTGGCATTGTTCTCTA	CTTCAGAGGCAGGAAACAGG
Ifnb1	AGCACTGGGTGGAATGAGAC	TCCCACGTCAATCTTTCCTC
IL-6	CCGGAGAGGAGACTTCACAG	TCCACGATTTCCCAGAGAAC
Cxcl10	CAGTGAGAATGAGGGCCATAGG	CTCAACACGTGGGCAGGAT
Itgax	ATGTTGGAGGAAGCAAATGG	TGGGGCTGACTTAGAGGAGA
Ccl2	CCCACTCACCTGCTACT	TCTGGACCCATTCCTTCTTG
Ccl3	ACCATGACACTCTGCAACCA	GATGAATTGGCGTGGAATCT
Nos2	GACGGATAGGCAGAGATTGG	CACATGCAAGGAAGGGAACT
Prnp	GGACCGCTACTACCGTGAAA	TCATCTTCACATCGGTCTCG

Slamf7	GCAGAACTCAGCAATGTCCA	GAAAGCCCAACCTCGATACA
Tlr3	AGCTTTGCTGGGAACTTTCA	ATCGAGCTGGGTGAGATTTG
Tlr4	GGCAGCAGGTGGAATTGTAT	AGGATTCGAGGCTTTTCCAT
Tlr7	GGCATTCCCACTAACACCAC	TTGGACCCCAGTAGAACAGG
Tlr8	TCGTCTTGACCATTTGTGGA	AATGCTCCATTTGGGATTTG
Tlr9	ACTTCGTCCACCTGTCCAAC	TCATGTGGCAAGAGAAGTGC
Tnf	CCACCACGCTCTTCTGTCTAC	GAGGGTCTGGGCCATAGAA

Table 6.2 Antibodies used for flow cytometry

Antigen	Clone	Vendor	Cat. No.
CD11a-eFluor450	M17/4	eBiosciences	48-0111
CD11b-AF700	M1/70	eBiosciences	56-0112-82
CD11b-V500	M1/70	BD Horizon	562127
CD172a-FITC	P84	BD Pharmingen	560316
CD200R-PerCP-eFluor710	OX110	eBiosciences	46-5201
CD45-PE	30-F11	BD Pharmingen	553081
CD86-AF700	GL1	BD Pharmingen	560581
F4/80-APC	BM8	eBiosciences	17-4801-82
GFAP-AF488	--	Cell Signaling	3655
LY6C-AF700	AL-21	BD Pharmingen	561237
SLAMF7-Fluorescein	--	R&D Systems	FAB4628F

CHAPTER SIX

CONCLUDING REMARKS

In humans, gestational infections have been linked to later neurological illness in offspring. The correlation between infection and neurological illness has been most often made for schizophrenia, a disease that usually does not manifest itself until late adolescence or early adulthood. While such complex neurological diseases cannot be fully reproduced in animal models, specific pathological symptoms can. For example, in animal models of schizophrenia, perinatal immune stimulation can replicate specific behavioral and cognitive disabilities, including the delayed onset.

The underlying mechanisms that may connect early infection with later neurological illness are unknown. In humans, a variety of infectious agents, including viruses, bacteria and parasites have been associated with neurological illness. In animal models, inoculation with infectious agents, TLR ligands or the cytokine IL-6 can lead to neurodevelopmental abnormalities. Collectively, this suggests it is a generalized response to infection that may increase one's risk of neurological illness. In this respect, the developing immune response in the brain is of particular interest.

To better understand how the neonatal immune response differs from other ages, it is helpful to directly compare the response of neonatal immune cells with those from older animals that are known to have a more mature immune system. Since weanling mice are less susceptible to neurological infection than neonatal mice, we compared the neonatal cytokine response to IC TLR4 or TLR9 stimulation with that of weanling mice.

In our comparisons of the cytokine response at each age, we found that production of many cytokines was increased in neonatal brains. This included pro-inflammatory cytokines that are elevated in a variety of neurological conditions, such as IL-1b, TNF and IL-6, as well as cytokines whose roles in neuroimmunity are not well characterized, such as IL-5. While some of these cytokines, such as IL-6, have previously been linked to neurodevelopmental illness in animal models of disease, others, such as IL-5, have not. Knowledge of cytokines that are elevated during the neonatal neuroinflammatory response may lead to important insights into their impact on neurodevelopment. The neonatal cytokine response we observed in the brain differed from what has been reported in some other tissues after TLR stimulation, including the ability to produce large amounts of strongly pro-inflammatory cytokines such as IL-1b and TNF. In future studies, it will be interesting to directly compare the production of these cytokines in the brains and peripheral tissues of neonates. It is somewhat surprising that their expression would be inhibited to a greater extent in peripheral tissues, than in the brain, where there is a greater risk of long-term damage.

Microglia and astrocytes are important immune- and TLR-responsive cells in the brain parenchyma. In addition, macrophages inhabit the perivascular spaces surrounding brain tissue. We sought to characterize the expression of activating and inhibitory receptors on these cells at each age. Although we came up against several unexpected obstacles in our attempts to characterize CNS immune-responsive populations ex vivo using flow cytometry, we did observe age-specific differences in expression of activating β_2-integrins and inhibitory CD172a on microglia. Rather unexpectedly, considering the more amoeboid phenotype of neonatal microglia, neonatal microglia did not express increased amounts of all activating proteins

examined, nor did they express lower levels of some of the inhibitory proteins examined, when compared with weanling microglia. In future studies, it would be interesting to directly compare regulation of microglial activation at each age, as our data could suggest some age-dependent differences in microglial regulation.

We also noted relatively high expression of SLAMF7 on neonatal microglia. Since many immunoregulatory proteins are expressed at lower levels on microglia than on other immune cell populations, it will be particularly interesting to examine how SLAMF7 influences neonatal microglial activation, as it may be particularly important for their function. Since microglial SLAMF7 has not been previously described, and SLAMF7 can have both activating and inhibitory functions, its role in microglial physiology is not immediately clear.

In addition, we observed age-specific differences in the ratios of different $CD45^{hi}$ populations in the brain, which could have important consequences for the immune response under a variety of conditions at each age.

REFERENCES

Ackman, J.B., et al., 2006. Fusion of microglia with pyramidal neurons after retroviral infection. Journal of Neuroscience. 26**,** 11413-11422.

Airaksinen, M.S., Saarma, M., 2002. The GDNF family: Signalling, biological functions and therapeutic value. Nat Rev Neurosci. 3**,** 383-394.

Aksoy, E., 2006. Interferon regulatory factor 3-dependent responses to lipopolysaccharide are selectively blunted in cord blood cells. Blood.

Alliot, F., Godin, I., Pessac, B., 1999. Microglia derive from progenitors, originating from the yolk sac, and which proliferate in the brain. Developmental Brain Research. 117**,** 145-152.

Angelone, D.F., et al., 2006. Innate immunity of the human newborn is polarized toward a high ratio of IL-6/TNF-alpha production in vitro and in vivo. Pediatric Research. 60**,** 205-209.

Arantes, C., et al., 2009. Prion protein and its ligand stress inducible protein 1 regulate astrocyte development. GLIA. 57**,** 1439-1449.

Auffray, C., et al., 2007. Monitoring of blood vessels and tissues by a population of monocytes with patrolling behavior. Science. 317**,** 666-670.

Azevedo, F.A.C., et al., 2009. Equal numbers of neuronal and nonneuronal cells make the human brain an isometrically scaled-up primate brain. Journal of Comparative Neurology. 513**,** 532-541.

Bainbridge, J., Walker, K.B., 2005. The normal cellular form of prion protein modulates T cell responses. Immunology Letters. 96**,** 147-150.

Ballerini, C., et al., 2006. Functional implication of cellular prion protein in antigen-driven interactions between T cells and dendritic cells. Journal of Immunology. 176**,** 7254-7262.

Barres, B.A., 2008. The Mystery and Magic of Glia: A Perspective on Their Roles in Health and Disease. Neuron. 60**,** 430-440.

Barton, G.M., Kagan, J.C., 2009. A cell biological view of Toll-like receptor function: regulation through compartmentalization. Nature Reviews Immunology. 9**,** 535-542.

Bechmann, I., et al., 2001. Turnover of rat brain perivascular cells. Experimental Neurology. 168**,** 242-249.

Bechmann, I., Galea, I., Perry, V.H., 2007. What is the blood-brain barrier (not)? Trends in Immunology. 28**,** 5-11.

Belderbos, M.E., et al., 2009. Skewed pattern of Toll-like receptor 4-mediated cytokine production in human neonatal blood: Low LPS-induced IL-12p70 and high IL-10 persist throughout the first month of life. Clinical Immunology. 133**,** 228-237.

2048 Bendheim, P.E., et al., 1992. NEARLY UBIQUITOUS TISSUE DISTRIBUTION OF THE SCRAPIE AGENT
2049 PRECURSOR PROTEIN. Neurology. 42**,** 149-156.

2050 Bessis, A., et al., 2007. Microglial control of neuronal death and synaptic properties. GLIA. 55**,** 233-238.

2051 Beyer, M., et al., 2012. High-Resolution Transcriptome of Human Macrophages. PLoS ONE. 7.

2052 Bilbo, S.D., Schwarz, J.M., 2009. Early-life programming of later-life brain and behavior: a critical role for
2053 the immune system. Frontiers in Behavioral Neuroscience. 3.

2054 Bischoff, T., et al., 2011. Definition of Leukocyte Subsets in Primate Central Nervous System by
2055 Polychromatic Flow Cytometry. Cytometry Part A. 79A**,** 436-445.

2056 Bolin, L.M., et al., 2005. Differential inflammatory activation of IL-6 (-/-) astrocytes. Cytokine. 30**,** 47-55.

2057 Bonthius, D.J., Perlman, S., 2007. Congenital viral infections of the brain: Lessons learned from
2058 lymphocytic choriomeningitis virus in the neonatal rat. PLoS Pathogens. 3**,** 1541-1550.

2059 Botelho, R.J., et al., 2000. Localized biphasic changes in phosphatidylinositol-4,5-bisphosphate at sites of
2060 phagocytosis. Journal of Cell Biology. 151**,** 1353-1367.

2061 Brown, A.S., et al., 2005. Maternal exposure to toxoplasmosis and risk of schizophrenia in adult
2062 offspring. American Journal of Psychiatry. 162**,** 767-773.

2063 Brown, D.R., Schmidt, B., Kretzschmar, H.A., 1996. Role of microglia and host prion protein in
2064 neurotoxicity of a prion protein fragment. Nature. 380**,** 345-347.

2065 Brown, D.R., et al., 1998. Microglial expression of the prion protein. NeuroReport. 9**,** 1425-1429.

2066 Bueler, H., et al., 1992. NORMAL DEVELOPMENT AND BEHAVIOR OF MICE LACKING THE NEURONAL
2067 CELL-SURFACE PRP PROTEIN. Nature. 356**,** 577-582.

2068 Bueler, H., et al., 1993. MICE DEVOID OF PRP ARE RESISTANT TO SCRAPIE. Cell. 73**,** 1339-1347.

2069 Butchi, N.B., et al., 2008. Analysis of the neuroinflammatory response to TLR7 stimulation in the brain:
2070 Comparison of multiple TLR7 and/or TLR8 agonists. Journal of Immunology. 180**,** 7604-7612.

2071 Butchi, N.B., Du, M., Peterson, K.E., 2010. Interactions Between TLR7 and TLR9 Agonists and Receptors
2072 Regulate Innate Immune Responses by Astrocytes and Microglia. GLIA. 58**,** 650-664.

2073 Butchi, N.B., et al., 2011. TLR7 and TLR9 Trigger Distinct Neuroinflammatory Responses in the CNS.
2074 American Journal of Pathology. 179**,** 783-794.

2075 Cao, Z.D., et al., 1996. TARF6 is a signal transducer for interleukin-1. Nature. 383**,** 443-446.

2076 Cardona, A.E., et al., 2006. Isolation of murine microglial cells for RNA analysis or flow cytometry. Nat.
2077 Protocols. 1**,** 1947-1951.

2078 Carson, M.J., et al., 2006. CNS immune privilege: hiding in plain sight. Immunological Reviews. 213**,** 48-
2079 65.

2080 Carvey, P.M., 2003. Prenatal Exposure to the Bacteriotoxin Lipopolysaccharide Leads to Long-term
2081 Losses of Dopamine Neurons in Offspring: A Potential, New Model of Parkinson's Disease.
2082 Frontiers in Bioscience. 8**,** s826-837.

2083 Caughey, B., et al., 2009. Getting a grip on prions: Oligomers, amyloids, and pathological membrane
2084 interactions. In: Annual Review of Biochemistry. Vol. 78, ed.^eds., pp. 177-204.

2085 Chelvarajan, L., et al., 2007. Molecular mechanisms underlying anti-inflammatory phenotype of neonatal
2086 splenic macrophages. Journal of Leukocyte Biology. 82**,** 403-416.

2087 Chelvarajan, R.L., et al., 2004. Defective macrophage function in neonates and its impact on
2088 unresponsiveness of neonates to polysaccharide antigens. Journal of Leukocyte Biology. 75**,** 982-
2089 994.

2090 Chen, G.H., et al., 2011. Acceleration of age-related learning and memory decline in middle-aged CD-1
2091 mice due to maternal exposure to lipopolysaccharide during late pregnancy. Behavioural Brain
2092 Research. 218**,** 267-279.

2093 Chinnery, H.R., Ruitenberg, M.J., McMenamin, P.G., 2010. Novel characterization of monocyte-derived
2094 cell populations in the meninges and choroid plexus and their rates of replenishment in bone
2095 marrow chimeric mice. Journal of neuropathology and experimental neurology. 69**,** 896-909.

2096 Clancy, B., Darlington, R.B., Finlay, B.L., 2001. Translating developmental time across mammalian
2097 species. Neuroscience. 105**,** 7-17.

2098 Clancy, B., et al., 2007a. Extrapolating brain development from experimental species to humans.
2099 NeuroToxicology. 28**,** 931-937.

2100 Clancy, B., et al., 2007b. Web-based method for translating neurodevelopment from laboratory species
2101 to humans. Neuroinformatics. 5**,** 79-94.

2102 Cordeiro, Y., et al., 2001. DNA converts cellular prion protein into the beta-sheet conformation and
2103 inhibits prion peptide aggregation. Journal of Biological Chemistry. 276**,** 49400-49409.

2104 Couderc, T., et al., 2008. A mouse model for chikungunya: Young age and inefficient type-I interferon
2105 signaling are risk factors for severe disease. PLoS Pathogens. 4.

2106 Cruz-Munoz, M.E., et al., 2009. Influence of CRACC, a SLAM family receptor coupled to the adaptor EAT-
2107 2, on natural killer cell function. Nature Immunology. 10**,** 297-305.

2108 Czyz, J., Wobus, A.M., 2001. Embryonic stem cell differentiation: The role of extracellular factors.
2109 Differentiation. 68**,** 167-174.

2110 Danbolt, N.C., 2001. Glutamate uptake. Progress in Neurobiology. 65**,** 1-105.

2111 Danis, B., et al., 2008. Interferon regulatory factor 7-mediated responses are defective in cord blood
2112 plasmacytoid dendritic cells. European Journal of Immunology. 38**,** 507-517.

2113 Dasari, P., Zola, H., Nicholson, I.C., 2011. Expression of Toll-like receptors by neonatal leukocytes.
2114 Pediatric Allergy and Immunology. 22**,** 221-228.

2115 de Almeida, C.J.G., et al., 2005. The cellular prion protein modulates phagocytosis and inflammatory
2116 response. Journal of Leukocyte Biology. 77**,** 238-246.

2117 Deleault, N.R., Lucassen, R.W., Supattapone, S., 2003. RNA molecules stimulate prion protein
2118 conversion. Nature. 425**,** 717-720.

2119 Deng, L., et al., 2000. Activation of the I kappa B kinase complex by TRAF6 requires a dimeric ubiquitin-
2120 conjugating enzyme complex and a unique polyubiquitin chain. Cell. 103**,** 351-361.

2121 Dick, A.D., et al., 1995. FLOW CYTOMETRIC IDENTIFICATION OF A MINORITY POPULATION OF MHC
2122 CLASS-II POSITIVE CELLS IN THE NORMAL RAT RETINA DISTINCT FROM CD45(LOW)CD11B
2123 C(+)CD4(LOW) PARENCHYMAL MICROGLIA. British Journal of Ophthalmology. 79**,** 834-840.

2124 Dodelet, V.C., Cashman, N.R., 1998. Prion protein expression in human leukocyte differentiation. Blood.
2125 91**,** 1556-1561.

2126 Dorschner, R.A., et al., 2003. Neonatal skin in mice and humans expresses increased levels of
2127 antimicrobial peptides: Innate immunity during development of the adaptive response. Pediatric
2128 Research. 53**,** 566-572.

2129 Doyle, S.L., O'Neill, L.A.J., 2006. Toll-like receptors: From the discovery of NFKB to new insights into
2130 transcriptional regulations in innate immunity. Biochemical Pharmacology. 72**,** 1102-1113.

2131 El Khoury, J., et al., 2007. Ccr2 deficiency impairs microglial accumulation and accelerates progression of
2132 Alzheimer-like disease. Nature Medicine. 13**,** 432-438.

2133 Ewald, S.E., et al., 2008. The ectodomain of Toll-like receptor 9 is cleaved to generate a functional
2134 receptor. Nature. 456**,** 658-U88.

2135 Fan, Y.H., et al., 2010. Lysine 63-linked Polyubiquitination of TAK1 at Lysine 158 Is Required for Tumor
2136 Necrosis Factor alpha- and Interleukin-1 beta-induced IKK/NF-kappa B and JNK/AP-1 Activation.
2137 Journal of Biological Chemistry. 285**,** 5347-5360.

2138 Färber, K., Kettenmann, H., 2005. Physiology of microglial cells. Brain Research Reviews. 48**,** 133-143.

2139 Färber, K., Kettenmann, H., 2006. Purinergic signaling and microglia. Pflugers Archiv European Journal of
2140 Physiology. 452**,** 615-621.

2141 Ferret-Bernard, S., et al., Cellular and molecular mechanisms underlying the strong neonatal IL-12
2142 response of lamb mesenteric lymph node cells to R-848. PLoS ONE. 5.

2143 Field, E.J., Joyce, G., Keith, A., 1969. FAILURE OF INTERFERON TO MODIFY SCRAPIE IN MOUSE. Journal of
2144 General Virology. 5**,** 149-&.

2145 Ford, A.L., et al., 1995. NORMAL ADULT RAMIFIED MICROGLIA SEPARATED FROM OTHER CENTRAL-
2146 NERVOUS-SYSTEM MACROPHAGES BY FLOW CYTOMETRIC SORTING - PHENOTYPIC DIFFERENCES

DEFINED AND DIRECT EX-VIVO ANTIGEN PRESENTATION TO MYELIN BASIC PROTEIN-REACTIVE CD4(+) T-CELLS COMPARED. Journal of Immunology. 154, 4309-4321.

Frade, J.M., Barde, Y.A., 1998. Microglia-derived nerve growth factor causes cell death in the developing retina. Neuron. 20, 35-41.

Gabus, C., et al., 2001. The prion protein has RNA binding and chaperoning properties characteristic of nucleocapsid protein NCp7 of HIV-1. Journal of Biological Chemistry. 276, 19301-19309.

Geissmann, F., Jung, S., Littman, D.R., 2003. Blood Monocytes Consist of Two Principal Subsets with Distinct Migratory Properties. Immunity. 19, 71-82.

Geissmann, F., et al., 2010. Development of monocytes, macrophages, and dendritic cells. Science. 327, 656-661.

Gelderblom, M., et al., 2009. Temporal and Spatial Dynamics of Cerebral Immune Cell Accumulation in Stroke. Stroke. 40, 1849-1857.

Gilch, S., et al., 2007. CpG and LPS can interfere negatively with prion clearance in macrophage and microglial cells. FEBS Journal. 274, 5834-5844.

Gilmore, J.H., Jarskog, L.F., 1997. Exposure to infection and brain development: Cytokines in the pathogenesis of schizophrenia. Schizophrenia Research. 24, 365-367.

Ginhoux, F., et al., 2010. Fate Mapping Analysis Reveals That Adult Microglia Derive from Primitive Macrophages. Science. 330, 841-845.

Gioannini, T.L., et al., 2004. Isolation of an endotoxin-MD-2 complex that produces Toll-like receptor 4-dependent cell activation at picomolar concentrations. Proceedings of the National Academy of Sciences of the United States of America. 101, 4186-4191.

Gitik, M., et al., 2011. Myelin down-regulates myelin phagocytosis by microglia and macrophages through interactions between CD47 on myelin and SIRPalpha (signal regulatory protein-alpha) on phagocytes. Journal of Neuroinflammation. 8, 24.

Gottfried-Blackmore, A., et al., 2009. Acute in vivo exposure to interferon-gamma enables resident brain dendritic cells to become effective antigen presenting cells. Proceedings of the National Academy of Sciences of the United States of America. 106, 20918-20923.

Graeber, M.B., 2010. Changing Face of Microglia. Science. 330, 783-788.

Gresser, I., Maury, C., Chandler, R.L., 1983. FAILURE TO MODIFY SCRAPIE IN MICE BY ADMINISTRATION OF INTERFERON OR ANTI-INTERFERON GLOBULIN. Journal of General Virology. 64, 1387-1389.

Hacker, H., et al., 2006. Specificity in Toll-like receptor signalling through distinct effector functions of TRAF3 and TRAF6. Nature. 439, 204-207.

Hamilton, J.A., Anderson, G.P., 2004. Mini Review GM-CSF Biology. Growth Factors. 22, 225-231.

2180 Hanisch, U.K., Kettenmann, H., 2007. Microglia: Active sensor and versatile effector cells in the normal
2181 and pathologic brain. Nature Neuroscience. 10**,** 1387-1394.

2182 Herms, J.W., et al., 1997. Increase of intracellular free Ca2+ in microglia activated by prion protein
2183 fragment. GLIA. 21**,** 253-257.

2184 Hernangómez, M., et al., 2012. CD200-CD200R1 interaction contributes to neuroprotective effects of
2185 anandamide on experimentally induced inflammation. GLIA. 60**,** 1437-1450.

2186 Hesske, L., et al., 2010. Induction of inhibitory central nervous system-derived and stimulatory blood-
2187 derived dendritic cells suggests a dual role for granulocyte-macrophage colony-stimulating
2188 factor in central nervous system inflammation. Brain. 133**,** 1637-1654.

2189 Hickey, W.F., Kimura, H., 1988. Perivascular microglial cells of the CNS are bone marrow-derived and
2190 present antigen in vivo. Science. 239**,** 290-292.

2191 Honda, K., Takaoka, A., Taniguchi, T., 2006. Type I inteferon gene induction by the interferon regulatory
2192 factor family of transcription factors. Immunity. 25**,** 349-360.

2193 Hornig, M., et al., 1999. An infection-based model of neurodevelopmental damage. Proceedings of the
2194 National Academy of Sciences of the United States of America. 96**,** 12102-12107.

2195 Hu, X.Z., et al., 2010. beta(2)-Integrins in demyelinating disease: not adhering to the paradigm. Journal
2196 of Leukocyte Biology. 87**,** 397-403.

2197 Husebye, H., et al., 2006. Endocytic pathways regulate Toll-like receptor 4 signaling and link innate and
2198 adaptive immunity. EMBO Journal. 25**,** 683-692.

2199 Hynes, R.O., 2002. Integrins: Bidirectional, allosteric signaling machines. Cell. 110**,** 673-687.

2200 Irie-Sasaki, J., et al., 2001. CD45 is a JAK phosphatase and negatively regulates cytokine receptor
2201 signalling. Nature. 409**,** 349-354.

2202 Ishibashi, D., et al., 2012. Protective Role of Interferon Regulatory Factor 3-Mediated Signaling against
2203 Prion Infection. Journal of Virology. 86**,** 4947-4955.

2204 Ishibashi, M., et al., 2005. Signaling cascade coordinating growth of dorsal and ventral tissues of the
2205 vertebrate brain, with special reference to the involvement of Sonic Hedgehog signaling.
2206 Anatomical science international. 80**,** 30-6.

2207 Islam, M.A., et al., 2012a. Expression of Toll-like receptors and downstream genes in lipopolysaccharide-
2208 induced porcine alveolar macrophages. Veterinary Immunology and Immunopathology.

2209 Islam, M.A., et al., 2012b. Age-related changes in phagocytic activity and production of pro-
2210 inflammatory cytokines by lipopolysaccharide stimulated porcine alveolar macrophages.
2211 Cytokine.

2212 J. D. Isaacs, G.S.J.D.M.A., 2006. The role of the cellular prion protein in the immune system. Clinical and
2213 Experimental Immunology. 146**,** 1-8.

2214 Johnson, G.B., et al., 2002. Receptor-mediated monitoring of tissue well-being via detection of soluble
2215 heparan sulfate by toll-like receptor 4. Journal of Immunology. 168**,** 5233-5239.

2216 Jokic, M., et al., 2000. Fetal distress increases interleukin-6 and interleukin-8 and decreases tumour
2217 necrosis factor-alpha cord blood levels in noninfected full-term neonates. British Journal of
2218 Obstetrics and Gynaecology. 107**,** 420-425.

2219 Jutila, D.B., Kurk, S., Jutila, M.A., 1994. DIFFERENCES IN THE EXPRESSION OF LY-6C ON NEUTROPHILS
2220 AND MONOCYTES FOLLOWING PI-PLC HYDROLYSIS AND CELLULAR ACTIVATION. Immunology
2221 Letters. 41**,** 49-57.

2222 Kagan, J.C., Medzhitov, R., 2006. Phosphoinositide-mediated adaptor recruitment controls toll-like
2223 receptor signaling. Cell. 125**,** 943-955.

2224 Kagan, J.C., et al., 2008. TRAM couples endocytosis of Toll-like receptor 4 to the induction of interferon-
2225 beta. Nature Immunology. 9**,** 361-368.

2226 Kaul, D., et al., 2012. Expression of Toll-Like Receptors in the Developing Brain. PLoS ONE. 7.

2227 Kawagoe, T., et al., 2008. Sequential control of Toll-like receptor-dependent responses by IRAK1 and
2228 IRAK2. Nature Immunology. 9**,** 684-691.

2229 Keshet, G.I., et al., 1999. Scrapie-infected mice and PrP knockout mice share abnormal localization and
2230 activity of neuronal nitric oxide synthase. Journal of Neurochemistry. 72**,** 1224-1231.

2231 Kettenmann, H., et al., 2011. Physiology of Microglia. Physiological Reviews. 91**,** 461-553.

2232 Khosravani, H., et al., 2008. Prion protein attenuates excitotoxicity by inhibiting NMDA receptors.
2233 Journal of Cell Biology. 181**,** 551-565.

2234 Kim, Y.-M., et al., 2008. UNC93B1 delivers nucleotide-sensing toll-like receptors to endolysosomes.
2235 Nature. 452**,** 234-U80.

2236 Kocisko, D.A., et al., 2006. Potent antiscrapie activities of degenerate phosphorothioate
2237 oligonucleotides. Antimicrobial Agents and Chemotherapy. 50**,** 1034-1044.

2238 Kollmann, T.R., et al., 2009. Neonatal innate TLR-mediated responses are distinct from those of adults.
2239 Journal of Immunology. 183**,** 7150-7160.

2240 Krebs, B., et al., 2006. Prion protein induced signaling cascades in monocytes. Biochemical and
2241 Biophysical Research Communications. 340**,** 13-22.

2242 Kurpius, D., et al., 2006. Early activation, motility, and homing of neonatal microglia to injured neurons
2243 does not require protein synthesis. GLIA. 54**,** 58-70.

2244 Latz, E., et al., 2004. TLR9 signals after translocating from the ER to CpG DNA in the lysosome. Nature
2245 Immunology. 5**,** 190-198.

Lazarini, F., Deslys, J.P., Dormont, D., 1991. REGULATION OF THE GLIAL FIBRILLARY ACIDIC PROTEIN, BETA-ACTIN AND PRION PROTEIN MESSENGER-RNAS DURING BRAIN-DEVELOPMENT IN MOUSE. Molecular Brain Research. 10**,** 343-346.

Lee, K.S., et al., 2007. Hemin interactions and alterations of the subcellular localization of prion protein. Journal of Biological Chemistry. 282**,** 36525-36533.

Leifer, C.A., et al., 2004. TLR9 Is localized in the endoplasmic reticulum prior to stimulation. Journal of Immunology. 173**,** 1179-1183.

Lent, R., et al., 2012. How many neurons do you have? Some dogmas of quantitative neuroscience under revision. European Journal of Neuroscience. 35**,** 1-9.

Levy, O., et al., 2004. Selective impairment of TLR-mediated innate immunity in human newborns: Neonatal blood plasma reduces monocyte TNF-alpha induction by bacterial lipopeptides, lipopolysaccharide, and imiquimod, but preserves the response to R-848. Journal of Immunology. 173**,** 4627-4634.

Levy, O., et al., 2006a. The adenosine system selectively inhibits TLR-mediated TNF-alpha production in the human newborn. Journal of Immunology. 177**,** 1956-1966.

Levy, O., et al., 2006b. Unique efficacy of Toll-like receptor 8 agonists in activating human neonatal antigen-presenting cells. Blood. 108**,** 1284-1290.

Levy, O., 2007. Innate immunity of the newborn: basic mechanisms and clinical correlates. Nature Reviews Immunology. 7**,** 379-390.

Li, X.X., Stark, G.R., 2002. NF kappa B-dependent signaling pathways. Experimental Hematology. 30**,** 285-296.

Lieberburg, I., 1987. DEVELOPMENTAL EXPRESSION AND REGIONAL DISTRIBUTION OF THE SCRAPIE-ASSOCIATED PROTEIN MESSENGER-RNA IN THE RAT CENTRAL-NERVOUS-SYSTEM. Brain Research. 417**,** 363-366.

Lima, F.R.S., et al., 2007. Cellular prion protein expression in astrocytes modulates neuronal survival and differentiation. Journal of Neurochemistry. 103**,** 2164-2176.

Lin, H.H., et al., 2005. The macrophage F4/80 receptor is required for the induction of antigen-specific efferent regulatory T cells in peripheral tolerance. Journal of Experimental Medicine. 201**,** 1615-1625.

Lin, H.H., et al., 2010. F4/80: The Macrophage-Specific Adhesion-GPCR and its Role in Immunoregulation. In: Adhesion-Gpcrs: Structure to Function. Advances in Experimental Medicine and Biology, Vol. 706, S. Yona, M. Stacey, ed.^eds., pp. 149-156.

Linden, R., et al., 2008. Physiology of the prion protein. Physiological Reviews. 88**,** 673-728.

Ling, Z.D., et al., 2006. Progressive dopamine neuron loss following supra-nigral lipopolysaccharide (LPS) infusion into rats exposed to LPS prenatally. Experimental Neurology. 199**,** 499-512.

2281 Liu, D.Q., et al., 2008. Signal Regulatory Protein alpha Negatively Regulates beta(2) Integrin-Mediated
2282 Monocyte Adhesion, Transendothelial Migration and Phagocytosis. PLoS ONE. 3.

2283 Llinas, L., et al., 2011. Expression profiles of novel cell surface molecules on B-cell subsets and plasma
2284 cells as analyzed by flow cytometry. Immunology Letters. 134**,** 113-121.

2285 Lotscher, M., et al., 2007. Induced Prion Protein Controls Immune-Activated Retroviruses in the Mouse
2286 Spleen. PLoS ONE. 2.

2287 Lotz, M., et al., 2006. Postnatal acquisition of endotoxin tolerance in intestinal epithelial cells. Journal of
2288 Experimental Medicine. 203**,** 973-984.

2289 Manson, J., et al., 1992. THE PRION PROTEIN GENE - A ROLE IN MOUSE EMBRYOGENESIS. Development.
2290 115**,** 117-122.

2291 Manson, J.C., et al., 1994. 129/OLA MICE CARRYING A NULL MUTATION IN PRP THAT ABOLISHES
2292 MESSENGER-RNA PRODUCTION ARE DEVELOPMENTALLY NORMAL. Molecular Neurobiology. 8**,**
2293 121-127.

2294 Marc, D., Mercey, R., Lantier, F., 2007. Scavenger, transducer, RNA chaperone? What ligands of the
2295 prion protein teach us about its function. Cellular and Molecular Life Sciences. 64**,** 815-829.

2296 Marella, M., et al., 2002. Filipin prevents pathological prion protein accumulation by reducing
2297 endocytosis and inducing cellular PrP release. Journal of Biological Chemistry. 277**,** 25457-
2298 25464.

2299 Mariante, R.M., et al., 2012. Neuroimmunoendocrine regulation of the prion protein in neutrophils.
2300 Journal of Biological Chemistry. 287**,** 35506-35515.

2301 Marodi, L., 2006. Innate cellular immune responses in newborns. Clinical Immunology. 118**,** 137-144.

2302 Martin, G.R., et al., 2011. Endogenous Prion Protein Attenuates Experimentally Induced Colitis.
2303 American Journal of Pathology. 179**,** 2290-2301.

2304 Martino, D., Holt, P., Prescott, S., 2012. A novel role for interleukin-1 receptor signaling in the
2305 developmental regulation of immune responses to endotoxin. Pediatric Allergy and
2306 Immunology. 23**,** 567-572.

2307 Masocha, W., 2009. Systemic lipopolysaccharide (LPS)-induced microglial activation results in different
2308 temporal reduction of CD200 and CD200 receptor gene expression in the brain. Journal of
2309 Neuroimmunology. 214**,** 78-82.

2310 Mausberg, A.K., Jander, S., Reichmann, G., 2009. Intracerebral Granulocyte-Macrophage Colony-
2311 Stimulating Factor Induces Functionally Competent Dendritic Cells in the Mouse Brain. GLIA. 57**,**
2312 1341-1350.

2313 McKimmie, C.S., Fazakerley, J.K., 2005. In response to pathogens, glial cells dynamically and differentially
2314 regulate Toll-like receptor gene expression. Journal of Neuroimmunology. 169**,** 116-125.

McLennan, N.F., et al., 2004. Prion protein accumulation and neuroprotection in hypoxic brain damage. American Journal of Pathology. 165**,** 227-235.

Mednick, S.A., et al., 1988. ADULT SCHIZOPHRENIA FOLLOWING PRENATAL EXPOSURE TO AN INFLUENZA EPIDEMIC. Archives of General Psychiatry. 45**,** 189-192.

Meyer, U., et al., 2006. The time of prenatal immune challenge determines the specificity of inflammation-mediated brain and behavioral pathology. Journal of Neuroscience. 26**,** 4752-4762.

Meyer, U., Feldon, J., Fatemi, S.H., 2009. In-vivo rodent models for the experimental investigation of prenatal immune activation effects in neurodevelopmental brain disorders. Neuroscience and Biobehavioral Reviews. 33**,** 1061-1079.

Meyer, U., Feldon, J., 2010. Epidemiology-driven neurodevelopmental animal models of schizophrenia. Progress in Neurobiology. 90**,** 285-326.

Meylan, E., et al., 2004. RIP1 is an essential mediator of Toll-like receptor 3-induced NF-kappa B activation. Nature Immunology. 5**,** 503-507.

Mildner, A., et al., 2007. Microglia in the adult brain arise from Ly-6ChiCCR2+ monocytes only under defined host conditions. Nature Neuroscience. 10**,** 1544-1553.

Mildner, A., et al., 2011. Distinct and non-redundant roles of microglia and myeloid subsets in mouse models of Alzheimer's disease. Journal of Neuroscience. 31**,** 11159-11171.

Montero-Menei, C.N., et al., 1996. Early events of the inflammatory reaction induced in rat brain by lipopolysaccharide intracerebral injection: Relative contribution of peripheral monocytes and activated microglia. Brain Research. 724**,** 55-66.

Moser, M., et al., 1995. Developmental expression of the prion protein gene in glial cells. Neuron. 14**,** 509-517.

Murray, P.J., Wynn, T.A., 2011. Protective and pathogenic functions of macrophage subsets. Nature Reviews Immunology. 11**,** 723-737.

Nandi, P.K., et al., 2002. DNA-induced partial unfolding of prion protein leads to its polymerisation to amyloid. Journal of Molecular Biology. 322**,** 153-161.

Nasu-Nishimura, Y., et al., 2008. Cellular prion protein prevents brain damage after encephalomyocarditis virus infection in mice. Archives of Virology. 153**,** 1007-1012.

Nelson, K.B., Willoughby, R.E., 2000. Infection, inflammation and the risk of cerebral palsy. Current Opinion in Neurology. 13**,** 133-9.

Nguyen, M., et al., 2010. Acquisition of Adult-Like TLR4 and TLR9 Responses during the First Year of Life. PLoS ONE. 5.

2348 Nico, P.B.C., et al., 2005. Altered behavioural response to acute stress in mice lacking cellular prion
2349 protein. Behavioural Brain Research. 162**,** 173-181.

2350 Nimmerjahn, A., Kirchhoff, F., Helmchen, F., 2005. Neuroscience: Resting microglial cells are highly
2351 dynamic surveillants of brain parenchyma in vivo. Science. 308**,** 1314-1318.

2352 Ortega, A., Jadeja, V., Zhou, H.P., 2011. Postnatal development of lipopolysaccharide-induced
2353 inflammatory response in the brain. Inflammation Research. 60**,** 175-185.

2354 Ostuni, R., Zanoni, I., Granucci, F., 2010. Deciphering the complexity of Toll-like receptor signaling.
2355 Cellular and Molecular Life Sciences. 67**,** 4109-4134.

2356 Palsson-McDermott, E.M., et al., 2009. TAG, a splice variant of the adaptor TRAM, negatively regulates
2357 the adaptor MyD88-independent TLR4 pathway. Nature Immunology. 10**,** 579-U30.

2358 Pan, T., et al., 2002. Cell-surface prion protein interacts with glycosaminoglycans. Biochemical Journal.
2359 368**,** 81-90.

2360 Paolicelli, R.C., et al., 2011. Synaptic pruning by microglia is necessary for normal brain development.
2361 Science. 333**,** 1456-1458.

2362 Park, B., et al., 2008. Proteolytic cleavage in an endolysosomal compartment is required for activation of
2363 Toll-like receptor 9. Nature Immunology. 9**,** 1407-1414.

2364 Pasupuleti, M., et al., 2009. Antimicrobial activity of human prion protein is mediated by its N-terminal
2365 region. PLoS ONE. 4.

2366 Pekny, M., et al., 1998. Impaired induction of blood-brain barrier properties in aortic endothelial cells by
2367 astrocytes from GFAP-deficient mice. GLIA. 22**,** 390-400.

2368 Pelvig, D.P., et al., 2008. Neocortical glial cell numbers in human brains. Neurobiology of Aging. 29**,**
2369 1754-1762.

2370 Peterson, K.E., et al., 2006. Increased proinflammatory cytokine and chemokine responses and
2371 microglial infection following inoculation with neural stem cells infected with polytropic murine
2372 retroviruses. Virology. 354**,** 143-153.

2373 Petrova, P., et al., 2003. MANF: A new mesencephalic, astrocyte-derived neurotrophic factor with
2374 selectivity for dopaminergic neurons. Journal of Molecular Neuroscience. 20**,** 173-187.

2375 Prinz, M., et al., 2003. Prion pathogenesis in the absence of Toll-like receptor signalling. Embo Reports.
2376 4**,** 195-199.

2377 Prinz, M., et al., 2011. Heterogeneity of CNS myeloid cells and their roles in neurodegeneration. Nature
2378 Neuroscience. 14**,** 1-9.

2379 Ransohoff, R.M., Cardona, A.E., 2010. The myeloid cells of the central nervous system parenchyma.
2380 Nature. 468**,** 253-262.

Rolls, A., et al., 2007. Toll-like receptors modulate adult hippocampal neurogenesis. Nature Cell Biology. 9, 1081-1088.

Rosenberg, P.A., Aizenman, E., 1989. Hundred-fold increase in neuronal vulnerability to glutamate toxicity in astrocyte-poor cultures of rat cerebral cortex. Neuroscience Letters. 103, 162-168.

Roumier, A., et al., 2004. Impaired synaptic function in the microglial KARAP/DAP12-deficient mouse. Journal of Neuroscience. 24, 11421-11428.

Rudge, J.S., et al., 1995. CHANGES IN NEUROTROPHIC FACTOR EXPRESSION AND RECEPTOR ACTIVATION FOLLOWING EXPOSURE OF HIPPOCAMPAL NEURON ASTROCYTE COCULTURES TO KAINIC ACID. Journal of Neuroscience. 15, 6856-6867.

Rutkowski, M.J., et al., 2010. Complement and the central nervous system: emerging roles in development, protection and regeneration. Immunology and Cell Biology. 88, 781-786.

Ryman, K.D., et al., 2007. Early restriction of alphavirus replication and dissemination contributes to age-dependent attenuation of systemic hyperinflammatory disease. Journal of General Virology. 88, 518-529.

Sadeghi, K., et al., 2007. Immaturity of infection control in preterm and term newborns is associated with impaired toll-like receptor signaling. Journal of Infectious Diseases. 195, 296-302.

Saijo, K., Glass, C.K., 2011. Microglial cell origin and phenotypes in health and disease. Nature Reviews Immunology. 11, 775-787.

Sakurai-Yamashita, Y., et al., 2005. Female-specific neuroprotection against transient brain ischemia observed in mice devoid of prion protein is abolished by ectopic expression of prion protein-like protein. Neuroscience. 136, 281-287.

Samokhvalov, I.M., Samokhvalova, N.I., Nishikawa, S.I., 2007. Cell tracing shows the contribution of the yolk sac to adult haematopoiesis. Nature. 446, 1056-1061.

Sato, S., et al., 2005. Essential function for the kinase TAK1 in innate and adaptive immune responses. Nature Immunology. 6, 1087-1095.

Schafer, D.P., et al., 2012. Microglia Sculpt Postnatal Neural Circuits in an Activity and Complement-Dependent Manner. Neuron. 74, 691-705.

Schulz, C., et al., 2012. A Lineage of Myeloid Cells Independent of Myb and Hematopoietic Stem Cells. Science. 336, 86-90.

Sedgwick, J.D., et al., 1991. ISOLATION AND DIRECT CHARACTERIZATION OF RESIDENT MICROGLIAL CELLS FROM THE NORMAL AND INFLAMED CENTRAL-NERVOUS-SYSTEM. Proceedings of the National Academy of Sciences of the United States of America. 88, 7438-7442.

Sethi, S., et al., 2002. Postexposure prophylaxis against prion disease with a stimulator of innate immunity. Lancet. 360, 229-230.

2415 Shi, L.M., et al., 2003. Maternal influenza infection causes marked behavioral and pharmacological
2416 changes in the offspring. Journal of Neuroscience. 23**,** 297-302.

2417 Sierra, A., et al., 2010. Microglia shape adult hippocampal neurogenesis through apoptosis-coupled
2418 phagocytosis. Cell Stem Cell. 7**,** 483-495.

2419 Simard, A.R., et al., 2006. Bone marrow-derived microglia play a critical role in restricting senile plaque
2420 formation in Alzheimer's disease. Neuron. 49**,** 489-502.

2421 Sorensen, H.J., et al., 2009. Association Between Prenatal Exposure to Bacterial Infection and Risk of
2422 Schizophrenia. Schizophrenia Bulletin. 35**,** 631-637.

2423 Spinner, D.S., et al., 2008. Accelerated Prion Disease Pathogenesis in Toll-Like Receptor 4 Signaling-
2424 Mutant Mice. Journal of Virology. 82**,** 10701-10708.

2425 Stella, R., et al., Prion and TNFÎ±: TAC(E)it agreement between the prion protein and cell signaling. Cell
2426 Cycle. 9**,** 4616-4621.

2427 Stevens, B., et al., 2007. The Classical Complement Cascade Mediates CNS Synapse Elimination. Cell.
2428 131**,** 1164-1178.

2429 Sunyach, C., et al., 2003. The mechanism of internalization of glycosylphosphatidylinositol-anchored
2430 prion protein. Embo Journal. 22**,** 3591-3601.

2431 Suzuki, N., et al., 2002. Severe impairment of interleukin-1 and Toll-like receptor signalling in mice
2432 lacking IRAK-4. Nature. 416**,** 750-754.

2433 Swirski, F.K., et al., 2009. Identification of Splenic Reservoir Monocytes and Their Deployment to
2434 Inflammatory Sites. Science. 325**,** 612-616.

2435 Tabeta, K., et al., 2006. The Unc93b1 mutation 3d disrupts exogenous antigen presentation and signaling
2436 via Toll-like receptors 3, 7 and 9. Nature Immunology. 7**,** 156-164.

2437 Termeer, C., et al., 2002. Oligosaccharides of hyaluronan activate dendritic cells via toll-like receptor 4.
2438 Journal of Experimental Medicine. 195**,** 99-111.

2439 Tohmi, M., et al., 2007. The cellular and behavioral consequences of interleukin-1 alpha penetration
2440 through the blood-brain barrier of neonatal rats: A critical period for efficacy. Neuroscience.
2441 150**,** 234-250.

2442 Tollin, M., et al., 2005. Vernix caseosa as a multi-component defence system based on polypeptides,
2443 lipids and their interactions. Cellular and Molecular Life Sciences. 62**,** 2390-2399.

2444 Trgovcich, J., et al., 1999. TNF alpha, interferon, and stress response induction as a function of age-
2445 related susceptibility to fatal Sindbis virus infection of mice. Virology. 263**,** 339-348.

2446 Triantafilou, M., et al., 2004. Lateral diffusion of Toll-like receptors reveals that they are transiently
2447 confined within lipid rafts on the plasma membrane. Journal of Cell Science. 117**,** 4007-4014.

Ullian, E.M., et al., 2001. Control of synapse number by glia. Science. 291**,** 657-661.

Wakselman, S., et al., 2008. Developmental neuronal death in hippocampus requires the microglial CD11b integrin and DAP12 immunoreceptor. Journal of Neuroscience. 28**,** 8138-8143.

Wang, C., et al., 2001. TAK1 is a ubiquitin-dependent kinase of MKK and IKK. Nature. 412**,** 346-351.

Weinstock, M., 2008. The long-term behavioural consequences of prenatal stress. Neuroscience and Biobehavioral Reviews. 32**,** 1073-1086.

Weiss, S., et al., 1997. RNA aptamers specifically interact with the prion protein PrP. Journal of Virology. 71**,** 8790-8797.

West, A.P., Koblansky, A.A., Ghosh, S., 2006. Recognition and signaling by toll-like receptors. In: Annual Review of Cell and Developmental Biology. Annual Review of Cell and Developmental Biology, Vol. 22, ed.^eds., pp. 409-437.

Wolburg, H., Lippoldt, A., 2002. Tight junctions of the blood-brain barrier: Development, composition and regulation. Vascular Pharmacology. 38**,** 323-337.

Wright, S.D., et al., 1990. CD14, A RECEPTOR FOR COMPLEXES OF LIPOPOLYSACCHARIDE (LPS) AND LPS BINDING-PROTEIN. Science. 249**,** 1431-1433.

Yamamoto, M., et al., 2003. TRAM is specifically involved in the Toll-like receptor 4-mediated MyD88-independent signaling pathway. Nature Immunology. 4**,** 1144-1150.

Yan, S.R., et al., 2004. Role of MyD88 in diminished tumor necrosis factor alpha production by newborn mononuclear cells in response to lipopolysaccharide. Infection and Immunity. 72**,** 1223-1229.

Yin, S., et al., 2008. Binding of recombinant but not endogenous prion protein to DNA causes DNA internalization and expression in mammalian cells. The Journal of biological chemistry. 283**,** 25446-25454.

Zarewych, D.M., et al., 1996. LPS induces CD14 association with complement receptor type 3, which is reversed by neutrophil adhesion. Journal of Immunology. 156**,** 430-433.

Zhang, G.X., et al., 2002. Parenchymal microglia of naive adult C57BL/6J mice express high levels of B7.1, B7.2, and MHC class II. Experimental and Molecular Pathology. 73**,** 35-45.

Ziv, Y., et al., 2006. Immune cells contribute to the maintenance of neurogenesis and spatial learning abilities in adulthood. Nat Neurosci. 9**,** 268-275.